ARID

International Journal for Science and Technology

مَجلةُ أُريد الدَّوليةُ للعُلومِ والتِّكنولوجيا

VOL. 4 NO. 7 June 2021

ISSN : 2662-009X

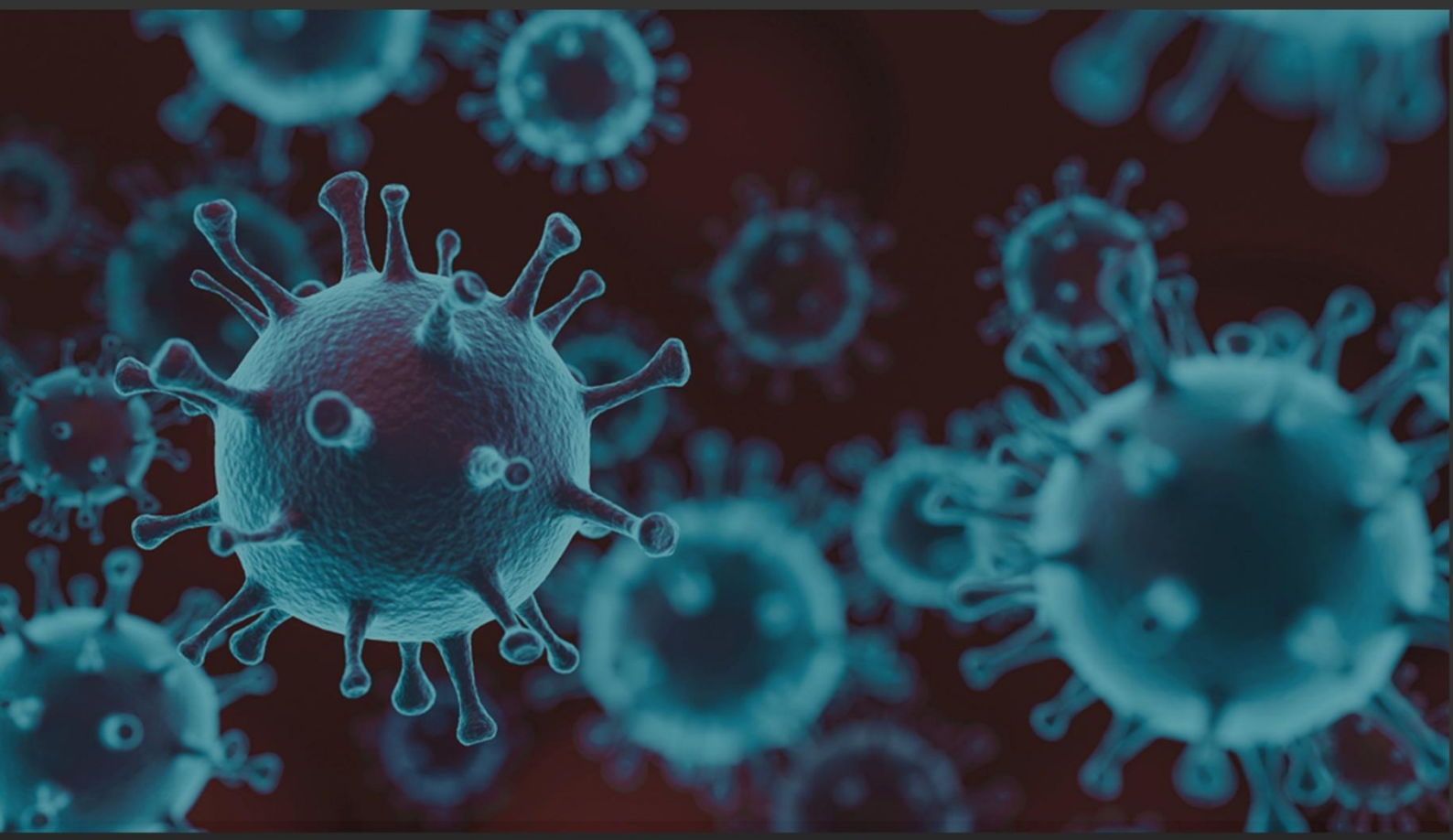

ARID PUBLICATIONS

ARID.MY/J/AIJST

ARAB RESEARCHER ID

ARID International Journal for Science and Technology (AIJST)

Published by Arabic Researcher ID (ARID)

The Board of Trustees مجلس الامناء

أ.د عبدالرازق مختار محمود
Prof. Dr.Abdel Razek Mokhtar

arid.my/0001-2264

أ.د سلوان كمال جميل العاني
Prof.Dr. Salwan K.J.Al-Ani

arid.my/0001-1999

أ.د محمود عبد العاطى ابو حسوب
Prof. Dr.Mahmoud Abdel-Aty

arid.my/0001-8321

أ.د. رحاب يوسف
Prof. Dr. Rehab Yousif

arid.my/0003-9655

أ.د. سعاد هادي حسن الطائي
Prof.Dr.Suaad AL-Taai

arid.my/0003-3810

أ.د. سعد سلمان عبد الله المشهداني
Prof. Dr.Saad Salman Abdallah

arid.my/0001-6136

د.سيف السويدي
Dr.Saif Al-Sewaidi

arid.my/0001-0001

أ.م.د . ناصر محمود احمد الراوي
Assoc. Prof.Dr.Naser Mahmoud

arid.my/0002-0775

أ.م.د.مصطفى عبدالله السويدي
Assoc. Prof.Dr.Mustafa Abdullah

arid.my/0001-7762

فهرس المجلة | Index

ARID Journals

ARID International Journal for Science and Technology (AIJST)
ISSN: 2662-009X

Journal home page: http://arid.my/j/aijst

مَجلةُ أُريد الدَّوليةُ للعُلومِ والتِّكنولوجيا

العدد 7 ، المجلد 4 ، حزيران 2021 م

رسالة المحرر

سوف يتم التركيز في هذه الرسالة على اتجاهات البحث العلمي بعد حدوث جائحة كورونا (كوفيد – 19)، حيث شهدت أنظمة التعليم في العالم خلال العام 2020م اضطراباً غير مسبوق بفعل جائحة كورونا، فوفقاً لأرقام حديثة صادرة عن معهد اليونسكو للإحصاء، فقد أغلقت معظم مدارس وجامعات العالم أبوابها أمام أكثر من 1.5 مليار تلميذ وطالب، أي ما يزيد على 90% من إجمالي الدارسين.

بالاضافة لذلك فقد تميز العام 2020م بظهور اتجاهات جديدة في التعليم مع بنية تحتية عالية الأتمتة باستخدام مُعطيات الثورة الصناعية الرابعة، وأنظمة الذكاء الاصطناعي، وأن ثمَّة تحوُّلات متوقَّعة سوف تكون كبيرة وهيكلية في أنماط التعليم العام أو الجامعي.

ومن أبرز تحوُّلات التعليم في زمن ما بعد كورونا:

- استخدام التقنيات المتقدِّمة.
- إنشاء مزيد من البوابات والمنصَّات، لمختلف مراحل التعليم، خاصة بعد أن أثبتت فاعليتها في وقت شِدة الجائحة.
- تعزيز التعليم عبر الإنترنت وبرمجيات التعلُّم التكيفية.
- أهم الأنماط الجديدة ذات البنية الرقمية في التعليم هي التعليم عن بُعد، التعليم الإلكتروني، الذكاء الاصطناعي، وإن إدماج التقنيات الجديدة في المناهج الدراسية والبحث العلمي يتطلّب التخطيط الجيّد.

بدأ مفهوم الاقتصاد الرقمي في العقد الأخير من القرن الماضي وتطور في كافة المرافق الاقتصادية من خلال الهواتف الذكية وشبكات التواصل الاجتماعي والمنصات التشاركية.

وزاد اهتمام الدول المتقدمة بالاقتصاد الرقمي نتيجة لنمو التكنولوجيات الرقمية وزيادة إعداد المستخدمين إلى نصف سكان الأرض، وتطبيقاته في التجارة الإلكترونية والنقل والتعليم والصحة وقطاعات أخرى. وتعد الاستراتيجيات الرقمية الوطنية مهمة لتحقيق النمو الاقتصادي والاجتماعي الضروري لبلوغ أهداف التنمية المستدامة.

ولا بد من الإشارة إلى الفجوة الكبيرة في مجال الاقتصاد الرقمي بين الاقتصاديات العربية والاقتصاديات المتقدمة، وضرورة حث الخطى باللحاق بالتحولات الناشئة في هذا المجال. وهناك تنافس أمريكي صيني في الحصول على الحصة الأكبر من الاقتصاد الرقمي. وتسعى الدول لتمكين الاقتصاد الرقمي وتوظيف التكنولوجيا في مجال المعلومات والاتصالات لخدمة التجارة على المستوى العالمي، وتوجيه الاستثمار في هذا القطاع الحيوي، وتدريب كوادر وطنية متخصصة في البرمجة والصيانة لتحقيق جودة البنية التحتية، وتواجه التحديات بتطوير برمجيات الحماية من القرصنة وبتشريعات محلية واقليمية ودولية.

وتشير التقارير الصادرة من قاعدة بيانات البنك الدولي أن الصادرات من السلع التكنولوجية من الدول العربية مجتمعة خلال الأعوام 2011، 2012، 2013م لم يتعدى الـ 1.7 مليار دولار بينما تعدت الصادرات السلعية للعالم 1.3 تريليون دولار وما يمثل 1 من الألف من الانتاج القومي العربي. وبلغت استثمارات الدول العربية في التكنولوجيا بعد جائحة كورونا الـ 16 مليار دولار في عام 2019م، ويتوقع لها الزيادة على الـ 20 مليار دولار في العام 2024م.

أما واقع البحث العلمي بعد تفشي جائحة كورونا فيمكن اجماله بالآتي:

- تأثرت البحوث الإجرائية بشكل كبير والسبب عدم إمكانية تطبيق التجربة في أكثر البحوث، فالبحوث التربوية تواجه إغلاق المؤسسات التعليمية.
- لم تتوقف حركة العلوم النظرية والرياضيات وتخصصات العلوم الإنسانية والتاريخ واللغات، واستمر النشر العلمي والتأليف وتوفر متسع من الوقت لنشر ما يمكن من المعلومات.
- تأثرت معظم مختبرات البحوث في العالم بسبب جائحة كورونا، حيث أدت إلى الإغلاق الجزئي أو الكلي للمختبرات البحثية من جهة وإلى نقص التمويل للبحوث العلمية بسبب الازمة الاقتصادية من جهة ثانية.
- مع كل الانحسار والاختناق الحاصل في مجال البحث العلمي إلا أن مختبرات البحوث قد عملت بالحد الأدنى خلال الجائحة، مع تكيف الباحثين مع الوضع الجديد باستخدام إجراءات السلامة والوقاية من الإصابة مثل التعقيم ولبس

الكمامات والتباعد الاجتماعي، واستمرت المختبرات بنشر نتائج البحوث حسب تخصصاتها لعدم توقف الجامعات عن التدريس على مستوى الدراسات الأولية والدراسات العليا ولكنها تحولت إلى التعليم الإلكتروني.

- أما الأبحاث التي تعتمد على البرامج الحاسوبية والمحاكاة فلم تتاثر كثيرا بسبب الجائحة نظرا لطبيعتها الملائمة لإجراءات التباعد الاجتماعي.
- البحوث القائمة على تجارب مختبرية وتتعلق بمشاركة الطلبة أيضا تأثرت لعدم إمكانية حضور الطلبة إلى المختبرات.
- البحوث المتعلقة ببعض القطاعات التي أغلقت بالكامل، تكاد تكون متوقفة تماما كالبحوث المتعلقة بسلوك الأطفال في أماكن اللعب والترفيه، أو البحوث المتعلقة بالسينما، فهذه القطاعات أغلقت منذ فبراير 2020 ولم تفتح حتى هذه اللحظة.
- تأثرت البحوث التي تعد الاستبانة أحد أهم أدواتها تأثرا شديدا على مستوى مصداقية هذه الأداة، والسبب أن أغلب الباحثين لجأوا إلى هذه الأداة لإنجاز بحوثهم، وفي العادة قليل من الناس يتجاوبون مع الاستبانة ويكلفوا أنفسهم عناء الرد، وبعد الجائحة لا يكاد يخلو يوم من إرسال هذه الاستبانات الأمر الذي أدى إلى عدم التجاوب – شبه التام – معها من قبل الفئة المستهدفة.
- البحوث التي تعتمد على الوثائق النادرة غير المنشورة إلكترونيا والتي تستوجب الذهاب إلى مكتبة أو متحف للحصول عليها تأثرت هي الأخرى بشكل كبير مع الإغلاق الحاصل أو مع تقليص عدد الموظفين وفي الغالب لجوئهم إلى عدم استقبال الباحثين.
- البحوث التي تعتمد على زيارة المواقع التاريخية أو ما يشابهها من ناحية احتياجات البحث، تأثرت هي الأخرى بسبب إغلاق هذه المواقع.

وكان من الطبيعي أن يحدث تحول في اتجاهات البحث العلمي بعد حدوث جائحة كورونا، والذي تمثل فيما يلي:

- وجه باحثو الطب بأنواعه والصيدلة وعلوم الحياة (البيولوجيا) على دراسة الفايروس المستجد وأطواره وعملية تحوره وكيفية الإصابة به والعوامل التي تساعد على انتشار أو انحسار الجائحة، وكذلك طرق الوقاية والتشخيص والعلاج.
- ساهمت بحوث الكيمياء في دعم البحوث البيولوجية، وفي نفس الوقت في تطوير المنظفات ووسائل التعقيم وملابس الوقاية.

- شاركت بحوث الفيزياء في تطوير أساليب التشخيص والتحليل.
- تناولت البحوث الهندسية كيفية تطبيق نتائج البحوث الأكاديمية ووضعها موضع التنفيذ من حيث تطوير أجهزة التشخيص والعلاج وأجهزة التنفس ووسائل وقاية الأطقم الطبية وتطوير طرق العزل وإيجاد حلول لما يطرأ من مشكلات.
- كشفت أزمة كورونا عن أهمية البحث العلمي، وحيوية الاستثمار في هذا القطاع الاستراتيجي الكفيل بتحويل الأزمات والمخاطر إلى محطات لاستخلاص النتائج وإرساء الاستراتيجيات الكفيلة بتحصين المستقبل.

ARID Journals

ARID International Journal for Science and Technology (AIJST)
ISSN: 2662-009X

Journal home page: http://arid.my/j/aijst

مَجلةُ أُريد الدَّوليةُ للعُلومِ والتِّكنولوجيا

العدد 7 ، المجلد 4 ، حزيران 2021 م

UNION AND INTERSECTION OF CHAOTIC GRAPHS WITH DENSITY VARIATION

Fathia Milad Alogab Ibtesam Milad Laqab

Mathematics department - Science College - Al-Asmarya Islamic University - Libya

اتحاد وتقاطع الكثافة للمخططات الفوضوية (المُشوّشة)

فتحية ميلاد العقاب ابتسام ميلاد العقاب

قسم الرياضيات - كلية العلوم - الجامعة الأسمرية الإسلامية - ليبيا

fathiaalagab@gmail.com
arid.my/0003-9675
https://doi.org/10.36772/arid.aijst.2021.471

ARTICLE INFO

Article history:
Received 18/01/2021
Received in revised form 10/03/2021
Accepted 17/05/2021
Available online 15/06/2021
https://doi.org/10.36772/arid.aijst.2021.471

ABSTRACT

The aim of the present study is to discuss the union and intersection operations on chaotic graphs with density variation; the adjacency and incidence matrices representing the chaotic graphs induced from these operations will be introduced when physical characters of chaotic graphs have the same properties.

There are several applications that have been utilized on chaotic graphs with density variation. The most practical applications of these kinds of operations on chaotic graphs with density variation are the internet signal speeds and the variation of green color for different parts of the plant. For example, in botany, in some cases several plants suffer from a lack of chlorophyll in the damaged parts of the plant. In this case the plant is represented by a chaotic graph and the proportion of chlorophyll is represented by the density property, then the appropriate process is applied to increase the chlorophyll percentage in the appropriate place, so these operations helps us to choose the suitable operator that satisfy our desires and requests.

Keywords*:* adjacency matrix, incidence matrix, chaotic graph, density, union, intersection.

.

الملـخــص

في هذا البحث سوف يتم مناقشة بعض العمليات الجبرية على المخططات الفوضوية (المُشوّشة) التي تحمل خاصية الكثافة و هما عمليتا الإتحاد والتقاطع، كذلك سيتم استعراض نتائج هذه العمليات في صورة مصفوفتي التأثير(المجاورة) والوقوع (الاسقــاط) عندما يكون المخطط المشوش يحمل خاصية واحدة.

هذا البحث يناقش تأثير هذه العمليات على مستوى الكثافة لدى المخططات المشوّشة (الفوضوية)، حيث يمكننا تمثيل خاصية الكثافة بتركيز مادة الكلوروفيل في النباتات أو بسرعة إشارات الإنترنت على الشبكة، فعلى حسب متطلبات التطبيق المختار للمخطط المشوّش يمكن إختيار العملية المناسبة لذلك فمن الممكن زيادة أو تحفيز سرعة الإنترنت في مناطق معينة من الشبكة دون الأخرى، كذلك يمكننا تحفيز نسبة الكلوروفيل في أجزاء معينة من النباتات المعرضة للتلف لإنعاشها دون التأثير على أجزاء النباتات الأخرى.

استخدام التطبيق المناسب مع العملية المناسبة يُمكّنُنا الحصول على النتائج المطلوبة و أهمية الحصول عليها، دراسة مصفوفتي التأثير(المجاورة) والوقوع (الإسقــاط) تساعد الباحث في فهم نقاط الإرتكاز للمخطط المشوّش وتساعده في عملية التركيز على مستوى الكثافة للأجزاء المطلوبة للمخطط المشوش.

الكلمـات المفـتاحـيـة: مصفوفة التأثير (المجاورة)، مصفوفة الوقوع (الإسقاط)، المخطط الفوضوي (المشوش)، كثافة، إتحاد، تقاطع.

1. INTRODUCTION

Scientists of all physical systems are searching for a simple structure that describe the topology of the system in a simple way which help them to develop the performance of the system, the theory of chaotic graphs is introduced to describe most of these physical systems, it visualizes the topology of the system, so scientist can apply their physical character on the system and understand the behavior of the physical character. In this research, the physical character is presented by the density character; the density character can represent many physical applications in different fields such as biology fields (i.e. Chlorophyll degree, Bacterial grows, nerve system), chemical systems (i.e. atoms topology), internet technology (i.e. web internet signal speed) and many other different fields. [1, 2]

Our interest is applying the algebraic part of the chaotic graph and translated on the chosen applications, so the theory of chaotic graphs can help scientists to understand and control their applications.

Basic topological definitions and backgrounds are relevant to this article are cited in this background**.**

1.1. Definitions and backgrounds

- Simple graph $G(V,E)$: Is a graph with no loops or multiple edges [3].
- Adjacency and incidence: Let v and w be vertices of a graph, if v and w are joined by an edge e , then v and w are said to be adjacent. Moreover, v and w are said to be incident with e , and e is said to be incident with v and w [4, 5, 6].
- The adjacency matrix: Let G be a graph without loops, with n-vertices labeled $1,2,3,...,n$ the "adjacency matrix" $A(G)$ is the $n \times n$ matrix in which the entry in row i and column j is the number of edges joining the vertices i and j [4, 5, 6].

- The incidence matrix: Let G be a graph without loops, with n-vertices labeled 1,2,3,...,n and m- edges labeled 1,2,3,...,m.The" incidence matrix" $I(G)$ is the $n \times m$ matrix in which the entry in row i and column j is 1 if vertex i is incident with edge j and 0 otherwise [4, 5, 6].

Example: Consider the graph G in Figure (1):

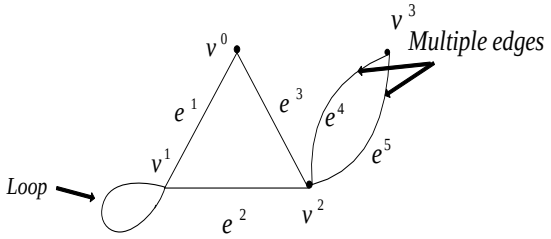

Figure (1): Multiple graph

The adjacency matrix $A(G)$ is: $A(G) = \begin{bmatrix} 0 & 1 & 1 & 0 \\ 1 & 1 & 1 & 0 \\ 1 & 1 & 0 & 2 \\ 0 & 0 & 2 & 0 \end{bmatrix}$

And its incidence matrix $I(G)$ is: $I(G) = \begin{bmatrix} 1 & 0 & 1 & 0 & 0 \\ 1^1 & 1 & 0 & 0 & 0 \\ 0 & 1 & 1 & 1 & 1 \\ 0 & 0 & 0 & 1 & 1 \end{bmatrix}$

Noting that the symbol (1^1) in the second row and first column means that we have one loop at the vertex v^1 with the edge e^1. Also, if we have two loops at the same above vertex, we symbolize it by 1^{11}. Moreover, if we have an infinite number of loops at any vertex, say v^i, we use the symbol $1^{1111..}$ to represent them [1].

- Chaotic graph $G_h(V_h, E_h)$: Is a geometric graph that carries many physical characters, these geometric graphs might have similar properties or different [5, 7, 8, 9].

- Null graph: Is a graph consists of a set of vertices and no edges [9, 10].
- Loop: A loop is an edge which starts and ends on the same vertex [6, 7, 8].
- Multiple edges: Tow or more edges joining the same pair of vertices are called "multiple edges" [2].
- Density (d): Is a physical property of matter, as each element and compound has a unique density associated with it [11].
- The "union" G of two graphs G_1 and G_2 is a graph $G = G_1 \bigcup G_2$ having $V(G) = V(G_1) \bigcup V(G_2)$ and $E(G) = E(G_1) \bigcup E(G_2)$ such that $V(G_1) \bigcap V(G_2) = \phi$ [10].
- The "intersection" of two graphs $G_1 = (V_1, E_1)$ and $G_2 = (V_2, E_2)$, with at least one vertex in common than their intersection will be the graph of vertices and edges defined as follows: $V(G_1 \bigcap G_2) = V(G_1) \bigcap V(G_2)$ and $E(G_1 \bigcap G_2) = E(G_1) \bigcap E(G_2)$ [9].

1.2. The matrix representation for fixed and different densities of chaotic graphs:

In this part we will obtain the adjacent and incidence matrices for two cases:

1. When degree of density is fixed, for example degree of green color of a leave is a perfect green.

2. Degree of density is different and various between chaotic levels and areas. For example degree of green color of a leave is various between different parts of a leave.

We will denote the degree of each area on the chaotic graph by d_{pq}, where p denotes level of chaotic graph, while q denotes different areas on each level of chaotic graph [11] .See Figure (2)

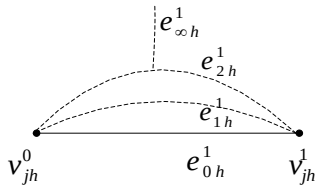

Figure (2): 1-Simplicial chaotic graph

And the adjacent and incidence matrices are:

$$A(G_h)=\begin{bmatrix} 0_{(0123..\infty)_{d_{pq}}h} & 1_{(0123..\infty)_{d_{pq}}h} \\ 1_{(0123..\infty)_{d_{pq}}h} & 0_{(0123..\infty)_{d_{pq}}h} \end{bmatrix}, I(G_h)=\begin{bmatrix} 1_{(0123..\infty)_{d_{pq}}h} \\ 1_{(0123..\infty)_{d_{pq}}h} \end{bmatrix}.$$

2. Union and intersection of chaotic graphs with density variations:

2.1. Union of chaotic graphs with density variation

This part will discuss and explain the union of two chaotic graphs with density variation, we shall show the union of two simple and multiple chaotic graphs inducing the adjacent and incidence matrices of the resulted, discussion can be understand it clearly via examples.

Consider two simple chaotic graphs with density variation $G_h^{\,1}$ and $G_h^{\,2}$ which are

$G_h^1=\{v^0_{jh}e^1_{0h}v^1_{jh};\ j=0,1,2...\infty\}$, $G_h^2=\{v^2_{jh}e^2_{jh}v^3_{jh}e^3_{jh}v^4_{jh}e^4_{jh}v^2_{jh};\ j=0,1,2,...\infty\}$ and their union

$G_h^1\cup G_h^2=\{v^0_{jh}e^1_{jh}v^1_{jh}v^2_{jh}e^2_{jh}v^3_{jh}e^3_{jh}v^4_{jh}e^4_{jh}v^2_{jh};\ j=0,1,2,...\infty\}$ is shown in Figure (3)

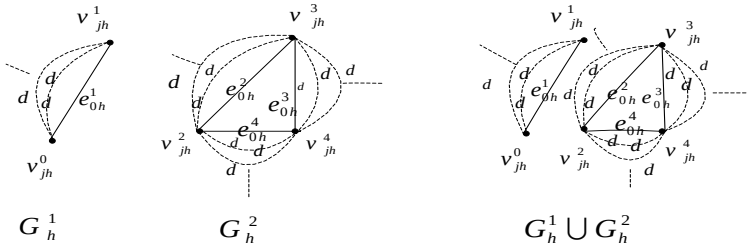

Figure (3): Union of two simple chaotic graphs

Both the adjacent and incidence matrices of G_h^1 , G_h^2 and $G_h^1 \bigcup G_h^2$ respectively are:

$$A_h^1 = \begin{bmatrix} 0_{(012..\infty)_{d_{pq}}h} & 1_{(012..\infty)_{d_{pq}}h} \\ 1_{(012..\infty)_{d_{pq}}h} & 0_{(012..\infty)_{d_{pq}}h} \end{bmatrix} \; I_h^1 = \begin{bmatrix} 1_{(012..\infty)_{d_{pq}}h} \\ 1_{(012..\infty)_{d_{pq}}h} \end{bmatrix} \; A_h^2 = \begin{bmatrix} 0_{(012..\infty)_{d_{pq}}h} & 1_{(012..\infty)_{d_{pq}}h} & 1_{(012..\infty)_{d_{pq}}h} \\ 1_{(012..\infty)_{d_{pq}}h} & 0_{(012..\infty)_{d_{pq}}h} & 1_{(012..\infty)_{d_{pq}}h} \\ 1_{(012..\infty)_{d_{pq}}h} & 1_{(012..\infty)_{d_{pq}}h} & 0_{(012..\infty)_{d_{pq}}h} \end{bmatrix}$$

$$I_h^2 = \begin{bmatrix} 1_{(012..\infty)_{d_{pq}}h} & 0_{(012..\infty)_{d_{pq}}h} & 1_{(012..\infty)_{d_{pq}}h} \\ 1_{(012..\infty)_{d_{pq}}h} & 1_{(012..\infty)_{d_{pq}}h} & 0_{(012..\infty)_{d_{pq}}h} \\ 0_{(012..\infty)_{d_{pq}}h} & 1_{(012..\infty)_{d_{pq}}h} & 1_{(012..\infty)_{d_{pq}}h} \end{bmatrix}.$$

And $A_h = \begin{bmatrix} 0_{(012..\infty)_{d_{pq}}h} & 1_{(012..\infty)_{d_{pq}}h} & 0_{(012..\infty)_{d_{pq}}h} & 0_{(012..\infty)_{d_{pq}}h} & 0_{(012..\infty)_{d_{pq}}h} \\ 1_{(012..\infty)_{d_{pq}}h} & 0_{(012..\infty)_{d_{pq}}h} & 0_{(012..\infty)_{d_{pq}}h} & 0_{(012..\infty)_{d_{pq}}h} & 0_{(012..\infty)_{d_{pq}}h} \\ 0_{(012..\infty)_{d_{pq}}h} & 0_{(012..\infty)_{d_{pq}}h} & 0_{(012..\infty)_{d_{pq}}h} & 1_{(012..\infty)_{d_{pq}}h} & 1_{(012..\infty)_{d_{pq}}h} \\ 0_{(012..\infty)_{d_{pq}}h} & 0_{(012..\infty)_{d_{pq}}h} & 1_{(012..\infty)_{d_{pq}}h} & 0_{(012..\infty)_{d_{pq}}h} & 1_{(012..\infty)_{d_{pq}}h} \\ 0_{(012..\infty)_{d_{pq}}h} & 0_{(012..\infty)_{d_{pq}}h} & 1_{(012..\infty)_{d_{pq}}h} & 1_{(012..\infty)_{d_{pq}}h} & 0_{(012..\infty)_{d_{pq}}h} \end{bmatrix}$,

$$I_h = \begin{bmatrix} 1_{(012..\infty)_{d_{pq}}h} & 0_{(012..\infty)_{d_{pq}}h} & 0_{(012..\infty)_{d_{pq}}h} & 0_{(012..\infty)_{d_{pq}}h} \\ 1_{(012..\infty)_{d_{pq}}h} & 0_{(012..\infty)_{d_{pq}}h} & 0_{(012..\infty)_{d_{pq}}h} & 0_{(012..\infty)_{d_{pq}}h} \\ 0_{(012..\infty)_{d_{pq}}h} & 1_{(012..\infty)_{d_{pq}}h} & 0_{(012..\infty)_{d_{pq}}h} & 1_{(012..\infty)_{d_{pq}}h} \\ 0_{(012..\infty)_{d_{pq}}h} & 1_{(012..\infty)_{d_{pq}}h} & 1_{(012..\infty)_{d_{pq}}h} & 0_{(012..\infty)_{d_{pq}}h} \\ 0_{(012..\infty)_{d_{pq}}h} & 0_{(012..\infty)_{d_{pq}}h} & 1_{(012..\infty)_{d_{pq}}h} & 1_{(012..\infty)_{d_{pq}}h} \end{bmatrix}$$

As the above result the total density of the resulted graph is increased.

Consider two multiple chaotic graphs with density variation $G_h^1(V_h^1, E_h^1)$ and $G_h^2(V_h^2, E_h^2)$ such that

$V_h^1 = \{v_{jh}^0, v_{jh}^1; j = 0,1,2...\infty\}$ $E_h^1 = \{e_{jh}^1; j = 0,1,2...\infty\}, V_h^2 = \{v_{jh}^2, v_{jh}^3, v_{jh}^4; j = 0,1,2...\infty\},$

$E_h^2 = \{e_{jh}^2, e_{jh}^3, e_{jh}^4, e_{jh}^5; j = 0,1,2...\infty\}$ .See Figure (4)

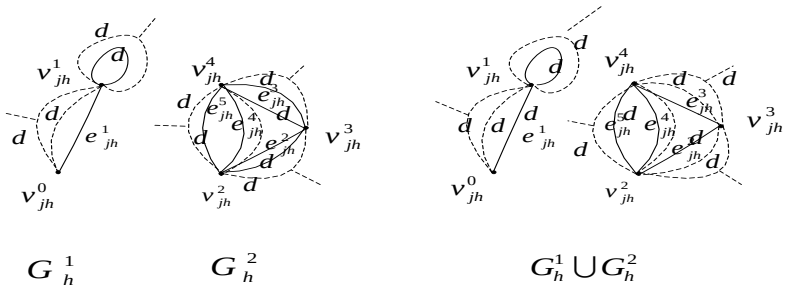

Figure (4): Union of two multiple chaotic graphs

Both the adjacent and incidence matrices of G_h^1, G_h^2 and $G_h^1 \cup G_h^2$ respectively are:

$$A_h^1 = \begin{bmatrix} 0_{(012..\infty)_{d_{pq}}h} & 1_{(012..\infty)_{d_{pq}}h} \\ 1_{(012..\infty)_{d_{pq}}h} & 1_{(012..\infty)_{d_{pq}}h} \end{bmatrix}, I_h^1 = \begin{bmatrix} 1_{(012..\infty)_{d_{pq}}h} \\ 1^1_{(012..\infty)_{d_{pq}}h} \end{bmatrix}, A_h^2 = \begin{bmatrix} 0_{(012..\infty)_{d_{pq}}h} & 1_{(012..\infty)_{d_{pq}}h} & 2_{(012..\infty)_{d_{pq}}h} \\ 1_{(012..\infty)_{d_{pq}}h} & 0_{(012..\infty)_{d_{pq}}h} & 1_{(012..\infty)_{d_{pq}}h} \\ 2_{(012..\infty)_{d_{pq}}h} & 1_{(012..\infty)_{d_{pq}}h} & 0_{(012..\infty)_{d_{pq}}h} \end{bmatrix}$$

$$I_h^2 = \begin{bmatrix} 1_{(012..\infty)_{d_{pq}}h} & 0_{(012,,\infty)_{d_{pq}}h} & 1_{(012..\infty)_{d_{pq}}h} & 1_{(012..\infty)_{d_{pq}}h} \\ 1_{(012..\infty)_{d_{pq}}h} & 1_{(012..\infty)_{d_{pq}}h} & 0_{(012..\infty)_{d_{pq}}h} & 0_{(012..\infty)_{d_{pq}}h} \\ 0_{(012..\infty)_{d_{pq}}h} & 1_{(012..\infty)_{d_{pq}}h} & 1_{(012..\infty)_{d_{pq}}h} & 1_{(012..\infty)_{d_{pq}}h} \end{bmatrix}$$

$$A_h = \begin{bmatrix} 0_{(012..\infty)_{d_{pq}}h} & 1_{(012..\infty)_{d_{pq}}h} & 0_{(012..\infty)_{d_{pq}}h} & 0_{(012..\infty)_{d_{pq}}h} & 0_{(012..\infty)_{d_{pq}}h} \\ 1_{(012..\infty)_{d_q}h} & 1_{(012..\infty)_{d_{pq}}h} & 0_{(012..\infty)_{d_{pq}}h} & 0_{(012..\infty)_{d_{pq}}h} & 0_{(012..\infty)_{d_{pq}}h} \\ 0_{(012..\infty)_{d_{pq}}h} & 0_{(012..\infty)_{d_{pq}}h} & 0_{(012..\infty)_{d_{pq}}h} & 1_{(012..\infty)_{d_{pq}}h} & 2_{(012..\infty)_{d_{pq}}h} \\ 0_{(012..\infty)_{d_{pq}}h} & 0_{(012..\infty)_{d_{pq}}h} & 1_{(012..\infty)_{d_{pq}}h} & 0_{(012..\infty)_{d_{pq}}h} & 1_{(012..\infty)_{d_{pq}}h} \\ 0_{(012..\infty)_{d_{pq}}h} & 0_{(012..\infty)_{d_{pq}}h} & 2_{(012..\infty)_{d_{pq}}h} & 1_{(012..\infty)_{d_{pq}}h} & 0_{(012..\infty)_{d_{pq}}h} \end{bmatrix},$$

$$I_h = \begin{bmatrix} 1_{(012..\infty)_{d_{pq}}h} & 0_{(012..\infty)_{d_{pq}}h} & 0_{(012..\infty)_{d_{pq}}h} & 0_{(012..\infty)_{d_{pq}}h} & 0_{(012..\infty)_{d_{pq}}h} \\ 1^1_{(012..\infty)_{d_{pq}}h} & 0_{(012..\infty)_{d_{pq}}h} & 0_{(012..\infty)_{d_{pq}}h} & 0_{(012..\infty)_{d_{pq}}h} & 0_{(012..\infty)_{d_{pq}}h} \\ 0_{(012..\infty)_{d_{pq}}h} & 1_{(012..\infty)_{d_{pq}}h} & 0_{(012..\infty)_{d_{pq}}h} & 1_{(012..\infty)_{d_{pq}}h} & 1_{(012..\infty)_{d_{pq}}h} \\ 0_{(012..\infty)_{d_{pq}}h} & 1_{(012..\infty)_{d_{pq}}h} & 0_{(012..\infty)_{d_{pq}}h} & 1_{(012..\infty)_{d_{pq}}h} & 0_{(012..\infty)_{d_{pq}}h} \\ 0_{(012..\infty)_{d_{pq}}h} & 0_{(012..\infty)_{d_{pq}}h} & 1_{(012..\infty)_{d_{pq}}h} & 1_{(012..\infty)_{d_{pq}}h} & 1_{(012..\infty)_{d_{pq}}h} \end{bmatrix}.$$

The union of two chaotic graphs with density variation is another chaotic graph with more extremer density value to the resulted chaotic graph. The adjacent and incidence matrices representing the union of two chaotic graphs can be obtained from the adjacent and incidence matrices of representing each of the given chaotic graphs constituting such a union of both of them by adding to them some chaotic zero matrices**.**

2.2. Intersection of chaotic graphs with density variation:

The operation of intersection on chaotic graphs is quite interesting compared to the operation of union; the following discussion explains the intersection of any two chaotic graphs with density variation by examples in several cases (i.e. disjoint, common vertices and common edges). The results of intersection of any two chaotic graphs are based on the intersection of any two geometric graphs.

2.2.1. Disjoint intersection of chaotic graphs with density variation:

Consider two simple chaotic graphs with density variation $G_h^1 = \{v_{jh}^0 e_{jh}^1 v_{jh}^1; j = 0,1,2,...\}$ and $G_h^2 = \{v_{jh}^2 e_{jh}^2 v_{jh}^3 e_{jh}^3 v_{jh}^4; j = 0,1,2,...\}$. See Figure (5)

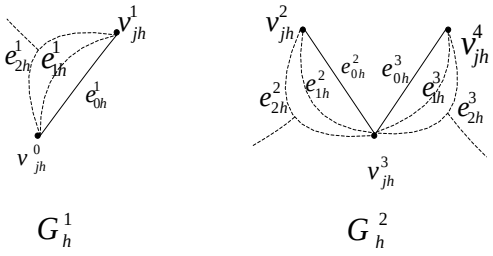

Figure (5): Two simple chaotic graphs

Applying the intersection on G_h^1 and G_h^2, (i.e. $G_h^1 \bigcap G_h^2$) results the empty graph, and both the adjacent and incidence matrices representing the chaotic graphs with density variation G_h^1, G_h^2 and $G_h^1 \bigcap G_h^2$ are:

$$A_h^1 = \begin{bmatrix} 0_{(012..\infty)_{d_{pq}}h} & 1_{(012..\infty)_{d_{pq}}h} \\ 1_{(012..\infty)_{d_{pq}}h} & 0_{(012..\infty)_{d_{pq}}h} \end{bmatrix}, I_h^1 = \begin{bmatrix} 1_{(012..\infty)_{d_{pq}}h} \\ 1_{(012..\infty)_{d_{pq}}h} \end{bmatrix},$$

$$A_h^2 = \begin{bmatrix} 0_{(012..\infty)_{d_{pq}}h} & 1_{(012..\infty)_{d_{pq}}h} & 0_{(012..\infty)_{d_{pq}}h} \\ 1_{(012..\infty)_{d_{pq}}h} & 0_{(012..\infty)_{d_{pq}}h} & 1_{(012..\infty)_{d_{pq}}h} \\ 0_{(012..\infty)_{d_{pq}}h} & 1_{(012..\infty)_{d_{pq}}h} & 0_{(012..\infty)_{d_{pq}}h} \end{bmatrix}, I_h^2 = \begin{bmatrix} 1_{(012..\infty)_{d_{pq}}h} & 0_{(012..\infty)_{d_{pq}}h} \\ 1_{(012..\infty)_{d_{pq}}h} & 1_{(012..\infty)_{d_{pq}}h} \\ 0_{(012..\infty)_{d_{pq}}h} & 1_{(012..\infty)_{d_{pq}}h} \end{bmatrix}.$$

While the adjacent and incidence matrices of the intersected chaotic graph $G_h^1 \bigcap G_h^2$ is the ϕ -matrix, (I.e. $A_h = \phi - matrix$, $I_h = \phi - matrix$).

So; if any two chaotic graphs with density variation are disjoint, then both of the adjacent and incidence matrices representing that intersection are $\phi-$matrix, and the density value of the intersected graph is zero.

2.2.2. The intersection of two chaotic graphs with density variation common in one vertex or more vertices:

Consider two simple chaotic graphs with density variation $G_h^1 = \{v_{jh}^0 e_{jh}^1 v_{jh}^1; j = 0,1,2,3...\}$ and $G_h^2 = \{v_{jh}^0 e_{jh}^2 v_{jh}^1 e_{jh}^3 v_{jh}^2; j = 0,1,2,3...\}$, then their intersection $G_h^1 \bigcap G_h^2$ is the null graph of only two chaotic vertices $\{v_{jh}^0, v_{jh}^1; j = 0,1,2...\}$. See Figure (6).

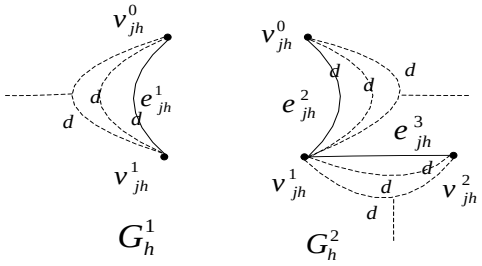

Figure (6): Two chaotic graphs common in two vertices

The density value in the intersected graph is greater than the original two chaotic graphs. The adjacent and incidence matrices of G^1_h, G^2_h and $G^1_h \bigcap G^2_h$ are:

$$A^1_h = \begin{bmatrix} 0_{(012..\infty)_{d_{pq}}h} & 1_{(012..\infty)_{d_{pq}}h} \\ 1_{(012..\infty)_{d_{pq}}h} & 0_{(012..\infty)_{d_{pq}}h} \end{bmatrix}, I^1_h = \begin{bmatrix} 1_{(012..\infty)_{d_{pq}}h} \\ 1_{(012..\infty)_{d_{pq}}h} \end{bmatrix},$$

$$A^2_h = \begin{bmatrix} 0_{(012..\infty)_{d_{pq}}h} & 1_{(012..\infty)_{d_{pq}}h} & 0_{(012..\infty)_{d_{pq}}h} \\ 1_{(012..\infty)_{d_{pq}}h} & 0_{(012..\infty)_{d_{pq}}h} & 1_{(012..\infty)_{d_{pq}}h} \\ 0_{(012..\infty)_{d_{pq}}h} & 1_{(012..\infty)_{d_{pq}}h} & 0_{(012..\infty)_{d_{pq}}h} \end{bmatrix}, I^2_h = \begin{bmatrix} 1_{(012..\infty)_{d_{pq}}h} & 0_{(012..\infty)_{d_{pq}}h} \\ 1_{(012..\infty)_{d_{pq}}h} & 1_{(012..\infty)_{d_{pq}}h} \\ 0_{(012..\infty)_{d_{pq}}h} & 1_{(012..\infty)_{d_{pq}}h} \end{bmatrix}$$

$$A_h = \begin{bmatrix} 0_{(\overline{012}..\bar{\infty})_{\bar{d}_{pq}}h} & 0_{(\overline{012}..\bar{\infty})_{\bar{d}_{pq}}h} \\ 0_{(\overline{012}..\bar{\infty})_{\bar{d}_{pq}}h} & 0_{(\overline{012}..\bar{\infty})_{\bar{d}_{pq}}h} \end{bmatrix}, I_h = \begin{bmatrix} 0_{(\overline{012}..\bar{\infty})_{\bar{d}_{pq}}h} \\ 0_{(\overline{012}..\bar{\infty})_{\bar{d}_{pq}}h} \end{bmatrix}.$$

The adjacent and incidence matrices of the intersection of two chaotic vertices with density variation in the case if they are common in one vertex or many vertices and without any common edges are zeros matrices, but they have a double density in the intersected chaotic vertices.

2.2.3. The intersection of two chaotic graphs with density variation common in more than one edge:

Consider two simple chaotic graphs with density variation

$G^1_h = \{v^0_{jh} e^1_{jh} v^1_{jh} e^2_{jh} v^2_{jh} e^3_{jh} v^3_{jh};\ j = 0,1,2,3,...\}$ and $G^2_h = \{v^1_{jh} e^2_{jh} v^2_{jh} e^3_{jh} v^3_{jh} e^4_{jh} v^4_{jh};\ j = 0,1,2,3,...\}$ .See Figure (7)

The intersection of $G_h^1 \bigcap G_h^2$ results another simple chaotic graph with denser value at these locations, and the adjacent and incidence matrices of G_h^1, G_h^2 and $G_h^1 \bigcap G_h^2$ are:

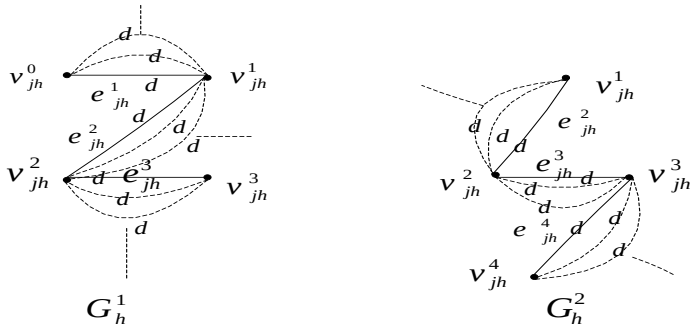

Figure (7): Intersection of two simple chaotic graphs common in two edges

$$A_h^1 = \begin{bmatrix} 0_{(012..\infty)_{d_{pq}}h} & 1_{(012..\infty)_{d_{pq}}h} & 0_{(012..\infty)_{d_{pq}}h} & 0_{(012..\infty)_{d_{pq}}h} \\ 1_{(012..\infty)_{d_{pq}}h} & 0_{(012..\infty)_{d_{pq}}h} & 1_{(012..\infty)_{d_{pq}}h} & 0_{(012..\infty)_{d_{pq}}h} \\ 0_{(012..\infty)_{d_{pq}}h} & 1_{(012..\infty)_{d_{pq}}h} & 0_{(012..\infty)_{d_{pq}}h} & 1_{(012..\infty)_{d_{pq}}h} \\ 0_{(012..\infty)_{d_{pq}}h} & 0_{(012..\infty)_{d_{pq}}h} & 1_{(012..\infty)_{d_{pq}}h} & 0_{(012..\infty)_{d_{pq}}h} \end{bmatrix} = A_h^2,$$

$$I_h^1 = \begin{bmatrix} 1_{(012..\infty)_{d_{pq}}h} & 0_{(012..\infty)_{d_{pq}}h} & 0_{(012..\infty)_{d_{pq}}h} \\ 1_{(012..\infty)_{d_{pq}}h} & 1_{(012..\infty)_{d_{pq}}h} & 0_{(012..\infty)_{d_{pq}}h} \\ 0_{(012..\infty)_{d_{pq}}h} & 1_{(012..\infty)_{d_{pq}}h} & 1_{(012..\infty)_{d_{pq}}h} \\ 0_{(012..\infty)_{d_{pq}}h} & 0_{(012..\infty)_{d_{pq}}h} & 1_{(012..\infty)_{d_{pq}}h} \end{bmatrix} = I_h^2$$

$$, A_h = \begin{bmatrix} 0_{(\overline{012}..\bar{\infty})_{\bar{d}_{pq}}h} & 1_{(\overline{012}..\bar{\infty})_{\bar{d}_{pq}}h} & 0_{(\overline{012}..\bar{\infty})_{\bar{d}_{pq}}h} \\ 1_{(\overline{012}..\bar{\infty})_{\bar{d}_{pq}}h} & 0_{(\overline{012}..\bar{\infty})_{\bar{d}_{pq}}h} & 1_{(\overline{012}..\bar{\infty})_{\bar{d}_{pq}}h} \\ 0_{(\overline{012}..\bar{\infty})_{\bar{d}_{pq}}h} & 1_{(\overline{012}..\bar{\infty})_{\bar{d}_{pq}}h} & 0_{(\overline{012}..\bar{\infty})_{\bar{d}_{pq}}h} \end{bmatrix}, \; I_h = \begin{bmatrix} 1_{(\overline{012}..\bar{\infty})_{\bar{d}_{pq}}h} & 0_{(\overline{012}..\bar{\infty})_{\bar{d}_{pq}}h} \\ 1_{(\overline{012}..\bar{\infty})_{\bar{d}_{pq}}h} & 1_{(\overline{012}..\bar{\infty})_{\bar{d}_{pq}}h} \\ 0_{(\overline{012}..\bar{\infty})_{\bar{d}_{pq}}h} & 1_{(\overline{012}..\bar{\infty})_{\bar{d}_{pq}}h} \end{bmatrix}.$$

If any two chaotic graphs with density variation are intersected in one edge or in many edges, then both the adjacent and incidence matrices representing that intersection are not zero matrices and they are not sub matrices of those representing the given two chaotic graphs and the total

density of the intersected graph will be reduced as it is a sub-graph of the two graphs, while it is increased in the intersected area.

2.2.4. The intersection of two chaotic graphs with density variation common in more than one edge and vertex in another way:

Consider two multiple chaotic graphs with density variation $\{e^{i}_{jh};\{i=1,2,3,5,8,9,\ j=0,1,2...\}\}$ and $G^{2}_{h}=\{v^{i}_{jh};i=\{1,2,3,4\}\ \&\ \{j=0,1,2,3,...\}\};\ \ \{e^{i}_{jh};\{i=2,3,4,5,6,7,8,\ j=0,1,2...\}\}$. See Figure (8).

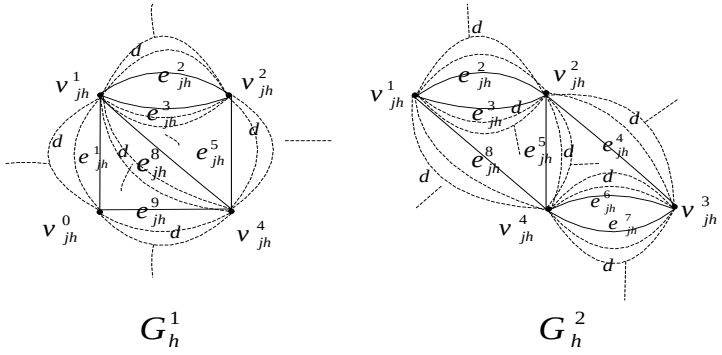

Figure (8): Intersection of two chaotic graphs common in more than one vertex and edge

The adjacent and incidence matrices of G^{1}_{h}, G^{2}_{h} and $G^{1}_{h}\cap G^{2}_{h}$ are:

$$A^{1}_{h}=\begin{bmatrix} 0_{(012..\infty)_{d_{pq}}h} & 1_{(012..\infty)_{d_{pq}}h} & 0_{(012..\infty)_{d_{pq}}h} & 1_{(012..\infty)_{d_{pq}}h} \\ 1_{(012..\infty)_{d_{pq}}h} & 0_{(012..\infty)_{d_{pq}}h} & 2_{(012..\infty)_{d_{pq}}h} & 1_{(012..\infty)_{d_{pq}}h} \\ 0_{(012..\infty)_{d_{pq}}h} & 2_{(012..\infty)_{d_{pq}}h} & 0_{(012..\infty)_{d_{pq}}h} & 1_{(012..\infty)_{d_{pq}}h} \\ 1_{(012..\infty)_{d_{pq}}h} & 1_{(012..\infty)_{d_{pq}}h} & 1_{(012..\infty)_{d_{pq}}h} & 0_{(012..\infty)_{d_{pq}}h} \end{bmatrix}$$

$$I_h^1 = \begin{bmatrix} 1_{(012..\infty)_{d_{pq}}h} & 0_{(012..\infty)_{d_{pq}}h} & 0_{(012..\infty)_{d_{pq}}h} & 0_{(012..\infty)_{d_{pq}}h} & 0_{(012..\infty)_{d_{pq}}h} & 1_{(012..\infty)_{d_{pq}}h} \\ 1_{(012..\infty)_{d_{pq}}h} & 1_{(012..\infty)_{d_{pq}}h} & 1_{(012..\infty)_{d_{pq}}h} & 0_{(012..\infty)_{d_{pq}}h} & 1_{(012..\infty)_{d_{pq}}h} & 0_{(012..\infty)_{d_{pq}}h} \\ 0_{(012..\infty)_{d_{pq}}h} & 1_{(012..\infty)_{d_{pq}}h} & 1_{(012..\infty)_{d_{pq}}h} & 1_{(012..\infty)_{d_{pq}}h} & 0_{(012..\infty)_{d_{pq}}h} & 0_{(012..\infty)_{d_{pq}}h} \\ 0_{(012..\infty)_{d_{pq}}h} & 0_{(012..\infty)_{d_{pq}}h} & 0_{(012..\infty)_{d_{pq}}h} & 1_{(012..\infty)_{d_{pq}}h} & 1_{(012..\infty)_{d_{pq}}h} & 1_{(012..\infty)_{d_{pq}}h} \end{bmatrix},$$

$$A_h^2 = \begin{bmatrix} 0_{(012..\infty)_{d_{pq}}h} & 2_{(012..\infty)_{d_{pq}}h} & 0_{(012..\infty)_{d_{pq}}h} & 1_{(012..\infty)_{d_{pq}}h} \\ 2_{(012..\infty)_{d_{pq}}h} & 0_{(012..\infty)_{d_{pq}}h} & 1_{(012..\infty)_{d_{pq}}h} & 1_{(012..\infty)_{d_{pq}}h} \\ 0_{(012..\infty)_{d_{pq}}h} & 1_{(012..\infty)_{d_{pq}}h} & 0_{(012..\infty)_{d_{pq}}h} & 2_{(012..\infty)_{d_{pq}}h} \\ 1_{(012..\infty)_{d_{pq}}h} & 1_{(012..\infty)_{d_{pq}}h} & 2_{(012..\infty)_{d_{pq}}h} & 0_{(012..\infty)_{d_{pq}}h} \end{bmatrix},$$

$$I_h^2 = \begin{bmatrix} 1_{(012..\infty)_{d_{pq}}h} & 1_{(012..\infty)_{d_{pq}}h} & 0_{(012..\infty)_{d_{pq}}h} & 0_{(012..\infty)_{d_{pq}}h} & 0_{(012..\infty)_{d_{pq}}h} & 0_{(012..\infty)_{d_{pq}}h} & 1_{(012..\infty)_{d_{pq}}h} \\ 1_{(012..\infty)_{d_{pq}}h} & 1_{(012..\infty)_{d_{pq}}h} & 1_{(012..\infty)_{d_{pq}}h} & 1_{(012..\infty)_{d_{pq}}h} & 0_{(012..\infty)_{d_{pq}}h} & 0_{(012..\infty)_{d_{pq}}h} & 0_{(012..\infty)_{d_{pq}}h} \\ 0_{(012..\infty)_{d_{pq}}h} & 0_{(012..\infty)_{d_{pq}}h} & 1_{(012..\infty)_{d_{pq}}h} & 0_{(012..\infty)_{d_{pq}}h} & 1_{(012..\infty)_{d_{pq}}h} & 1_{(012..\infty)_{d_{pq}}h} & 0_{(012..\infty)_{d_{pq}}h} \\ 0_{(012..\infty)_{d_{pq}}h} & 0_{(012..\infty)_{d_{pq}}h} & 0_{(012..\infty)_{d_{pq}}h} & 1_{(012..\infty)_{d_{pq}}h} & 1_{(012..\infty)_{d_{pq}}h} & 1_{(012..\infty)_{d_{pq}}h} & 1_{(012..\infty)_{d_{pq}}h} \end{bmatrix},$$

$$A_h = \begin{bmatrix} 0_{(\overline{012}..\bar{\infty})_{\bar{d}_{pq}}h} & 2_{(\overline{012}..\bar{\infty})_{\bar{d}_{pq}}h} & 1_{(\overline{012}..\bar{\infty})_{\bar{d}_{pq}}h} \\ 2_{(\overline{012}..\bar{\infty})_{\bar{d}_{pq}}h} & 0_{(\overline{012}..\bar{\infty})_{\bar{d}_{pq}}h} & 1_{(\overline{012}..\bar{\infty})_{\bar{d}_{pq}}h} \\ 1_{(\overline{012}..\bar{\infty})_{\bar{d}_{pq}}h} & 1_{(\overline{012}..\bar{\infty})_{\bar{d}_{pq}}h} & 0_{(\overline{012}..\bar{\infty})_{\bar{d}_{pq}}h} \end{bmatrix},$$

$$I_h = \begin{bmatrix} 1_{(\overline{012}..\bar{\infty})_{\bar{d}_{pq}}h} & 1_{(\overline{012}..\bar{\infty})_{\bar{d}_{pq}}h} & 0_{(\overline{012}..\bar{\infty})_{\bar{d}_{pq}}h} & 1_{(\overline{012}..\bar{\infty})_{\bar{d}_{pq}}h} \\ 1_{(\overline{012}..\bar{\infty})_{\bar{d}_{pq}}h} & 1_{(\overline{012}..\bar{\infty})_{\bar{d}_{pq}}h} & 1_{(\overline{012}..\bar{\infty})_{\bar{d}_{pq}}h} & 0_{(\overline{012}..\bar{\infty})_{\bar{d}_{pq}}h} \\ 0_{(\overline{012}..\bar{\infty})_{\bar{d}_{pq}}h} & 0_{(\overline{012}..\bar{\infty})_{\bar{d}_{pq}}h} & 1_{(\overline{012}..\bar{\infty})_{\bar{d}_{pq}}h} & 1_{(\overline{012}..\bar{\infty})_{\bar{d}_{pq}}h} \end{bmatrix}$$

An important point is that both the adjacent and incidence matrices of the intersection of two multiple chaotic graphs are not sub matrices of those representing the given two multiple chaotic graph.

3. Applications

There are several applications applied on chaotic graphs with density variation such as the internet signal speeds and the variation of green color for different parts of the plant, for example, in botany, in some cases some plants suffer from a lack of chlorophyll, in this case the plant is represented by a chaotic graph and the proportion of chlorophyll is represented by the

density property, and then the appropriate process is applied to increase the chlorophyll percentage in the appropriate place.

4. Conclusions

In this paper, the union and intersection of chaotic graphs with density variation was discussed. The union of two chaotic graphs result a new chaotic graph with more extremer density value. The intersection operation discussed in several cases, in all cases the density value will increase in the intersected area, but the total density of the resulted graph will be reduced compared to the original two graphs. If any two chaotic graphs with density variation are disjoint, then both the adjacent and incidence matrices representing that intersection are $\phi-\text{matrix}$, and the density value of the intersected graph is zero, while the adjacent and incidence matrices of the intersection of two chaotic graphs common in more than one vertex with density variation and without any common edges are zeros matrices, but they have a double density at the intersected chaotic vertices.

If any two chaotic graphs with density variation are intersected in more than one edge, then both the adjacent and incidence matrices representing that intersection are not zero matrices and they are not sub matrices of those representing the given two chaotic graphs such as the case of the intersection of two geometric graphs and the total density of the intersected graph will be reduced as it is a sub-graph of the two graphs, while it is increased in the intersected area.

The intersection of two chaotic graphs with density variation common in more than one edge and vertex resulted more extremer density in the intersected area as the total density will be reduced as it is a sub-graph of the intersected two graphs and both the adjacent and incidence matrices of the intersection of those graphs are not sub matrices of those representing the given two multiple chaotic graph.

In future work, more advanced study on chaotic graphs will be discussed such as the unfolding transform and how it effects on the density value of the chaotic graph. Moreover; a comparison study will be discussed between the un-folding and folding transform which had been studied in previous paper.

List of Abbreviations:

d	density
$A_h(G)$	Adjacency matrix of chaotic graph
$I_h(G)$	Incidence matrix of chaotic graph
h	An index represents chaotic graph
G	graph
G_h	Chaotic graph

REFERENCES:

[1] J.L. Gross,and T.W .Tucker, Topological Graph Theory, John Wiley & Sons Inc. Canada 1987.
[2] M. El-Ghoul, A. El-Ahmady, and T. Homoda, On chaotic graphs and applications in physics and biology, Chaos Solutions and Fractals, 27, No.1, UK, January (2006) 159-173.
[3] M. EL-Ghoul, A. EI- Ahmady, and T. Homoda, Retraction of simplicial complexes, International Journal of Applied Mathematics and statistics, India, 4, No. J06 (2006) 54-67.
[4] A.Gibbons, Algorithmic graph theory, Cambridge University Press, Cambridge, UK, 1995.
[5] M. Abu-Saleem, Topological folding on the chaotic edge graphs and their fundamental group, International Journal of Pure and Applied Mathematics, 119, No.12, (2018)15479-15487.
[6] A. El-Ahmady, and H. M .Shamara, Fuzzy deformation retract of fuzzy horospheres, Indian Journal of Pure & Applied Mathematics, 32, No.10, October (2001)1501-1506.
[7] R.J. Wilson, Introduction to graph theory, Oliver & *Boyed, Edinburgh, 1972.*
[8] S. Nada, and E.EL- Shafey, Chaotic graph an the sphere, British Journal of Mathematics & Computer Science, 10(3), No.BJMCS.18791, January (2015) 1-27
[9] M. Abu-Saleem, Folding on the chaotic graph operations and their fundamental group, October 25th 2019, DOI: 10.5772/intechopen.88553.
[10] M. El-Ghoul ,H. Ahmed, and M. M. Khalil, Algorithm on tape graph and their geometric transformations, International Journal of Applied Science and Technology, 3,No.5,May (2013) 45-52.
[11] F. M. Alogab, Folding Simple chaotic graphs with density variation, Journal of Humanities and Applied Science (JHAS) ,2, No. 29, December (2016) 56-73.

ARID Journals

ARID International Journal for Science and Technology (AIJST)
ISSN: 2662-009X

Journal home page: http://arid.my/j/aijst

مَجلةُ أُريد الدَّوليةُ للعُلومِ والتِّكنولوجيا

العدد 7 ، المجلد 4 ، حزيران 2021 م

CLINICAL STUDY TO EVALUATE THE RETENTION OF LOWER COMPLETE DENTURES WITH DIFFERENT TECHNIQUES

NARIMAN YASSIN MARAKA

DEPARTMENT OF REMOVABLE PROSTHODONTICS. FACULTY OF DENTISTRY. HAMA UNIVERSITY, HAMA, SYRIA

دراسة سريرية لتقييم ثبات أطقم الأسنان الكاملة السفلية بتقنيات مختلفة

ناريمان ياسين مرقا

قسم التعويضات المتحركة – كلية الأسنان - جامعة حماه- حماه – سوريا

dr.nmaraka@gmail.com
arid.my/0005-6196
https://doi.org/10.36772/arid.aijst.2021.472

ARTICLE INFO

Article history:
Received 22/01/2021
Received in revised form 10/03/2021
Accepted 19/05/2021
Available online 15/06/2021
https://doi.org/10.36772/arid.aijst.2021.472

ABSTRACT

The retention of the lower denture, was one of the most important factors for success the complete dentures (CD) for edentulous patients with resorbed mandibular ridge. Therefore, this study was conducted to compare the retention of the lower complete denture for patients with full resuscitation treated by traditional complete denture and denture manufactured by silicon materials. The studied sample consisted of (12) patients (5 males and 7 females) between the ages of (55-71) years, with an average age of (63) years. Two lower dentures were made in two different ways: the conventional method and the silicon material method opposite to one upper whole denture. The retention of the lower denture was measured on the digital forces meter when the dentures was delivered to the patient. Three readings were recorded for each technique.

The results showed a difference in the retention of the lower denture. The retention value by Newton (N) In set of lower manufactured using silicon materials of the lower denture were (7.03) higher in the set of lower denture manufactured in the traditional way.

Keywords: adsorbed alveolar mandibular ridge, CD, conventional method, silicon material, retention of dentures.

الملخص

يعتبرُ ثبات الطقم السّفليّ من أهم عوامل نجاح أطقم الأسنان الكاملة Complete denture (CD) لدى مرضى الدّرد الكامل ذوي الارتفاع السّنخي السّفليّ الممتص، لذلكَ تمَّ إجراءُ هذَا البحثِ لمقارنةِ ثبات الطقم الكامل السّفليّ عندَ مرضَى الدردِ الكاملِ المُعالجينَ بالأطقمِ الكاملةِ التقليديَّةِ والأطقم الكاملة المصنّعة بطريقة الموادّ السّيليكونيّة. تكونَت العينةُ المدروسةُ من (12) مريض درد كامِل (5 ذكور و7 إناث) تراوحَت أعمارهُم بينَ (55 -71) سنة بمتوسطِ عمرٍ (63) سنة. تمَّ صنعُ طقمين سفليين بطريقتين مختلفتين هما الطّريقة التّقليديّة وطريقة الموادّ السّليكونيّة مقابل طقم كامل علويّ واحد، وتمّ قياس ثبات الطقمين السّفليين بمقياس القوّة الرّقميّ عند تسليم الأطقم للمريض، تمّ تسجيل ثلاث قراءات لكلّ تقنيّة من التّقنيتين. أظهرتِ النتائجُ اختلاف في ثبات الطقمين السّفليين وكانت قيم قوّة الثّبات Newton (N) في مجموعة الأطقم السّفليّة المصنّعة بطريقة الموادّ السّليكونيّة أكبر بمقدار7.03 منها في مجموعة الأطقم السّفليّة المصنّعة بالطريقة التّقليديّة.

الكلماتُ المفتاحيّةُ: سنخٌ سفليٌّ ممتص، (CD)، الطّريقة التّقليديّة، الموادّ السّليكونيّة، ثبات الأطقم .

1- المقدمة:

إن تأمين ثبات CD يعتبر أحد أهم أهداف المعالجة التّعويضيّة عند مرضى الدّرد الكامل والهدف من طبّ الأسنان تعويض المريض عن الناحية الجمالية والوظيفية وتحسين الناحية الصّحية انطلاقاً من إزالة النخر حتى التعويض عن الأسنان المفقودة [1]. هذا وتعتبر الأطقم الكاملة المتحركة أجهزة ميكانيكية رئيسية تؤدي وظيفتها في الحفرة الفموية وارتداء هذه الأطقم يتناسق ويتلاءم مع وظائف الجملة العصبية العضلية وقد يكون له تأثير معاكس على الصحة الفموية والنسج الداعمة للجهاز[2].

كما أن نجاح CD يعتمد على تأمين الخصائص الثلاثة (الثبات والاستقرار والدعم) حيث تظهر الأطقم السّفليّة الكاملة للأسناخ الممتصّة صعوبة في تحقيق هذه الخصائص بسبب القيود التشريحية وتأثر ثباتها بعوامل عديدة منها: الالتصاق، اللزوجة، الضغط الجويّ، العوامل الخارجية الناشئة عن عضلات الفم والوجه [3].

1-1-الطقم السّفليّ للفكّ الأدرد الممتص:

يشكل تحديات تقنية كبيرة لطبيب الأسنان وأحياناً تطرح تحدي مهم للمريض ومع ذلك فإن المبادئ الأساسية لطبعات الطقم السفلي مشابهة لتلك الخاصة بالطقم العلوي. إن كل من مناطق الدعم والمنطقة المحيطية أو المنطقة الحدية ستكون بتماس مع سطح الطبعة أو مع الطقم المناسب المنطبق يجب أن تمتد قاعدة الطقم السفلي أبعد ما أمكن دون تداخل مع صحة أو وظيفة الأنسجة. يأتي دعم الطقم السفلي من جسم الفك السفلي ويتأمن الختم المحيطي من شكل حواف الطقم المحدد بالمناطق التشريحية الوصفية. كما أن وجود اللسان وحجمه وحركته تصعب من إجراءات أخذ طبعة الطقم السفلي ويقلل من ثباته[4].

1-2-العضلات المؤثّرة في ثبات الطقم السّفليّ:

تقسم العضلات التي تحيط بالطقم إلى مجموعتين منفصلتين:

- العضلات المزيحة للطقم: التي تؤدي إلى إزاحة الطقم من موضعه الصحيح خلال عملها.

- العضلات المثبّتة: التي تعمل على تثبيت الطقم في موضعه بوساطة الضغط المطبّق على السطوح الملمعة. كما ويمكن تقسيم هذه العضلات وفقاً لموضعها بالنسبة للطقم إلى:

- دهليزية (شفوية وخدية) – لسانية[3].

1-3-طرق أخذ الطبعات النهائية للفك السفلي الممتص:

1-3-1-الطريقة التقليدية:

يملكُ الحلُّ التعويضيُّ بطقم كَاملٍ تقليديٍّ مُصمم جيداً إيجابيةً كونهُ معالجةً قابلةً للتغييرِ عندَ وجودِ شكٍّ بقدرةِ المريضِ علَى تقبُّلِ المعالجةِ التعويضيَّةِ خُصوصاً مرضَى الدردِ الكاملِ كبارِ السنِّ ذوِي تجربةٍ سابقةٍ فِي عدمِ تحمُّلِهم للتعويضِ.

هذهِ المعالجةُ منَ المرجَّحِ أَن تكونَ ناجحةً عندَ ترافقهَا معَ حافةٍ سنخيَّةٍ جيدةٍ وعلاقةٍ فكيةٍ طبيعيَّة وعندَ الحاجةِ لتحسينِ الوظيفةِ أَو الناحيَةِ التجميليَّةِ للمريضِ.

1-3-1-1-العواملُ المؤثرَةُ فِي الطريقة التقليديَّةِ :

تحتاج هذه الطريقة خِبرةٌ سابقَةٌ جيدةٌ عند تصميم و تصنيع الأَطقم الكاملَة، واستقرارٌ كافٍ يتعلق بشكلِ السَنخ وتتميز بالمعالجَة البسيطَة والتكلفَة الأقَل والتخلُّصُ منَ الجراحَة.[5]

1-3-1-2-الآثارُ السلبيَّةُ الناتجةُ عَن المُعالجةِ بالأطقم الكاملةِ التقليديَّةِ :

اِنخفَاض قوَّة العَض Bite force مِن (200-50) باوند/ إنش^2،فبعد خمس عشرة سنة من استخدام الأطقم التقليدية تنخفض قوَّة العَض إلى (6) باوند/ إنش^2،واِنخفَاض فعاليَّة المَضغ، كما إن اِستخدَامُ الأدويةِ مِن أجلِ معالجةِ الاضطراباتِ المَعِديَّةِ المِعَويَّةِ المتشكِلَة ومحدوديَّة فِي اختيارِ الأطعمَة، واِنخفَاض فِي كميَّة الأغذيَة الصحيَّة المتناولَة[2]. يستخدم في الطبعة النهائية بالطريقة التقليدية معجون الطبع Impression Paste (IP) مع طبعة حواف بمركب الطبع الأخضر العصا الخضراء بوضعية الفم المفتوح[6] وعندما تصبح الحافة السنخية الممتصة غير قادرة على تأمين الدعم وسببت انزياح الجهاز بالطريقة التقليدية والنتيجة لم تعد مرضية كان لا بد من إجراء التعديلات على الطبعات، فكانت الطرق الآتية للتغلب على هذه السلبيات:

الطّريقة المركّبة [7]، طريقة مركّب الطّبع الأخضر[8]، طريقة الطّبعة الوظيفيّة والفم مغلق[9]، طريقة الكوكتيل[10]' طريقة الموادّ السّليكونيّة[11] . تقنيات الطبعات هذه تتمتع بالصفات التالية:

يمكن التحكم بسهولة للحصول على أقصى حد من التغطية، يمكن تصحيحها بسهولة، يمكن استخدامها بدقة وتحديد انطباعات الأغشية المخاطية، يمكن استخدامها للضغط المباشر للمناطق الحاملة و السفوح المتبقية للارتفاع السنخي السفلي[12].

1-3-2-طريقة المواد السيلوكونية المرنة :

طبعة المواد المرنة (المطاط) تؤخذ بها الطبعة النهائية حيث يتم استخدام درجة لاصقة على الحدود داخل وخارج السطح الاكريلي للطابع الإفرادي ليسهل ثبات السليكون (إضافة المادة السليكونية) وهي المسماة فينيل بوليسيلوكسان حراري لوني للتشكيل الأول للطبعة مع ثبات نهائي مرن يزيد من زمن العمل في الفم، يوضع الطابع في الفم ويطلب من المريض تحريك لسانه وفقا لمعايير الانطباع. تزال الطبعة ويطبق الفينيل ذو اللزوجة المنخفضة للحصول على الدقة العالية للنسج مع وقت سريع في الصلابة[11]. وُجدت دراسات كثيرة درست تقنيّة الطّبعات وتأثيرها على ثبات الأطقم، ناقش الباحثين Murray and Darvell 1993 [13] التقنيات لعدة سنوات، ووجد لكل تقنية مزايا وعيوب تتعلق بدرجة النشاط العضلي والمنطقة التي

يحدث فيها انزياح الطقم، بالنسبة للأفراد امتصاص العظم وحدته تجعل الحصول على الثبات الجيد والاستقرار الكامل صعب لوجود العضلات بالقرب من قمة السنخ حيث سجلت التقنية الوظيفية أعلى قيمة لها من حيث متوسط الثبات. وجد الباحث Winkler 2005 [9] أن تقنيات الفم المغلق لها مزايا، وهي: توفير الوقت، استخدام الصفيحة القاعدية لأخذ الطبعة يقلل من تدخل الطبيب في الحركات. كما أن وينكلر وجد عيوباً لهذه التقنية:لا يتحكم طبيب الأسنان في حركة المريض التي قد تُنتج حدود ناقصة أو مفرطة ،مثل حركة اللسان الأمامية التي قد تغير وتشوه الحواف اللسانية للطقم. وجد الباحث Smith وزملائه 1979 [14]أن تقنية المواد المرنة سجلت ثاني أعلى قيمة لها في دراسة سابقة وتمتعت هذه التقنية بمزايا وهي: أخذ حدود الطقم في خطوة واحدة والحركة الوظيفية للمريض كانت تتم أثناء أخذ الحدود ووجد أنّ المريض لا يتحمل الحرارة الناجمة عن مركبات الطبع.

- كما أن الباحث Tan وزملائه 1996 [15] وجدوا أن مواد البولي فينيل سيلوكسان تتطلب وقتاً أقل لأخذ حدود الأطقم مقارنة مع الطريقة التقليدية.

وجد الباحث Applebaum وزملائه 1984 [11] أن المعجون الرخو هو المادة المناسبة لأخذ كامل انطباعات الفك السفلي وتحقق نتائج أفضل ووقت أقل وأقل إزعاجا للمريض والطبيب وكذلك فني الأسنان.

- وجد الباحث Praveen وزملائه 2011 [10]أن تقنية الكوكتيل تلغي عيوب وينكلر من إصابته بتأثر خلع العضلات على امتداد الطقم بشكل غير صحيح والاستفادة الكاملة من تثبيت الأنسجة الإيجابي والسلبي للأسنان.

والفك السفلي يقع في علاقة مناسبة مع الفك العلوي لتحقيق الاستقرار في علبة مخصصة ومنع النزوح الأفقي للطابع أثناء الانطباع النهائي. ومن ميزات هذا الطابع الذي يؤدي مباشرة إلى تشكيل مادة الطبع بحركات وظيفية ومن قبل العضلات ومجاوراتها من النسج على حدود قاعدة الطقم.

كما بين كلاً من الباحثين Mccord and Tyson 1997 [7] ضرورة استخدام تقنية الطبعة المركبة للانطباعات السنخية الضامرة، ووجد ميزة تسجيل موقف وظيفي للعضلات في خطوة واحدة ووقت قصير وكلفة أقل مقارنة مع مكيف الأنسجة أو مادة التبطين.

ووجد الباحثPetrie وزملائه 2005 [16] أن الطريقة التقليدية باستخدام مركب الطبع الأخضر وأكسيد الزنك والأوجينول هي المواد الأكثر شعبية للحصول على الانطباع الكامل، حيث وجدوا: إعدادها سريع استنساخ التفاصيل الدقيقة وسهلة التعامل مع عدم وجود تغيرات مهمة في الأبعاد بعد التصلب، ومساوءها كانت: وقت عمل قصير وتصلب سريع.

- وجد الباحث Yadav وزملائه 2014 [17] في دراسة له أن الطريقة التقليدية أظهرت أقل قيمة ثبات مقارنة مع خمس طرق أخرى بينما احتلّت طريقة الموادّ السليكونيّة المرتبة الثّانية فيها.

- دعى الباحث Tan وزملائه ببداية 2009 [18]إلى استخدام الانطباع الوظيفي باستخدام المواد المرنة (السيليكونية) التي تحد هذه الطريقة من الطريقة التقليدية.

الهدف من البحث:

هو مقارنة ثبات الأطقم الكاملة السفلية بالطريقة التقليدية وطريقة المواد السيليكونية عند مرضى الدرد الكامل، الّذين يعانون من نقص ثبات الطقم السّفليّ بسبب الامتصاص السّنخيّ.

2-المواد والطرائقُ :

انتقاءُ المرضَى: تكونَتْ عيّنةُ الدراسةِ مِن 12 مريضا ومريضة درد كامِل منَ المرضَى المُراجعين لقسمِ التعويضاتِ السنيّةِ المتحرِّكةِ فِي كليّةِ طبِّ الأسنانِ - جامعةِ حماة. وقَد اِعتُمدَت بطاقةُ التشخيصِ الموجودة فِي قسمِ التعويضاتِ السنيَّةِ المُتحرِّكةِ أثناءَ الفحصِ السريريِّ الفمويِّ للمرضَى، وتمَّ إجراءُ الفحصِ الشعاعيِّ للصورِ البانوراميَّة .الشّكل(1) وَقد تـمَّ اِنتقـاءُ أفرادِ العيّنـةِ بناءً علَى اِســتمارةٍ تشـخيصيَّـةٍ خاصّـةٍ لهذَا البحــثِ .

وفقاً لتوافُرِ معاييرِ الإدخال التاليةِ:

دردٌ كاملٌ عُلويٌّ وسفلِي، للمريضِ قدرةٌ كافيةٌ علَى الفهمِ والإجابةِ علَى الأسئلةِ المطروحةِ عليهِ، أنْ يكونَ المريضُ قادراً علَى الإتصالِ والتردِدِ إلَى الباحِث، متطلباتُ المريضِ ورغباتُه قليلةٌ تتعلَّقُ في المقامِ الأوَّلِ بثباتِ الطقمِ الكاملِ السُفلي، المريضُ لا يستطيعُ تحمّل المعالجةِ بالزّرعات. المريضُ على علمٍ بالبحثِ و الموافقةُ قد أخذت منهُ .

2-1-المرحلةُ التعويضيَّةُ (صنعُ الأطقم الكاملَة):

تمَّ إنجازُ كافةِ المراحلِ السريريَّةِ للتعويضِ مِن قبلِ الباحثِة نفسِها ولكلِّ مرضَى العينةِ فِي عيادةِ التعويضاتِ السنيّةِ المُتحرّكةِ " الدراسَات العُليا"، كليّةُ طبِّ الأسنانِ - جامعةُ حماة .

كَما تمَّ إنجازُ المراحِل المخبريَّةِ المُتعلّقَة بطبخِ الأطقم عندَ فنِّي أسنَان لجميعِ أفرادِ العيِّنةِ، وقَد تمَّ اتباعُ جميعِ الخُطواتِ نفسهَا لكلِّ مرضَى العينَة.

2-2-المراحل السريريّة المتبعة لصنع الأطقم الكاملة :

- فك سفلي أدرد _ الشكل (2) - .
- سُجِّلَت الطبعاتُ الأوليَّةُ للفكينِ العُلويِّ والسفليِّ بِاستخدامِ الألجيناتِ –الشّكل (3) - .

- ثمَّ صُبَّت الطبعاتُ الأوليّةُ بِاستخدامِ الجبسِ السنيِّ للحُصولِ علَى الأمثلةِ الأوليَّةِ العُلويَّةِ والسفليّةِ –الشّكل (4)- .
- قُمنَا بصُنعِ جميعِ الطوابعِ الإفراديَّةِ العُلويَّةِ والسفليَّةِ علَى الأمثلةِ الأوليَّةِ الناتجةِ بِاستخدامِ راتنج Polymethyl methacrylate (PMMA) –الشّكل (5)- .
- بحيث حصلنا على طابعين إفراديين سفليين تمّ صنعهما على نفس المثال الجبسيّ الأوليّ .
- بعدَ فحصِ الطوابعِ الإفراديَّةِ فِي فمِ المريضِ، تمَّ أخذُ طبعةِ الحوافِّ العُلويَّةِ والسفليَّةِ لجميعِ أفرادِ العيّنةِ بِاستخدامِ شمعِ الحَوافِKerr للطّريقة التّقليديّة-الشّكل(6)- .
- تمَّ تهيئةُ الطابعِ الإفراديِّ مِن أجلِ الطبعةِ النهائيَّةِ للطّريقة التّقليديّة-الشّكل(7)- .
- قُمنَا بِاستخدامِ معجونِ الطبعِ أُكسيدِ الزنكِ والأوجينولِ Impression Paste (IP)لتسجيلِ الطبعَاتِ النهائيَّةِ للطّريقةِ التّقليديّة-الشّكل(8)- .

بالنّسبةِ لطريقةُ الموادِّ السّيليكونيّة**:** تؤخذ طبعة الفكّ السّفليّ كالآتي:

- يطبّق الّلاصق على حدود الطّابعِ الإفراديّ من الدّاخلِ والخارج لتأمين ثبات مادّة الطّبع مع الطّابع الإفراديّ.
- تمّ تطبيق المادّة السليكونية المرتفعُة اللّزوجة لأخذ طبعة الحوافّ ويطلب من المريض إجراء كامل الحركات الوظيفيّة وشدّ الخدود والشّفاه في آن واحد –الشّكل(11و12و13)- .
- بعد ذلك تطبق المادّة السليكونية المنخفضة اللّزوجة باستخدام جهاز خاص لحقن المادّة وفق معايير ثابتة -الشّكل(14)- .
- يتمُّ الحصولُ على طبعتين نهائيتين سفليتين بطريقتين مختلفتين مع طبعةٍ علويّةٍ واحدة .
- تمَّ تعليبُ جميعِ الطبعاتِ النهائيَّةِ وصبّهَا بِاستخدامِ جبسِBagostone، وتمَّ الحصولُ علَى الأمثلةِ النهائيّةِ العُلويّةِ والسُفليّةِ –الشّكل(9)- .
- ثمَّ صُنعَت الصفائحُ القاعديَّةُ بِاستخدامِ راتنج (PMMA).
- وَقُمنَا بصنعِ الإرتفاعاتِ الشمعيَّةِ –الشّكل(17و18)- .
- تمَّ تحديدُ المُستوياتِ الإطباقيَّةِ الأماميَّةِ والخلفيَّةِ سريريَّاً، ثمَّ تمَّ تحديدُ البُعدِ العموديِّ الإطباقيِّ Vertical Dimension Occlusion (VDO)-الشّكل(19)- .
- سُجِّلَتْ العلاقَة الفكيَّةُ المركزيّةُ Centric Relation(CR) لكلِّ مريضٍ وتمَّ اِستخدامُ المعجونِ اللاصقِ Bony Plus مِن أجلِ تثبيتِ الصفائحِ القاعديَّةِ أثناءَ أخذِ العلاقةِ المركزيَّة.

- كَما تمَّ اِستخدامُ القوسِ الوجهيِّ Hanau ear face Baw فِي نقلِ العلاقةِ الفكيَّةِ الخلفيّةِ إلَى مطبقٍ نصفِ مُعدَّلH2HANO-الشّكل(22)- .
- تمَّ اِختيارُ الأسنَانِ الاِصطناعيَّةِ الأكريليَّةِ Major وتمَّ تنضيدُهَا لجميعِ الأطقم مِن قبلِ الباحثِ نفسهِ وبِاستخدامِ أسلوبِ التنضيدِ نفسهِ، حيثُ تمَّ اِختيارُ الأسنانِ الستَّةِ الأماميَّةِ العُلويَّةِ والسفليَّةِ بحيثُ تحققُ الناحيةَ التجميليَّةَ للمريضِ، وتمَّ تنضيدُ الأسنانِ الخلفيّةِ بالإطباقِ المُتوازنِ ثُنائيِّ الجانِب-الشّكل(24)- .
- تمَّت مرحلةُ التجربةِ السريريَّةِ وقُمنَا بإزالةِ الإعاقاتِ الإطباقيّةِ والتأكُّدِ منَ (VDO) و(CR) وفحصِ الناحيةِ التجميليَّة.
- تمَّتْ مرحلةُ التشميعِ للجهازينِ العُلويِّ والسُفليِّ لكلِّ مريضٍ، ومِنْ ثُمَّ طُبخَتْ الأطقم.
- تمَّ إنهاءُ الأطقم وَتلميعُهَا وتسليمُهَا إلَى المريضِ .
- ملاحظة: يتمُّ طبخُ الطقمين السّفليين بكلا الطّريقتينِ في ظلِّ ظروف طبخٍ واحدة، نفسَ مزيجِ PMMA المعدُّ للطّبخِ، والضّغطُ متماثِلٌ أثناءَ الطّبخِ، وأثناءَ تّنزيل الأطقم في البواتق المعدنيةِ تجنّباً لفوارقَ مخبريّةٍ قد تؤثّرعلى ثباتِ الأطقم، لذلك تمّ توحيد شروطِ إعداد الأطقم.

2-3-قياس ثبات الأطقم: يتمّ بعدها فحص الدّعم والثّبات والاستقرار لكلا الطقمين في فم المريض للمقارنةِ بينَ الأطقم. تمَّ استخدام مقياس القوّة الرّقميّ الّذي استخدمه الباحث Burns وزملائه 1995 [19] حيث يوضعُ المريضُ على الكرسيّ السّنّيّ و ظهرهُ على استقامة والرّأس مشدود إلى مسندِ الكرسيّ. يوضعُ الطقم السّفليّ في فمِ المريضِ يوضعهِ الصّحيحِ واللسان في وضعهِ السّلبيّ في أرضِ الفم بحيثُ تمسُّ حوافّهُ السّطوحَ اللسانيةِ لأسنانِ الطقم. يتمُّ تثبيتِ الحلقةِ المعدنيّةِ ذات القطرِ (5مم) بحيثُ يتناسبُ هذا القطر مع قطرِ خطّافِ مقياسِ القوّة على مركز السّطوحِ اللسانيّةِ للثنايا السّفليّةِ. يتمُّ وضعُ خطّافِ الجهازِ ضمنَ الحلقةِ المثبّتةِ و تطَبّقُ قوّةٌ ضاغطةٌ عموديّةٌ لإزاحةِ الطقم السّنّيّ السّفليّ والمريضُ جالسٌ باستقامةٍ والسّطوحُ الإطباقيّةِ للطقمِ السّنّيّ السّفليّ موازية لمستوى الأرضِ. يتمُّ تسجيلُ ثلاثُ قراءاتٍ لكل طريقة منهما من قبلِ ثلاثة أخصّائيين(كل أخصائيّ قراءة) في قسم التّعويضاتِ السّنيّةِ في كلّيّةِ طبِّ الأسنان في حماه تلافياً للخطأ البشريّ. يبلغُ مقدارَ القوّةِ المطبّقةِ من المقياسِ حتّى 196 N-الشّكل(28)- .

الشّكل(1): صورة شعاعيّة

الشكل(2): فكٌّ سفليٌ

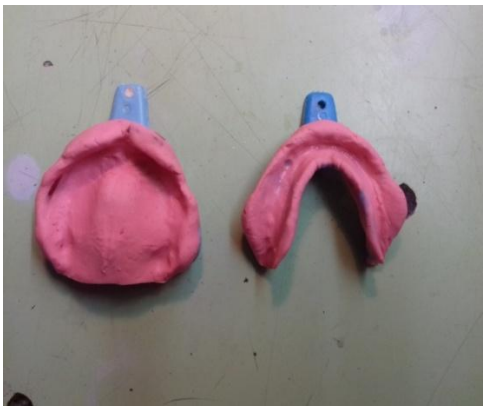

الشّكل(3): الطبعات الأوّلية

الشكل(4): الأمثلة الأوليّة

الشّكل(5): الطوابع الإفراديّة

الشكل(6): طبعة الحواف بالطّريقة التّقليديّة

الشّكل(7): تهيئة الطّوابع للطّريقة التّقليديّة

الشّكل(8): الطّبعة النّهائية للطّريقة التّقليديّة

الشّكل(9): الأمثلة النّهائيّة للطّريقة التّقليديّة

الشّكل(10): تطبيق لاصق المادّة السّليكونيّة

الشّكل(11): كمّيتان متساويتان من الموادّ السّليكونيّة

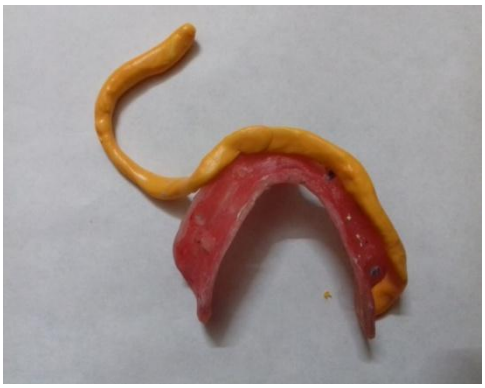

الشّكل(12): تطبيق المادّة مرتفعة اللزوجة

الشّكل(15): مثالٌ جبسيّ نهائي لطبعة الموادّ السّليكونيّة

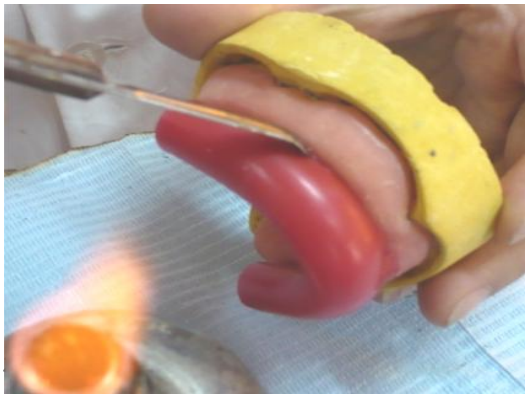

الشّكل(16): صنع الارتفاع الشّمعيّ

الشّكل(17): الصّفائح مع الارتفاعات الشّمعية بالطّريقة التّقليديّة

الشّكل(18): الصّفيحة مع الارتفاع الشّمعيّ بطريقة الموادّ السّليكونيّة

الشّكل (19) : تسجيل العلاقة الفكّيّة

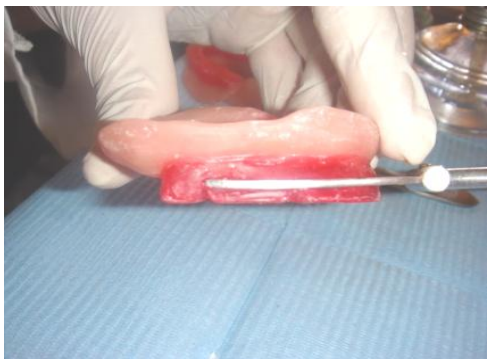

الشّكل (20) : تثبيت الشّوكة للارتفاع الشّمعيّ العلويّ

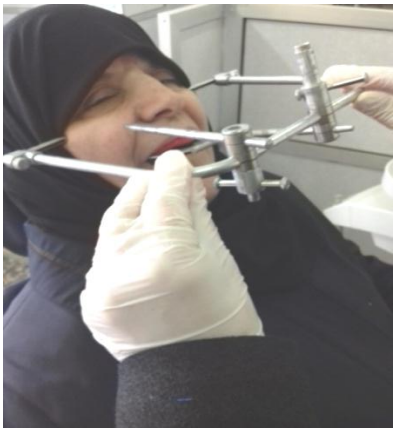

الشّكل(21) أ: نقل العلاقة باستخدام القوس الوجهيّ

الشّكل(22): نقل العلاقة باستخدام القوس

الشّكل(24): تنضيد الأسنان

الشّكل(23): تثبيت الأمثلة في مطبق هانو

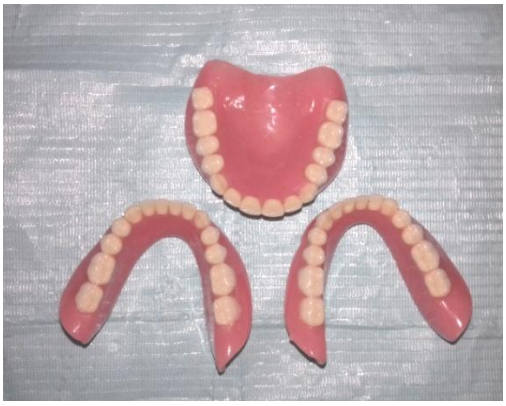

الشّكل(25): طقمين سفليين مقابل جهازٍ واحدٍ علويّ

الشّكل(26): تثبيت الحلقات المعدنيّة للطقمين السّفليين

الشّكل(27): وضع الطقم مع الحلقة في فم المريض

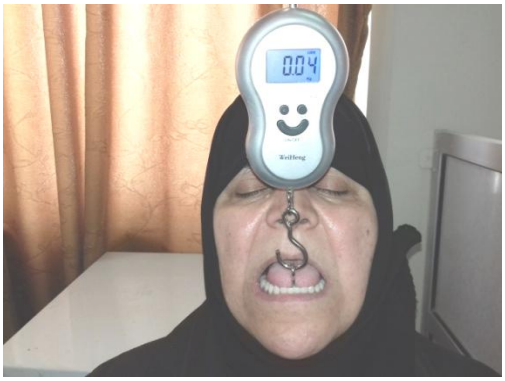

الشّكل(28): قياس ثبات الطقم

3-الدّراسة الإحصائيّة:

- دراسة تأثير طريقة تصنيع الطقم المتبعة في قيم مقدار قوة الثبات في عينة البحث:

تم إجراء اختبار T ستيودنت للعينات المستقلة لدراسة دلالة الفروق في متوسط مقدار قوة الثبات (N) بين مجموعة الأطقم السفلية المصنّعة بطريقة الموادّ السيليكونية ومجموعة الأطقم السفلية المصنّعة بالطريقة التقليدية في عينة البحث كما يلي:

- إحصاءات وصفية: جدول رقم (1) يبين المتوسط الحسابي والانحراف المعياري والخطأ المعياري والحد الأدنى والحد الأعلى لمقدار قوة الثبات (N) في عينة البحث وفقاً لطريقة تصنيع الطقم المتبعة.

جدول(1): يبين المتوسط الحسابي والانحراف المعياري والخطأ المعياري

المتغير المدروس = مقدار قوة الثبات (بالنيوتن)						
طريقة تصنيع الجهاز المتبعة	عدد الأجهزة	المتوسط الحسابي	الانحراف المعياري	الخطأ المعياري	الحد الأدنى	الحد الأعلى
جهاز سفلي مصنّع بطريقة الموادّ السيليكونية	12	11.43	1.27	0.37	8.92	14.27
جهاز سفلي مصنّع بالطريقة التقليدية	12	4.40	0.69	0.20	3.20	5.39

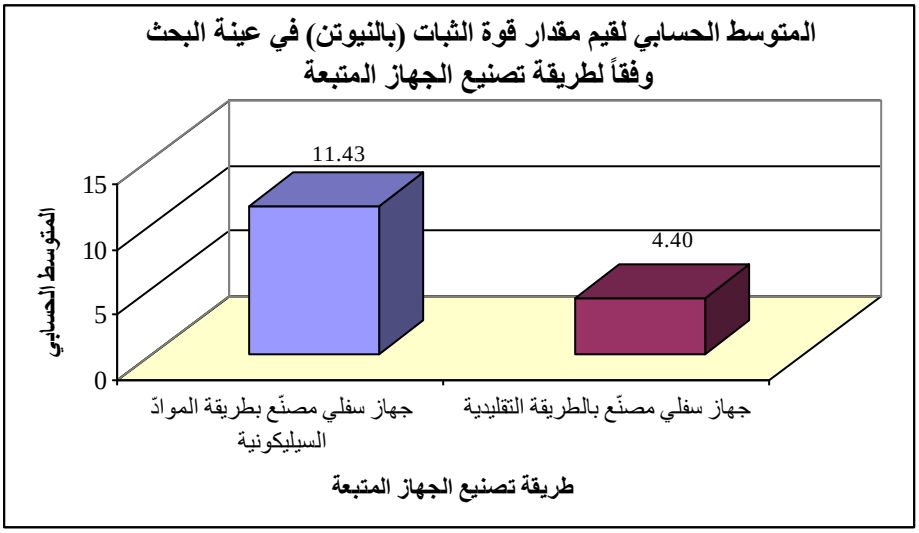

مخطط رقم (1): يمثل المتوسط الحسابي لمقدار قوة الثبات (N) في عينة البحث وفقاً لطريقة تصنيع الطقم المتبعة.

- ***نتائج اختبار T ستيودنت للعينات المستقلة:***

جدول رقم (2) يبين نتائج اختبار T ستيودنت للعينات المستقلة لدراسة دلالة الفروق في متوسط مقدار قوة الثبات (N) بين مجموعة الأطقم السفلية المصنّعة بطريقة الموادّ السيليكونية ومجموعة الأطقم السفلية المصنّعة بالطريقة التقليدية في عينة البحث.

جدول(2): يبين نتائج اختبار T ستيودنت للعينات المستقلة

المتغير المدروس = مقدار قوة الثبات (N)					
قيمة t المحسوبة	درجات الحرية	الفرق بين المتوسطين	الخطأ المعياري للفرق	قيمة مستوى الدلالة	دلالة الفروق
16.838	22	7.03	0.42	0.000	توجد فروق دالة

يبين الجدول أعلاه أن قيمة مستوى الدلالة أصغر بكثير من القيمة 0.05، أي أنه عند مستوى الثقة 95% توجد فروق دالة إحصائياً في متوسط مقدار قوة الثبات (N) بين مجموعة الأطقم السفلية المصنّعة بطريقة الموادّ السيليكونية ومجموعة الأطقم السفلية المصنّعة بالطريقة التقليدية في عينة البحث، وبدراسة قيم المتوسطات الحسابية نستنتج أن قيم قوة الثبات في مجموعة الأطقم السفلية المصنّعة بطريقة الموادّ السيليكونية كانت أكبر منها في مجموعة الأطقم السفلية المصنّعة بالطريقة التقليدية في عينة البحث.

4-المناقشة:

هذه الدراسة هي دراسة تطلعية سريرية لتقييم ثبات الأطقم الكاملة السفلية لمرضى الدرد وتأثير تقنية الطبعة النهائية المستخدمة والمقارنة بينهما. إن تأمين ثبات CD يعتبر أحد أهم أهداف المعالجة التّعويضيّة عند مرضى الدّرد الكامل والهدف من طبّ الأسنان هو تعويض المريض عن الناحية الجمالية والوظيفية وتحسين الناحية الصّحية انطلاقاً من إزالة النخر حتى التعويض عن الأسنان المفقودة[1] .واستخدمنا طريقة المواد السيليكونية (فينيل بوبي سيلوكان) الطابعة المعروفة بالسيليكون بتفاعل الإضافة لأنها أصبحت واسعة الانتشار خلال السنوات الأخيرة[20] ولقد استخدم النوع منخفض اللزوجة لهذه المادة عبر جهاز الحقن (المزج الآلي) بدلاً من المزج اليدوي وذلك للأسباب الآتية:

تمازج لوني جيد للأساس والمسرع، إدخال كمية هواء أقل إلى المزيج، إنقاص زمن المزج، احتمال تلوث أقل للمادة الطابعة[21] وتم استخدام الطريقة التقليدية للمقارنة مع طريقة المواد السليكونية كونها الطريقة الأكثر شعبية في دول العالم وتستخدم مركب طبع الحواف مع مركب أوكسيد الزنك والأوجينول. والتي تبدي عدم وجود تغييرات مهمة في الأبعاد بعد التصلب واستنتاج التفاصيل الدقيقة[9]. وعادة تؤخذ طبعات الحافة السنخية بالطريقة التقليدية أو طريقة المواد السليكونية وذلك بسبب الدقة الكامنة في هذه المواد وتوزيع الضغط المتوازن[22]. وبدراسة قيم المتوسطات الحسابية نستنتج أن قيم قوة الثبات (N) في مجموعة الأطقم السفلية المصنعة بطريقة المواد السيليكونية كانت أكبر منها في مجموعة الأطقم السفلية المصنعة بطريقة المواد التقليدية بمقدار قدره 7.03 نيوتن.

وتتّفق هذه النّتيجة مع دراسة كلٍّ من الباحثين Yadav 2014 [17] و Massad 2005 [23] و van Noort 2007 [24] فقد أصبحت تقنية استخدام السليكون العالي ومنخفض اللزوجة منتشرة بين أطباء الأسنان وتم تطوير هذه التقنية لما لها من مزايا حيث أنها تزيد من دقة الطبعة بتغلبها على تغير الأبعاد الكبير لأن معظم التقلص الحاصل أثناء عملية التبلمر (التقلص التصلبي) يحدث في النوع مرتفع اللزوجة فقط وبالتالي تكون الطبعة أكثر ثباتاً في الأبعاد، كما أنّ طريقةَ الموادّ السّليكونيّة تفوّقت على الطّريقة التّقليديّة حيث إن الانطباع الوظيفيّ باستخدام السّليكون يحدّ من استخدام مركّب طبع الحواف و IP [9,18] .

علماً أن الكثير من الدراسات أكدت أن العامل الأساسي لتأمين ثبات الأطقم السفلية الكاملة يتحقق بالتناسق العصبي العضلي مع استخدام تقنية المنطقة المحايدة [25]. وأن التقنية التقليدية كانت أقل ثبات من تقنية الطبعة الوظيفية بمقدار 8 N [26] . وغالبا ما تحتاج أطقم الأسنان السفلية الكاملة ذات الأسناخ شديدة الامتصاص إلى الجمع بين تقنيتين تقنية الانطباع الوظيفي و تقنية الانطباع المركب ومع ذلك هناك حاجة لدراسات أخرى لمعرفة التقنية الأفضل [27] .

5-الاستنتاجات :

ضمن حدود هذه الدراسة السريرية يمكن استخلاص الاستنتاجات الآتية:

1 - أبدى ثبات الطقم الكامل السفلي بطريقة المواد السيليكونية تفوقاً على الطريقة التقليدية لدى مرضى الدرد الكامل الذين يعانون من مشاكل في ثبات واستقرار الطقم السفلي.

التوصيات

1 - نوصي أن تكون طريقة المواد السيليكونية الطريقة المعتمدة في الكليات وذلك لسهولة المراحل السريرية لها وسهولة تطبيقها من قبل الطالب.

2 - نوصي باستخدام طريقة المواد السيليكونية لتوفير الوقت لطبيب الأسنان والمريض .

المقترحات

1 - إجراء دراسة سريرية لمقارنة ثبات الأطقم بعد فترة من استخدامها.

2 - إجراء دراسة سريرية مشابهة مع زيادة حجم العينة للوصول إلى نتائج أكثر دقة ودراسة متغيرات أخرى (مثل فعالية المضغ).

جدول بالمختصرات

ت	الاسم العلمي	المختصرات
1	Complete denture	CD
2	Newton	N
3	Impression Paste	IP
4	Polymethyl methacrylate	PMMA
5	Vertical Dimension Occlusion	VDO
6	Centric Relation	CR

المصادر:

[1]- E.Raviv, A. Turcotte, and M. Harel-Raviv, " Short dental implants in reduced alveolar bone height", *Quintessence international*, 41(2010) 575–579..

[2]- G. E. Carlsson, "Clinical morbidity and sequelae of treatment with complete dentures", *Journal of Prosthetic Dentistry*,79(1) (1998) 17–23.

[3]- K. Shay. Treatment of an edentulous patient with a dry mouth. *The Journal of Contemporary Dental Practice* ,1(2000)98.

[4]- C. Whitmyer, S. J. Esposito, and S. Alperin, "Longitudinal treatment of a severely atrophic mandible: a clinical report", J. *of Prosthetic Dentistry*,90(2) (2003) 116–120.

[5] -J.A. Hobkirk, R.M. Wotson, L .J. Searson, Introduction Dental Implants.6th ed, *Elsevier Science*, (2003) 63-79.

[6]- W. Greene J, Greene Brothers, "Clinical Course in Dental Prosthesis in Three Printed Lectures. New and Advanced-Test Methods in Impression", Articulation, Occlusion, Roofless Dentures, Refits and Renewals, *Detroit Dental Manufacturing Company*, Detroit, Mich, USA, 1916.

[7]- J. F. McCord and K. W. Tyson, "A conservative prosthodontic option for the treatment of edentulous patients with atrophic (flat) mandibular ridges", *British Dental Journal*,182(12)(1997) 469–472.

[8]-A. Tunkiwala and S. Ram, "Management of mandibular poor foundation: conventional complete dentures", *Dental Practice*,11(5) (2013) 34–37.

[9]-W.E.Winkler, "Re-identification methods for evaluating the confidentiality of analytically valid microdata", *Statistics*,9 (2005) 1-14.

[10]- G. Praveen, S. Gupta, S. Agarwal, and S. K. Agarwal, "Cocktail impression technique: a new approach to atwood's order vimandibular ridge deformity", *Journal of Indian Prosthodontist Society*,11(1)(2011) 32–35.

[11]- E. M. Applebaum and R. V. Mehra, "Clinical evaluation of polyvinylsiloxane for complete denture impressions", *The Journal of Prosthetic Dentistry*,52(4) (1984) 537–539.

[12]-V. C. Petropoulos and B. Rashedi, "Current concepts and techniques in complete denture final impression procedures", *Journal of Prosthodontics*,12(4) (2003) 280–287.

[13]- M.D. Murray, and B.W. Darvell, "The evolution of the complete denture base. Theories of complete denture retention—a review. Part 1", *Australian dental journal*,38(3) (1993) 216-219 .

[14]- D. E. SMITH, L. B. TOOLSON, C. L. BOLENDER, LORD, "One-step border molding of complete denture impressions using a polyether impression material", *Journal of Prosthetic Dentistry*,41(3) (1979) 347-351.

[15]- H.K. Tan, P.M. Hooper, and C.G, "Baergen, Variability in the shape of maxillary vestibular impressions recorded with modeling plastic and a polyether impression material", *International Journal of Prosthodontics*, 9(3) (1996)22.

[16]- C.S. Petrie, M.P. Walker, and K. Williams, "A survey of US prosthodontists and dental schools on the current materials and methods for final impressions for complete denture prosthodontics", *Journal of Prosthodontics: Implant, Esthetic and Reconstructive Dentistry*,14(4)(2005) 253-262.

[17]- B.Yadav, M. JAYNA, S. SURI, S. PHOGAT, R. MADAN, "Comparison of different final impression techniques for management of resorbed mandibular ridge: a case report", *Case reports in dentistry*, 2014.
[18]-K.M. Tan, M.T. Singer,R. Masri , C. F. DRISCOLL , "Modified fluid wax impression for a severely resorbed edentulous mandibular ridge", *J Prosthet Dent*,101(2009)279-28.
[19]- D. R. Burns, J. W. Unger, R. K. Elswick Jr., and D. A. Beck, "Prospective clinical evaluation of mandibular implant overdentures: part I-retention, stability, and tissue response", The *Journal of Prosthetic Dentistry*, 73(4) (1995) 354–363.
[20]- W.W.L Chee, Donovan TE. Polyvinyl siloxane impression materials, "A review of properties and techniques", *The Journal of Prosthetic Dentistry*,68(1992)728-32.
[21]- R. CRAIG, George,'S Restorative Dental Materials 12th edition, *Mosby*, (2006) 283-303.

[22] T. E. Jacobson and A. J. Krol, "A contemporary review of the factors involved in complete dentures. Part II: stability", *The Journal of Prosthetic Dentistry*,49 (2) (1983)165–172.
[23]- J.MASSAD, W. DAVIS,J. THORNTON, "Improving the Stability of maxillardentures:the use of polyvinyl siloxsan impression materials for edentulous impressions", *Dent Today*,33(21)(2005)24-6.
[24]-R.Van Noort, Introduction To Dental Materials, 3rd -E-Book, *Elsevier Health Sciences*,(2007) 186-207.

[25]-P.Shah, , R.K. Singh, and P. Suwal, "Stability-A Key To Success Using Neutral Zone Technique: A Case Report", *Guident*, 13(9)(2020).

[26]- N. Singh, G. Kaur, and K. Kaur, "Comparison of two impression techniques for secondary impression for complete denture", *Journal of Advanced Medical and Dental Sciences Research*, 6 (2018)9 .

[27]- S.Dash, S. Gunjan , S. Monika , "Management of Mandibular Resorbed Ridges by Combining Two Impression Techniques: A Literature Review and Case Report", *Indian Journal of Public Health Research & Development*,10 (9)(2019)1678-1683.

ARID Journals

ARID International Journal for Science and Technology (AIJST)
ISSN: 2662-009X

Journal home page: http://arid.my/j/aijst

مَجلةُ أُريد الدَّوليةُ للعُلومِ والتِّكنولوجيا

العدد 7 ، المجلد 4 ، حزيران 2021 م

Modification the Hysteresis Method of the Stator Currents Controller to SVM for Improving the Performance of the PMSM

Hamdy Mohamed Soliman

Department of Electrical Power and Machine Engineering, Faculty of Engineering,

Misr University for Science and Technology, 6th October Giza Egypt,

تعديل طريقة التباطؤ في تيار العضو الثابت الى المتجهات الفراغية المعدلة لتحسين أداء المحرك التزامنى ذو المغناطيس الدائم

حمدى محمد سليمان

قسم هندسة القوى والالات الكهربية – كلية الهندسة

جامعة مصر للعلوم والتكنولوجيا – 6 أكتوبر الجيزة مصر

Eldoctorhamdy70@gmail.com
arid.my/0002-4428
https://doi.org/10.36772/arid.aijst.2021.473

ARTICLE INFO
Article history:
Received 13/01/2021
Received in revised form 12/03/2021
Accepted 14/05/2021
Available online 15/06/2021
https://doi.org/10.36772/arid.aijst.2021.473

ABSTRACT

This paper aims to reduce the torque ripples in the motor torque, reduce the total harmonics distortion in the motor currents and improve the dynamic response of the permanent magnet synchronous motor. To carry out this study, a modification model was used and compared to conventional model. The main control method used here is a field-oriented control. It was used to generate two decoupled currents control. With help of rotor position, these currents changing into three-phase reference currents. These reference currents were compared to the actual three-phase motor currents. The errors among these currents are introduced to hysteresis current controller to get pulses. These pulses used to drive the voltage source inverter which produces three-phase voltage to drive the motor under study. This technique suffers from some problems as high torque ripples, high total harmonics distortion, the dynamic response isn't very high because at the beginning of the error and the deviation of the output signal becomes large. This is a conventional model. To overcome these problems, the hysteresis current controller was replaced by gain impedance. The output of this gain is the three-phase voltages. These voltages generate pulses through space vector modulation to drive the inverter to get suitable voltage for the permanent magnet synchronous motor. This modification has decreased the torque ripples and the THD in comparison to the conventional controller. To more improvement in the motor performance, one PI torque current controller and load torque estimator were used to damp the overshooting and decrease the rise time.

Keywords: Field orientated control; hysteresis current controller; PI controller; space vector modulation; THD.

الملخص

تهدف هذه الورقة الى تحسين تموجات عزم الدوران وتقليل التشوه في تيار العضو الثابت للمحرك التزامنى وتحسين الأداء الديناميكى للمحرك التزامنى ذو المغناطيس الدائم. لتوضيح ذلك دعنا نبدا بطريقة التحكم المستخدمة في هذه الورقة بدون اى اضافات ثم بعد ذلك سوف نقوم بتوضيح الإضافات التي تمت ومدى تاثيرها على الأداء. طريقة التحكم المستخدمة هنا هي التحكم بتوجيه المجال. انها تستخدم تيارين مرجعيين على محورين متعامدين اى ان اى منهما لا يؤثر على الاخر. يتم استخدام هذين التيارين مع زاوية المجال لتوليد تيارات ثلاثية الأوجه متغيرة مع الزمن. هذه التيارات المرجعية يتم مقارنتها بالتيارات الحقيقة الخاصة بالمحرك الكهربى الذى تحت الدراسة. الخطاء الناتج من هذه المقارنة يتم إدخاله الى وحدة تباطؤ التيار لتوليد نبضات تسلط على العاكس لانتاج جهد يسلط هذا الجهد المحرك الكهربى لادارته. هذا النموذج يعانى من بعض المشاكل مثل زيادة تموجات العزم وتشوهات التيار والمشاكل الديناميكية عند البدء. للتغلب على هذه المشاكل تم استبدال وحدة التحكم في التباطؤ بوحدة تسمى كسب المعاوقة. يتم ادخال الخطاء في التيار الى هذه الوحدة ويكون خرجها جهد متغير ثلاثى الأوجه الذى يتم إدخاله الى وحدة المتجهات الفراغية التي تقوم بناء على قيم هذا الجهد توليد نبضات تسلط على العاكس لانتاج جهد ثلاثى الأوجه يتم تسليطه على المحرك لادارته حيث نجد انه قد تم حدوث تحسن في تموجات العزم حيث انخفضت قيمتها وانخفض التشوه في التيار. ولتحسين الأداء الديناميكى تم إضافة وحدة تحكم تناسبى تكاملى للتحكم فى تيار العزم ونموذج حسابى لحساب عزم الحمل.

الكلمات المفتاحية: التحكم في التيار بالتباطؤ، التحكم بتوجيه المجال، التحكم التناسبي التكاملي، المتجهات الفراغية المعدلة، التشوه التوافقى الكلي.

1- INTRODUCTION

The Permanent Magnet Synchronous Motors (PMSM'S) spread in many industrial applications this because it has high efficiency, fast acceleration, and deceleration, no copper loss in the rotor, absent spark due to absent brushes, high torque to current ratio, high power to volume ratio, maintenance less and low maintenance cost.

There are many methods used to control PMSM'S. These methods can be classified into simple methods and complex methods. The simple methods as scalar control and the complex methods as vector control and direct torque control. The scalar control is favorite in the applications which don't require a high dynamic response but when this is required the vector and direct torque controls are used. Here the Field-Oriented Control (FOC) is used for this reason. The FOC appeared for the first time by Blaschke in Siemens company [1].

In FOC, the PMSM imitates the DC motor in the behavior. This can be done by splitting the resultant stator current vector in the space into two components one of them represents the flux and the other represents the torque. This can be applied by known the rotor position. To get that position sensor or encoder can be used to detect that. With constant parameters and constant load, the FOC works by good method but when the parameters change or load change, the controller will generate some errors to get rid of this problem some method of control can be used as the current control methods or voltage control methods.

Some researchers introduced effect of hysteresis current controller of the permanent magnet synchronous motors as in [2,3]. From that can be concluded that, the motor torque is highly torque ripples and the stator currents have highly Total Harmonic Distortion

(THD). Some methods of the controller used the hysteresis current to generate pulses to drive the inverter which produces three-phase voltages. These voltages were applied to the motor to drive it. Another research used AMESim software to show the advantages and disadvantages of Hysteresis Current Controller (HCC) as in [4]. The classical FOC with HCC can be seen in Fig. 1. This Fig. was represented by some of the blocks. These blocks are the main field orientation and stator current blocks, comparator block, hysteresis band block, voltage source inverter, and PMSM.

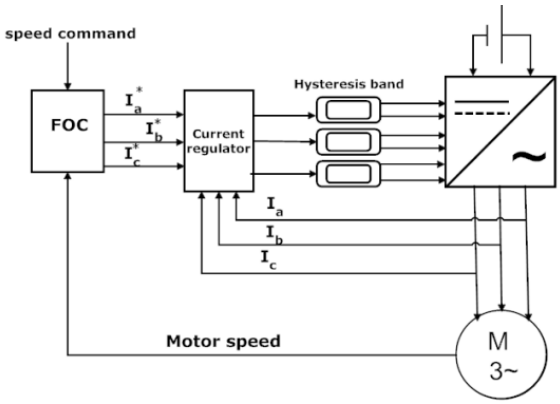

Fig. (1): Classical FOC with HCC

The inputs of the main field orientation block are reference motor speed and actual motor speed. The output of this block is the three-phase reference currents for different phases. In the comparator block, the three-phase reference currents are compared to the actual three-phase stator currents and errors introduced to the hysteresis band to generate the six pluses to drive the inverter to drive the motor. This method of switching has some drawbacks as highly distortion in the motor currents, highly distortion in the stator flux, and has more ripples in the torque. To overcome these problems, some paper design fast HCC to improve the dynamic response of FOC but the waveforms of the flux and current still have more distortion and the motor torque has high ripples as in [5]. The software was used to improve the performance of the PMSM as in [6] but it takes a very long time in calculations. P. Mamta et al [7] used a formula to adapt the hysteresis band but it doesn't

introduce more improvement in the motor current distortion and torque ripples. Hamdy Soliman, S. Hakim introduce an improvement in the THD and torque ripples with using HCC and Proportional Integrator (PI) controller but this leads to increase in the switching frequency of the inverter [8]. Some researches use the fuzzy logic controller to control in the hysteresis band to make the switching frequency of the inverter is constant this leads to some improvement in the ripples and reduces the harmonics as in [9] but these methods depend upon the learning and experiment. Also, predictive current controller is used to improve the performance of PMSM [10]. Another method to adapt the hysteresis band using fuzzy logic can be seen in [11]. Particle swarm used to improve the performance of the PMSM with HCC can be seen as in [12] but this method more complicated.

Also, some researchers used Space Vector Modulation (SVM) to improve the performance of the AC motor as in [13,14] who explains what is meant by SVM. Jacob & Chitra [15] use SVM with PI current controllers to improve the performance of the PMSM but this method suffers from slow response also, at the beginning of the error, the deviation of the output signal becomes large. Alsofyani and Lee [16] uses discrete Space Vector Modulation of PMSM without Flux Error-Sign and Voltage-Vector lookup table. In [17] SVM used with the multilevel inverter to improve the performance of the PMSM but this method has some drawbacks as using more IGBT's which make the system more complicated and has a higher cost. Haidari et al [18] uses predictive current control with SVM to improve the ripples in the motor torque and distortion in the motor currents but this method is also more complicated.

In this paper, the HCC was replaced by gain impedance. The input of the gain impedance is the error in the stator current. This error comes from comparing the reference stator current and actual stator current. The output of the gain impedance is the reference stator voltage. This reference voltage is the three-phase voltages. These three-phase voltages

were converted into two-phase voltages. These two-phase voltages used to generate six pulses to drive the inverter. The output voltage waveforms from the inverter applied to the motor to drive it. With this modification, the total harmonic distortion of the stator current will improve and the torque ripples will reduce. This modification is very good in reducing the distortion and ripples but it isn't approximately effecting the rise time, overshooting, and undershooting. This bad effect can be reduced by applying the PI torque current controller. The method was used in this paper is very simple, very fast response, reduces the torque ripples, reduces THD and improve the dynamic response. This paper can be divided into; the proposed system, a mathematical model of the three-phase induction motor, Pulse Width Modulation (PWM) control using Space Vector Modulation (SVM), simulation results, the conclusions and the recommendations.

2- Proposed System

Fig. 2 shows the proposed model to drive the PMSM. This Fig. contains some blocks. Each block has its own function. The first block is a field orientation block. it is used to generation $\chi\delta$-axes currents. This occurs through two signals (reference speed and measured speed). The measured speed has two functions. The first function is to deduce the reference flux current component through a lookup table ($i^*_{\chi s}$) and the other function is compared to the reference speed and the error between them introduced to the PI speed controller to generate the torque current component ($i^*_{\delta s}$). This occurred when the load torque is constant and this can be seen in Fig. 3 but when the load is varying the torque current component deduced by another method as in Fig. 4. From Fig. 4 can be deduced that

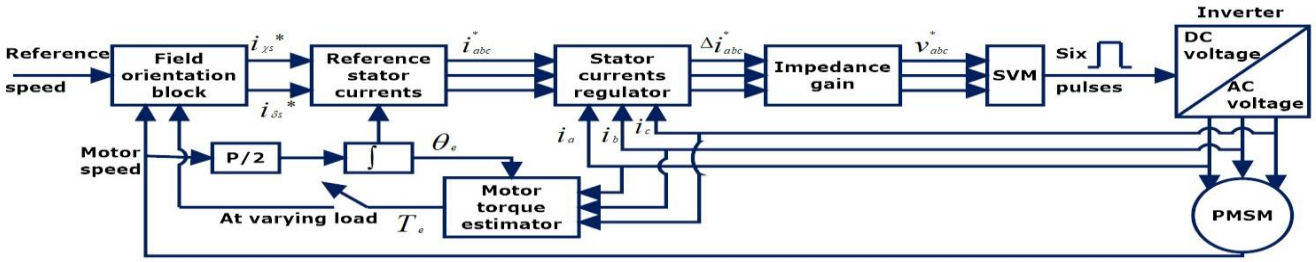

Fig. (2): Proposal model to drive the PMSM.

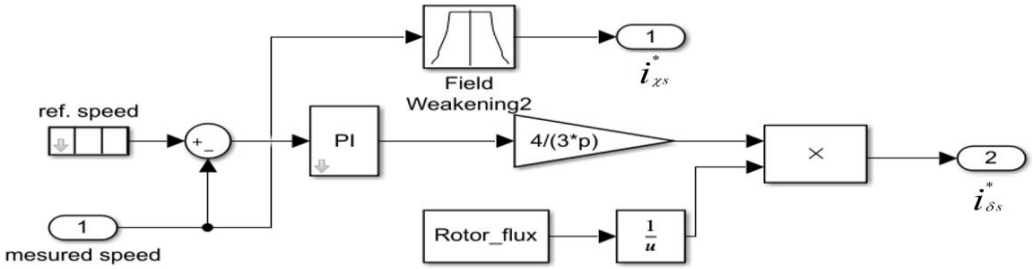

Fig. (3): Inside the field orientation block in case of constant load

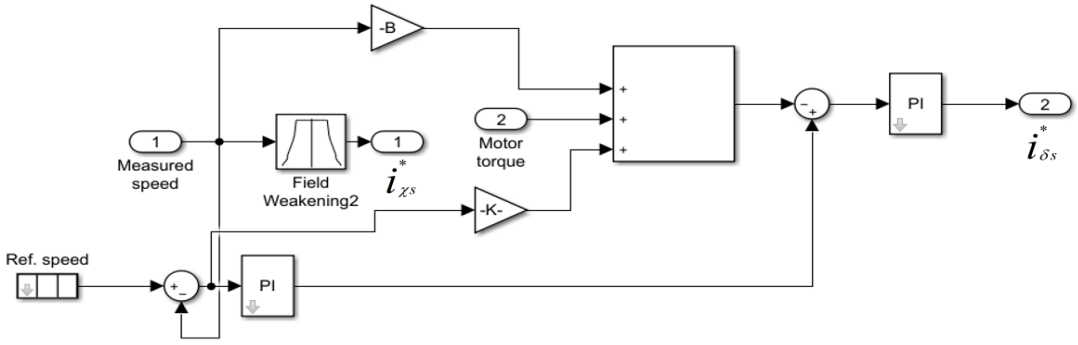

Fig. (4): Inside the field orientation block in case of varying load

The χ-axis flux current component can be deduced from the lookup table with help of measuring motor speed as before but the δ-axis torque current component can be deduced by estimating the motor torque with help of the stator current and rotor position and introduced to filed orientation block this estimating torque can be used with frictional torque and acceleration torque or deceleration torque to estimate the load torque. The frictional torque can be deduced from multiplying the measured speed in fractional coefficient (B) also, the acceleration torque or deceleration torque can be calculated by subtracting the reference

speed from the actual speed and the result divided into sampling time. The load torque compared to the reference toque and the error was introduced to the PI torque current controller to get the final δ-axis current component. The output of the orientation block ($i_{\chi s}$*&$i_{\delta s}$*) with the rotor position introduced into the reference stator current block use to get the reference stator current i^*_{abc}. These currents were compared to actual stator currents through the regulator current block to get the errors in the stator currents Δi^*_{abc}. These errors in the stator currents introduced to the impedance gain block to get the reference stator voltages v^*_{abc}. These reference stator voltages introduced to the SVM block to estimate the pulses of the inverter. These pulses were applied to the inverter to get suitable voltages to drive the PMSM.

3- Mathematical Model of the Three Phase PMSM

The mathematical model of the three-phase PMSM in synchronous frame is

$$v_{\chi s} = R_s i_{\chi s} + L_\chi \rho i_{\chi s} - \omega_e L_\delta i_{\delta s} \quad (1)$$

$$v_{\delta s} = R_s i_{\delta s} + L_\delta \rho i_{\delta s} + \omega_e L_\chi i_{\chi s} + \omega_e \psi_{pm} \quad (2)$$

$$T_e = \frac{3}{2}\frac{P}{2}\psi_{pm} i_{\delta s} \quad (3)$$

$$J\rho\omega_m = T_e - T_L - B\omega_m \quad (4)$$

$$\omega_e = \frac{P}{2}\omega_m \quad (5)$$

$$\theta_e = \int \omega_e dt \quad (6)$$

Where $v_{\chi s}, v_{\delta s}$ are χ, δ axes stator voltages, $i_{\chi s}, i_{\delta s}$ are χ, δ axes stator currents, L_{χ}, L_{δ} are χ, δ axes stator inductance, R_s is the stator resistance for each phase, T_e is electromagnetic torque, T_L is the load torque, B is the fractional coefficient, ω_m is the mechanical speed of the motor, ω_e is the electrical frequency of the motor, J is the moment of inertia, ρ is a derivative factor, θ_e is the electrical rotor position, P is the number of poles and is the permanent magnet of the rotor flux.

4- PWM CONTROL USING SVM

FOC is similar to separately excited DC motor so, the phasor diagram of the PMSM under FOC can be represented as shown in Fig. 5. With help of inverse Clark and Park transformation, the reference stator current can be calculated as,

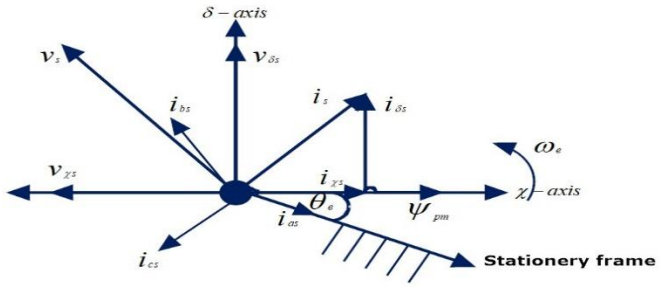

Fig. (5): Phasor diagram of PMSM with FOC and stator current

$$\begin{bmatrix} i_{as}^{*} \\ i_{bs}^{*} \\ i_{cs}^{*} \end{bmatrix} = \begin{bmatrix} \cos\theta_e & -\sin\theta_e \\ \cos(120^0 - \theta_e) & -\sin(120^0 - \theta_e) \\ \cos(240^0 - \theta_e) & -\sin(240^0 - \theta_e) \end{bmatrix} \begin{bmatrix} i_{\chi s}^{*} \\ i_{\delta s}^{*} \end{bmatrix} \quad (7)$$

These reference stator currents were compared to the actual stator currents to generate the errors in these currents. These errors in the stator currents are the input of impedance gain unit. The output of this unit is the reference stator voltages. These references of the voltages were used to generate the pulses of the inverter to reshape the output voltage of

the inverter. The pulses form depending upon some vector voltages. These voltage vectors are the zero-vector and non-zero vector (adjacent voltages). The switching states of the inverter have eight states. Two of them are non-active voltages (v_0-v_7). The others (six active voltages vector) are from v_1 to v_6. All active and non-active states can be seen in Fig. 6. From Fig. 6, the switching state and responding voltage can be seen in table 1.

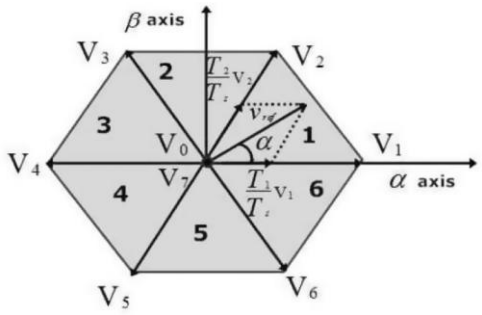

Fig. (6): Inverter hexagon and sector

The line to line and phase voltages depending upon the switching state of the inverter which shown in table 1 can be calculated as in eqs. 8 and 9. as follows,

$$\begin{bmatrix} v_{ab} \\ v_{bc} \\ v_{ca} \end{bmatrix} = \begin{bmatrix} 1 & -1 & 0 \\ 0 & 1 & -1 \\ -1 & 0 & 1 \end{bmatrix} \begin{bmatrix} a \\ b \\ c \end{bmatrix} V_{dc} \tag{8}$$

$$\begin{bmatrix} v_{an} \\ v_{bn} \\ v_{cn} \end{bmatrix} = \begin{bmatrix} 2 & -1 & -1 \\ -1 & 2 & -1 \\ -1 & -1 & 2 \end{bmatrix} \begin{bmatrix} a \\ b \\ c \end{bmatrix} \frac{V_{dc}}{3} \tag{9}$$

Where v_{ab}, v_{bc}, v_{ca} are line to line output voltage of inverter, v_{an}, v_{bn}, v_{cn} are phase output voltage of inverter, V_{dc} input voltage of inverter and a, b, c, operator of the phase voltages.

Depending upon the reference of three-phase stator voltages which entered to the SVM block to generate the pulses to drive the inverter can be simulated as,

Table(1): switching state and cross-ponding voltages

Voltage vector	Switching on	Line to neutral voltages			Line to line voltage		
		v_{an}	v_{bn}	v_{cn}	v_{ab}	v_{bc}	v_{ca}
V_0	T_1, T_3, T_5	0	0	0	0	0	0
V_1	T_2, T_3, T_5	2/3	−1/3	−1/3	1	0	−1
V_2	T_2, T_4, T_5	1/3	1/3	−2/3	0	1	−1
V_3	T_1, T_4, T_5	−1/3	2/3	−1/3	−1	1	0
V_4	T_1, T_4, T_6	−2/3	1/3	1/3	−1	0	1
V_5	T_1, T_3, T_6	−1/3	−1/3	2/3	0	−1	1
V_6	T_2, T_3, T_6	1/3	−2/3	1/3	1	−1	0
V_7	T_2, T_4, T_6	0	0	0	0	0	0

The three-phase reference voltages converter into two-phase voltages as follows,

$$\begin{bmatrix} v_{\alpha s} \\ v_{\beta s} \end{bmatrix} = \frac{2}{3}\begin{bmatrix} 1 & -\frac{1}{2} & -\frac{1}{2} \\ 0 & \frac{\sqrt{3}}{2} & -\frac{\sqrt{3}}{2} \end{bmatrix}\begin{bmatrix} v_{an} \\ v_{bn} \\ v_{cn} \end{bmatrix} \quad (10)$$

With these voltages, the reference voltage as the vector can be seen in Fig. 7 and can be calculated as,

$$v_{ref} = \sqrt{v_{\alpha s}{}^2 + v_{\beta s}{}^2} \quad \text{and} \quad \alpha = \tan^{-1}\frac{v_{\beta s}}{v_{\alpha s}} \quad (11)$$

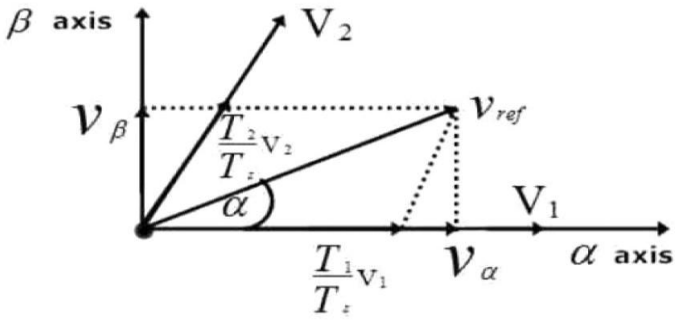

Fig. (7): The reference voltage

The time duration (T_1,T_2,T_s) can be calculated from Fig. 7 as,

$$\begin{aligned} \mathrm{m}_{\mathrm{in}\,dx}\, v_{ref} \cos\alpha &= \frac{T_1}{T_s} V_1 + \frac{T_2}{T_s} V_2 \cos\alpha \\ \mathrm{m}_{\mathrm{in}\,dx}\, v_{ref} \sin\alpha &= + \frac{T_2}{T_s} V_2 \sin 60^0 \\ T_0 &= T_s - (T_1 + T_2) \end{aligned} \tag{12}$$

Where $\mathrm{m}_{\mathrm{in}\,dx}$ is the modulation index and $T_s = \dfrac{1}{\text{switching frequency}}$

From (12) the duration time in each sector can be calculated as follows,

$$\begin{aligned} T_1 &= \frac{\sqrt{3}}{2} \mathrm{m}_{\mathrm{in}\,dx}\, T_s \sin(\frac{n\Pi}{3} - \alpha) \\ T_2 &= \frac{\sqrt{3}}{2} \mathrm{m}_{\mathrm{in}\,dx}\, T_s \sin(\frac{(n-1)\Pi}{3} - \alpha) \end{aligned} \tag{13}$$

Where n is the sector number

Depending upon this, the switching time can be written as in table 2 and the voltages can be gotten.

Table(2): Switching time calculation

Sector	Upper switches	Lower switches
1	$s_1 = T_1 + T_2 + \frac{T_0}{2}, s_3 = T_2 + \frac{T_0}{2}, s_5 = \frac{T_0}{2}$	$s_2 = \frac{T_0}{2}, s_4 = T_2 + \frac{T_0}{2}, s_6 = T_1 + T_2 + \frac{T_0}{2}$
2	$s_1 = T_2 + \frac{T_0}{2}, s_3 = T_1 + T_2 + \frac{T_0}{2}, s_5 = \frac{T_0}{2}$	$s_2 = T_2 + \frac{T_0}{2}, s_4 = \frac{T_0}{2}, s_6 = T_1 + T_2 + \frac{T_0}{2}$
3	$s_1 = T_1 + T_2 + \frac{T_0}{2}, s_3 = T_2 + \frac{T_0}{2}, s_5 = \frac{T_0}{2}$	$s_2 = T_1 + T_2 + \frac{T_0}{2}, s_4 = T_2 + \frac{T_0}{2}, s_6 = \frac{T_0}{2}$
4	$s_1 = \frac{T_0}{2}, s_3 = T_2 + \frac{T_0}{2}, s_5 = T_1 + T_2 + \frac{T_0}{2}$	$s_2 = T_1 + T_2 + \frac{T_0}{2}, s_4 = T_2 + \frac{T_0}{2}, s_6 = \frac{T_0}{2}$
5	$s_1 = T_2 + \frac{T_0}{2}, s_3 = \frac{T_0}{2}, s_5 = T_1 + T_2 + \frac{T_0}{2}$	$s_2 = T_2 + \frac{T_0}{2}, s_4 = T_1 + T_2 + \frac{T_0}{2}, s_6 = \frac{T_0}{2}$
6	$s_1 = T_1 + T_2 + \frac{T_0}{2}, s_3 = \frac{T_0}{2}, s_5 = T_2 + \frac{T_0}{2}$	$s_2 = \frac{T_0}{2}, s_4 = T_1 + T_2 + \frac{T_0}{2}, s_6 = T_2 + \frac{T_0}{2}$

5- Simulation Results

Here the simulation results of the proposed system were compared to the conventional system to show the advantages of the proposed system. This occurred at different loads. Theses loads are constant load. Dynamic load, sudden applied load, and sudden removal load. The motor data was used in this simulation can be seen in Table 3.

5-1 Constant Load

The shapes of the stator currents, motor torque, and motor speed with the conventional system and with the proposed system when the load is constant can be seen here. The variation of the stator current with conventional and proposal methods can be seen in Fig 8 and Fig 9 respectively. Fig. 8 shows that the stator currents are highly distorted (conventional system) and Fig. 9 shows the stator currents become less distorted with the proposed system. The variation in the motor torque with conventional and proposal methods can be seen in Fig 10 and Fig 11 respectively. Fig. 10 shows that the motor torque contains high ripples (conventional system) if it is compared to motor torque with the proposed system.

Fig 12 and Fig. 13 show that the variation of the motor speed with two methods under study. It is approximately the same.

Table(3): Motor data

Motor parameters	values
Power	900 Watt
voltage	110 Volt
Frequency	50 Hertz
Stator resistance	0.43 Ohm
χ -axis inductance	6.97 mH
δ -axis inductance	6.97 mH
Permanent magnet flux inductance	0.18 Weber
Moment of inertia	0.0011Kg.m^2
Frictional coefficient	0.001 Nm.sec/rad
Number of poles	6

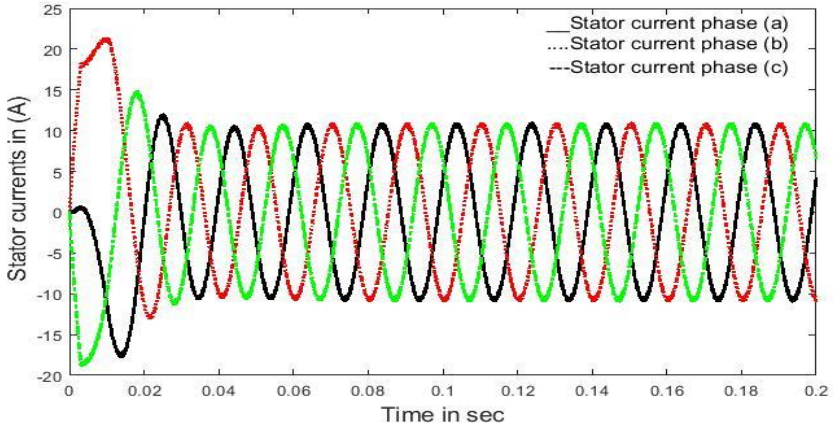

Fig. (8): The stator current with conventional system

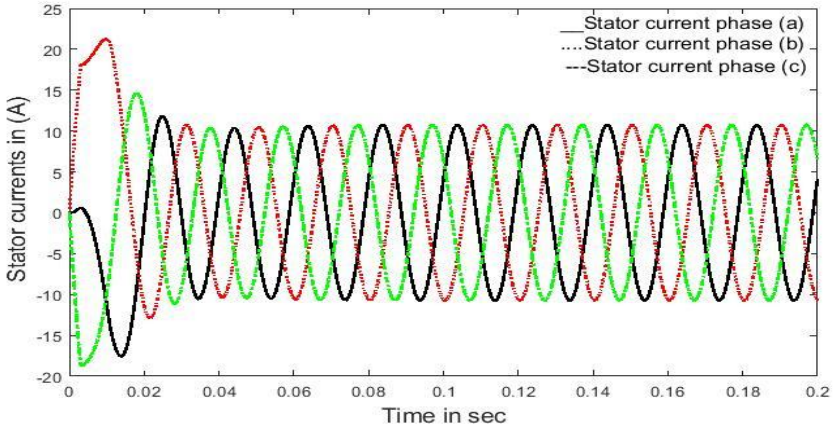

Fig. (9): The stator current with proposal system

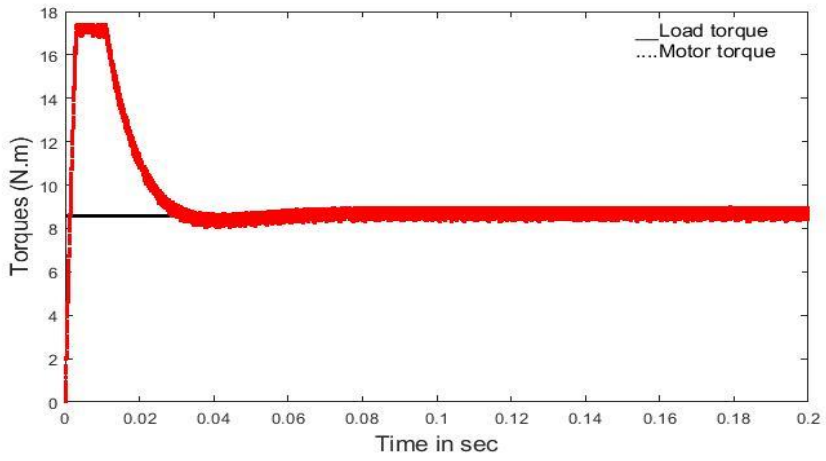

Fig. (10): The motor torque versus load torque with conventional system

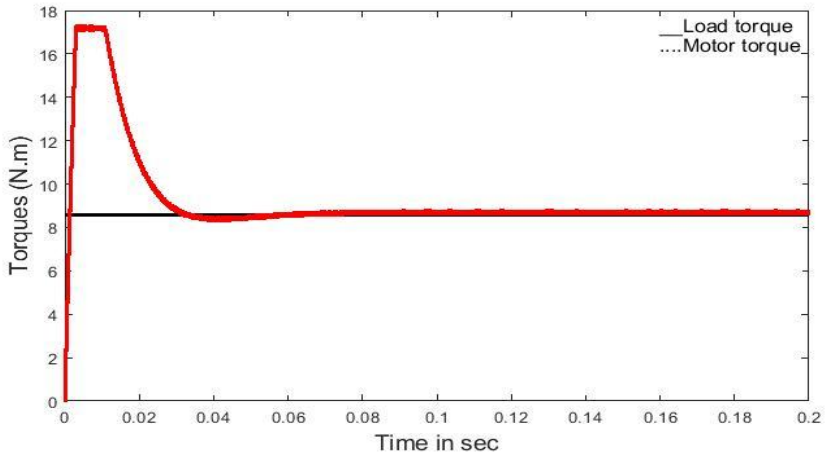

Fig. (11): The motor torque versus load torque with proposal system

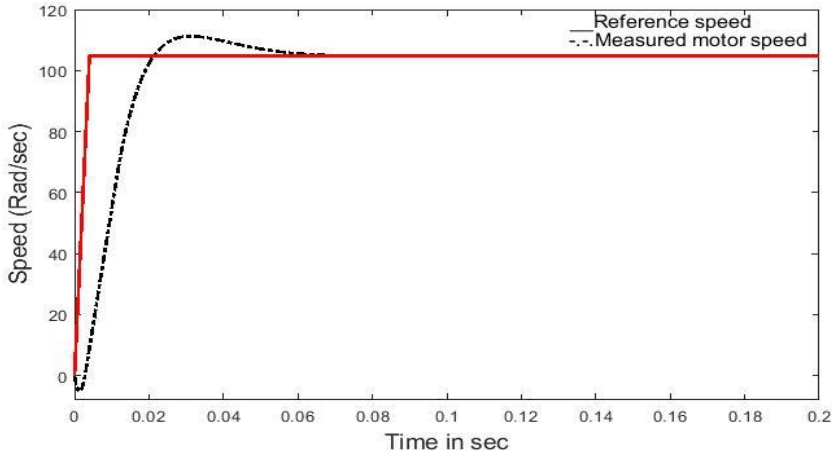

Fig. (12): The motor speed versus reference speed with conventional system

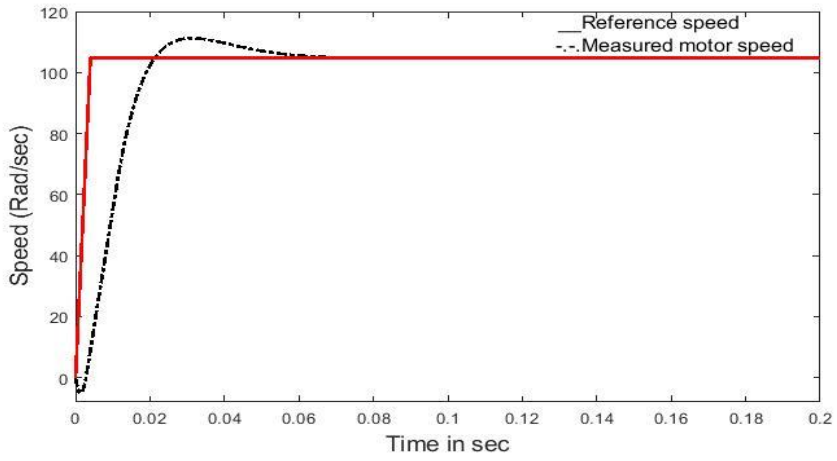

Fig. (13): The motor speed versus reference speed with proposal system

The following table (table 4) shows the value of the THD in the motor current and the torque ripples in the motor torque. From this table can be concluded that the THD was improved with the proposed system if it is compared to the conventional drive system. Also, when looking up to the torque ripples it is found that the torque ripples were improved with the proposed drive system compared to the conventional drive system.

Table(4): THD and torque ripples

System types	THD	Torque ripples
Conventional drive system	2.2	1.7
Proposed drive system	0.71	0.52

5-2 Dynamic Load

Here the dynamic load is applied from zero sec. up to 0.15 sec, the load increased gradually starting from no-load up to rated value, from 0.15 sec. up to 0.35 sec. the load still at rated value, from 0.35 sec up to 0.5 sec. the load decreased gradually from rated value up to no-load. When using the impedance gain it found that this gain improves only the torque ripples and THD in the current and in the motor flux but it isn't affecting the dynamic behavior so another modified was added to improve the dynamic performance. In this modified, the motor torque was estimated. With this torque, frictional torque, and with acceleration or deceleration torque the load torque is

calculated and compared to the reference torque. The error from this comparison introduced to another PI torque current controller and the output of this PI is a torque current component which used to improve the dynamic behavior and this can be seen here and when the load is gradually changing. The variation of the stator current with conventional and proposal methods can be seen in Fig 14 and Fig 15 respectively. Where Fig. 14 shows the stator currents with the conventional drive model and Fig. 15 shows the stator currents with the proposed system. From these Figs. It is found that the distortion of stator current decreased with the proposed drive system.

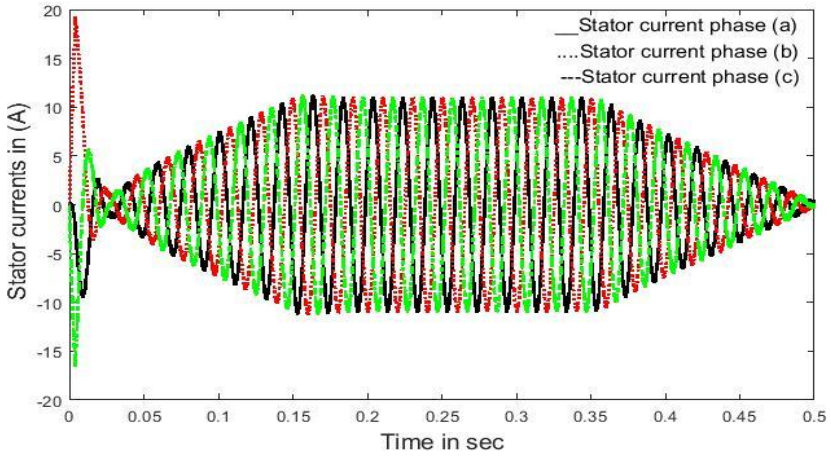

Fig. (14): The stator current with conventional system

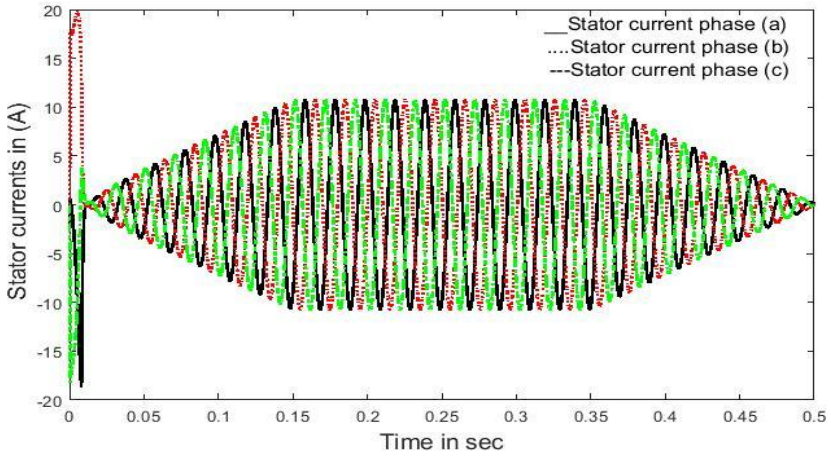

Fig. (15): The stator current with proposal system

The variation in the motor torque with conventional and proposal methods can be seen in Fig 16 and Fig 17 respectively. Fig. 16 shows that the motor torque contains high ripples (conventional system) if it is compared to motor torque with the proposed system. Fig 18 and Fig. 19 show the variation of the motor speed with two methods under study. From these Figs. It is found that the motor speed with proposed method is approximately not effecting by variation of the load if it is compared to conventional method due to estimate the load torque and use PI torque current component.

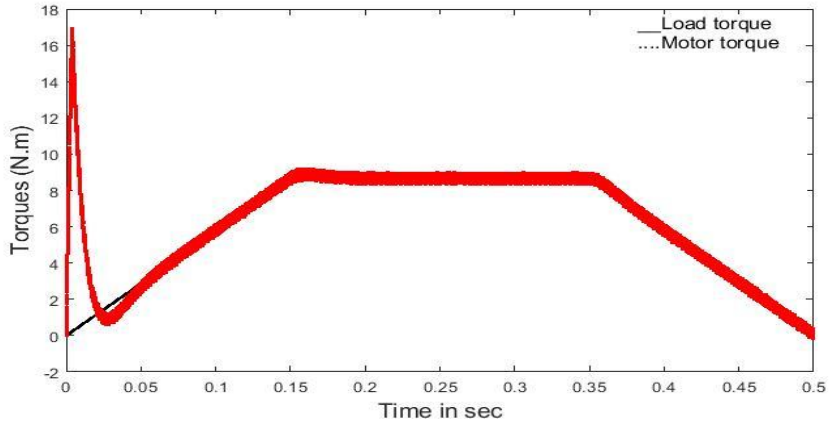

Fig. (16): The motor torque versus load torque with conventional system

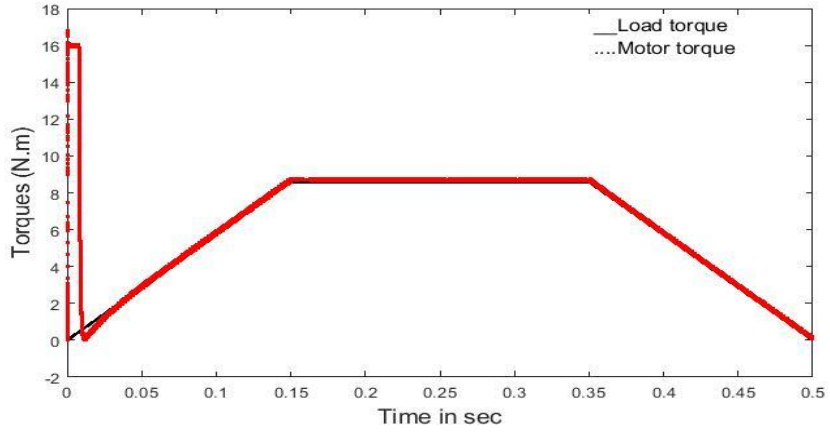

Fig. (17): The motor torque versus load torque with proposal system

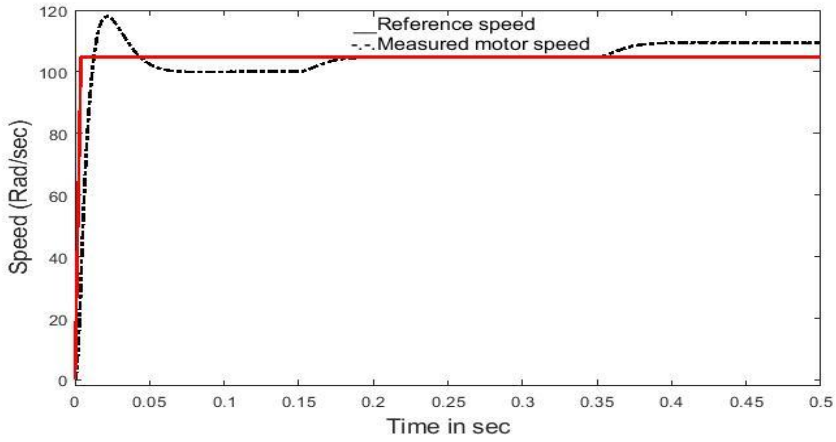

Fig. (18): The motor speed versus reference speed with conventional system

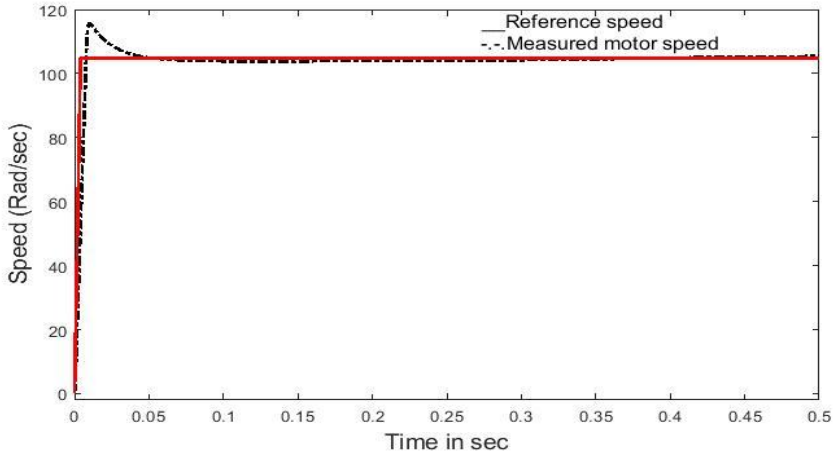

Fig. (19): The motor speed versus reference speed with proposal system

5-3 Sudden Applied Load and Sudden Removal Load

Here the shape of the load can be explained as follows; from zero sec. up to 0.15 sec, no-load is on the motor, at the instant of 0.15 sec. the rated load is suddenly applied and the motor continuous with this load up to 0.35 sec. at the instant of 0.35 sec the load was suddenly removed. The variation of the stator current with conventional and proposal methods can be seen in Fig 20 and Fig 21 respectively. Where Fig. 20 shows the stator currents with the conventional drive model and Fig. 21 shows the stator currents with the proposed system. From these Figs. It is found that the distortion of stator current decreased with the proposed drive system. The variation in the motor torque with conventional and proposal methods can be seen in Fig 22 and

Fig 23 respectively. Fig. 23 shows that the motor torque fewer ripples (proposed system) if it is compared to motor torque with the conventional system. Also, due to adding PI torque controller the effect of suddenly applied load or sudden removal load can be neglected with the proposed drive system if it compared to the conventional system.

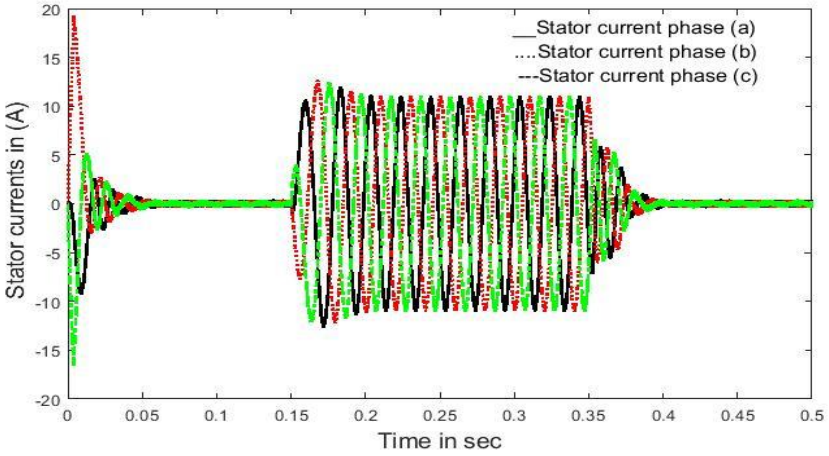

Fig. (20): The stator current with conventional system

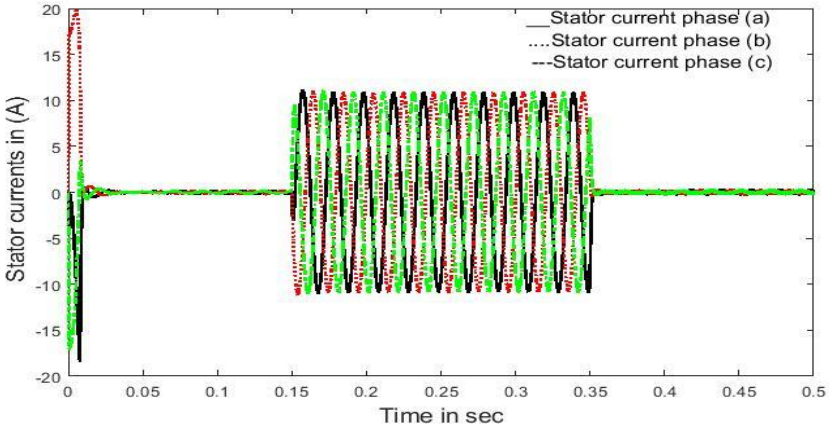

Fig. (21): The stator current with proposal system

Fig 24 and Fig. 25 show the variation of the motor speed with two methods under study. From these Figs. can be concluded that adding the PI torque current controller damped the effect of the variation of applied or remove the load. This means that the proposed model is more effective in the keeping of the motor speed if it compared to the conventional model.

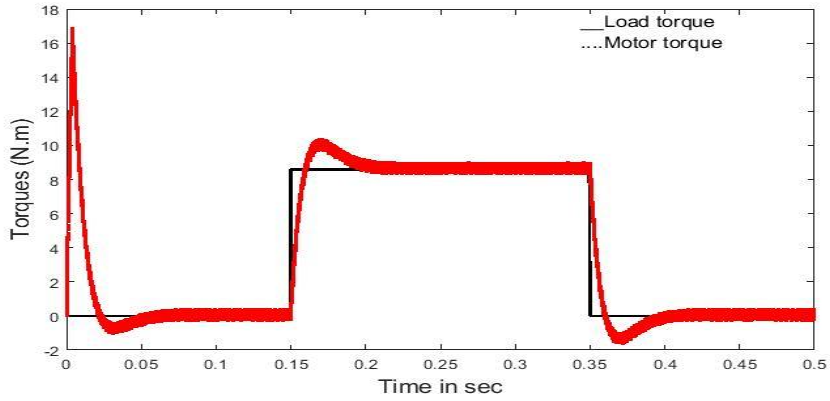

Fig. (22): The motor torque versus load torque with conventional system

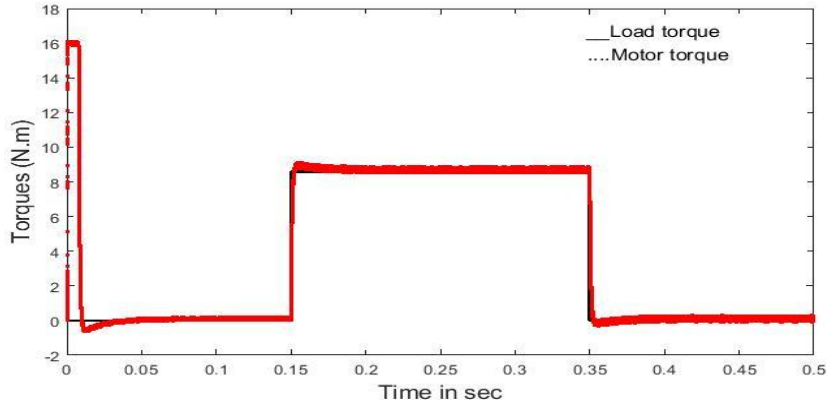

Fig. (23): The motor torque versus load torque with proposal system

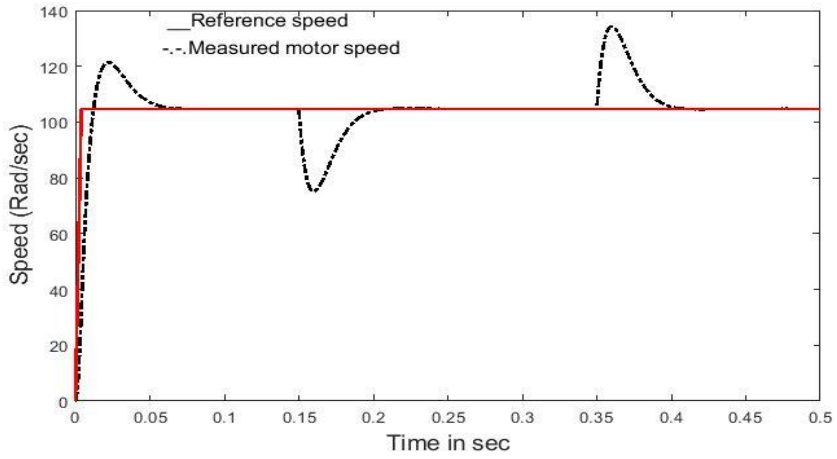

Fig. (24): The motor speed versus reference speed with conventional system

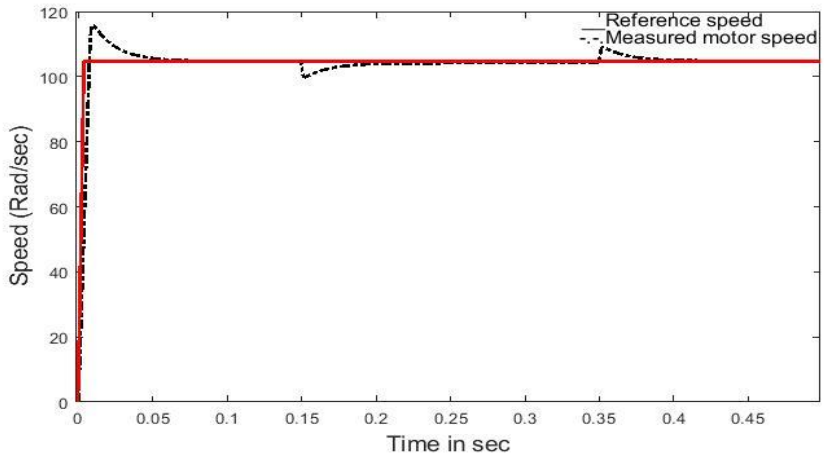

Fig. (25): The motor speed versus reference speed with proposal system

6- CONCLUSIONS

This paper studied the problems of the distortion in the stator current, the torque ripples of the PMSM, and the dynamic behavior of the PMSM. This paper produced solutions to these problems. These solutions depend upon improving the THD in the motor current, improving the torque ripples, and improving the dynamic behavior of the motor. The solution depends upon replacing the hysteresis controller by impedance gain to generate the reference voltages which improve the pluses introduced to the inverter through the SVM. Also, it used torque estimator and PI torque current controller to improve the dynamic performance of the PMSM. The simulation showed the importance of the proposed drive system to improve the performance of the PMSM overall.

7- RECOMMENDATIONS

The recommendation for the future work can be summarized as the follows;

1- Use the PMSM with taking into account the saturation effect.

2- Use the PMSM with taking into account the core loss effect.

3- Apply this modification on the other motors as induction motor.

List abbreviations

PMSM's	The Permanent Magnet Synchronous Motors
FOC	Field-Oriented Control
THD	Total Harmonic Distortion
HCC	Hysteresis Current Controller
PI	Proportional Integrator
SVM	Space Vector Modulation
PWM	Pulse Width Modulation

REFERENCES

[1] F. Blaschke,. The principle of field orientation as applied to the new transvector closed-loop control system for rotating-filed machines.Siemens, Bejing, 34, (1972) 217-220.

[2] U.B. Malkhandale, N.G. Bawane and P.M. Diagavane, "Study of Hysteresis Current Controller for Permanent Magnet Synchronous Motor Drives", International Conference on Smart Electric Drives & Power System, Nagpur, India, (2018), 334-339.

[3] Miraj Parsana, Jatinkumar Patel, "Field Oriented Vector Control Scheme of PMSM Using Hysteresis Current Control", International Research Journal of Modernization in Engineering Technology and Science, Vol. 2 (8), (2020), 1288-1291.

[4] Yu Lan Li*, Tie Zhu Zhang, Hong Zhao, Ji Zhang, "AMEsim, Hysteresis Current Control, Impedance Matrix, Permanent Magnet Synchronous Motor", Applied Mechanics and Materials Vol.700, (2014), 678-681.

[5] Cosmas Ogbuka, Cajethan Nwosu & Marcel, "A fast hysteresis current–controlled permanent magnet synchronous motor drive based on field orientation", Journal of electrical engineering, 67(2), (2016), 69-77.

[6] Mohamed Kadjoudj, Mohamed El Hachemi Benbouzid, Chawki Ghennai, and Demba Diallo, "A robust hybrid current control for permanent-magnet synchronous motor drive", IEEE transactions on energy conversion. 19(1), (2004), 109-115.

[7] P.Mamta, A.K Nadir and Beena Singh, 2015. "An adaptive hysteresis current controller for interior permanent magnet synchronous motor", IEEE Transactions on Industry Applications. 4 (7), (2015), 6026-6032.

[8] Hamdy Mohamed Soliman and S.M.EL. Hakim, "Improved hysteresis current controller to drive permanent magnet synchronous motors through the field-oriented control", International Journal of Soft Computing and Engineering. 2 (4), (2012), 40-46.

[9] Nabil Farah, M.H.N. Talib, Z. Ibrahim, Mat Isa S.N & J.M. Lazi, "variable hysteresis current controller with fuzzy logic controller-based induction motor drives",IEEE International Conference on System Engineering and Technology, (2017), 122-127.

[10] L. N. Ramya, A. Sivaprakasam, "Application of model predictive control for reduced torque ripple in orthopaedic drilling using permanent magnet synchronous motor drive", Electrical Engineering, Vol.102, (2020), 1469–1482

[11] M. Nasir Uddin & Ronald S. Rebeiro, "Fuzzy logic-based speed controller and adaptive hysteresis current controller based IPMSM drive for improved dynamic performance", IEEE international electric machine and drive conference, Niagara Falls, ON, Canada (2011), 1-6.

[12] Sanjaya Kumar Sahu, T. V. Dixit & D.D. Neema, "Particle swarm optimized fuzzy controller for indirect vector control of multilevel inverter f ed induction motor", International journal of computer science. 11 (4), (2014), 217-224.

[13] A. Maamoun, Y. M. Alsayed, & A. Shaltout, "Space-vector pwm inverter feeding a permanent-magnet synchronous motor", World Academy of Science, Engineering and Technology International Journal of Electrical and Computer Engineering, 4 (5), (2010), 829-833.

[14] Tingting Liu, Guojin Chen & Shigang Li, "Application of vector control technology for PMSM used in electric vehicles", Open automation and control systems journal, 6, (2014), 1334-1341.

[15] Jose Jacob and A.Chitra , "Field oriented control of space vector modulated multilevel inverter fed PMSM drive", international Conference on power engineering computing and control", VIT University, Chennai Campus, (2017), 966-973.

[16] Ibrahim Mohd Alsofyani and Kyo-Beum Lee, "Predictive Torque Control Based on Discrete Space Vector Modulation of PMSM without Flux Error-Sign and Voltage-Vector Lookup Table", electronics, MDPI, (2020), 1-15.

[17] Vidhi Patel, Concettina Buccella and Carlo Cecati, "Analysis and Implementation of Multilevel Inverter for Full Electric Aircraft Drives", energies, MDPI, (2020), 1-15.

[18] F. Haidari, A. Sheikholeslami, K. G. Firouzjah & S. Lesan, "Predictive field-oriented control of PMSM with space vector modulation technique ", Front. Electr. Electron. Eng. China. 5 (1), 2010, 91-9

ARID Journals

ARID International Journal for Science and Technology (AIJST)
ISSN: 2662-009X

Journal home page: http://arid.my/j/aijst

مَجلةُ أُريد الدَّوليةُ للعُلومِ والتِّكنولوجيا

العدد 7 ، المجلد 4 ، حزيران 2021 م

Evaluation of the Crack Model of V Type Longitudinal Ribs on Orthotropic Deck Using Finite Element Analysis

Fatih Alemdar

Department of Civil Engineering, Civil Engineering Faculty, Yıldız Technical University, Davutpaşa, Esenler, Istanbul 34220, Turkey.

تقييم نموذج التصدع للأضلاع الطولية من النوع V على سطح تقويمي باستخدام نموذج تحليل العناصر المحدودة

فاتح علم دار

قسم الهندسة المدنية، كلية الهندسة المدنية، جامعة يلدز التقنية-اسطنبول - تركيا

falemdar@yildiz.edu.tr
arid.my/0004-0654
https://doi.org/10.36772/arid.aijst.2021.474

ARTICLE INFO
Article history:
Received 28/01/2021
Received in revised form 16/03/2021
Accepted 19/05/2021
Available online 15/06/2021
https://doi.org/10.36772/arid.aijst.2021.474

Abstract

The long span orthotropic bridge decks applied around the world are used with open or closed cross-sectional longitudinal ribs placed below the steel deck to increase the strength of the deck. Fatigue cracks are developed in the longitudinal ribs due to traffic loadings. In this study, v type of longitudinal rib cross-sections are modelled and the stresses for the rib are evaluated under tire load loading using finite element analysis. Longitudinal ribs are used for long span steel bridges. The aim of this study is to compare the fatigue crack path of the longitudinal rib on a real bridge with the stress pattern in the finite element model.

Keywords: Finite Element, Orthotropic deck, Fatigue crack stop hole, Steel bridges, Longitudinal rib

الملخص

تُستخدم أسطح الجسر التقويمية طويلة المدى المنفذة حول العالم مع أضلاع طولية مقطعية مفتوحة أو مغلقة والموضوعة أسفل السطح الفولاذي لزيادة قوته ومتانته. حيث طورت شقوق الإجهاد في الأضلاع الطولية بسبب الأحمال المرورية الثقيلة. حيث تم، في هذه الدراسة، نمذجة النوع الخامس من المقاطع العرضية للأضلاع الطولية وتقييم ضغوط الضلع تحت حمل إطارات المركبات وذلك باستخدام مقياس تحليل العناصر المحدودة. وقد استخدمت الأضلاع الطولية للجسور الفولاذية الطويلة. إن الهدف من هذه الدراسة هو مقارنة مسار شق الإجهاد في الضلع الطولي على جسر حقيقي مع نمط الإجهاد في نموذج تحليل العناصر المحدودة.

كلمات مفتاحية: عنصر محدود، سطح متعامد، فتحة توقف صدع الاجهاد، جسور فولاذية، ضلع طولي.

1. Introduction

Longitudinal ribs constructed in the steel bridges are divided into two categories: (a) open cross-sectional ribs and (b) closed form longitudinal ribs. The strength of the open form longitudinal ribs are less than that of the closed form ribs and thus open form ribs are not utilized in practice (Fig. 1). Closed form longitudinal ribs generally consist of triangular and trapezoidal cross sections. The triangular longitudinal ribs were usually utilized in the steel bridges constructed before 1980s. Trapezoidal longitudinal ribs have been built in the bridges designed after 1980s. The main reason can be easier construction of the trapezoidal ribs than that of the triangular ribs. The secondary reasons may be considered as the top width of the trapezoidal rib is larger and less ribs are required for construction of bridges and thus labour is reduced.

The experimental studies on triangular longitudinal ribs are very few. Generally, steel bridge decks were modelled using finite element method (FEM) and the stresses at the critical regions were obtained. Stresses along the bridge decks were determined using different analysis programs [1-22]. Therefore; realistic information about the behaviour of the bridge decks under the loadings and the crack regions can be obtained. However, the stresses found by the analysis cannot reflect the real situations due to the assumptions done in the simulations. The results are getting closer to the real numbers depending on the assumptions made in the program and the formulae used in the analysis. Therefore; the finite element method is a well-recognized method in the World due to giving closer results to the real values.

Empirical equations were derived to calculate the construction expense of a bridge depending on the thickness of the plate and the minimum thickness of the plate to be used in the bridge was obtained [16]. This study was performed on the bridges having

less traffic loads and thus it may not be utilized for the bridges having long span and heavy traffic loads.

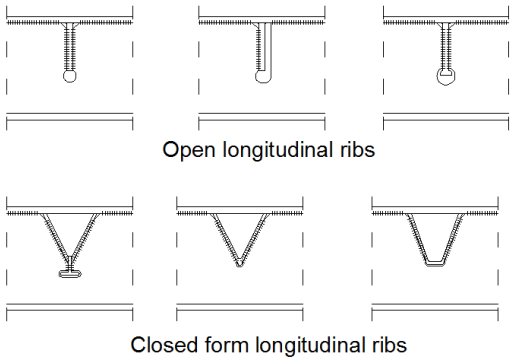

Figure(1): Steel orthotropic deck longitudinal rib types

2. Objectives

This study aims to investigate longitudinal rib body and diaphragm plate cracks modelling. The connection between the crack paths along the ribs on a real bridge and the stress distribution on the FE model is studied. The cracks on the rib – rib connection and rib – diaphragm plate connection are separately modelled. In the diaphragm plates cracks repaired with using different drilled holes diameter are evaluated. In addition, a parametric study is performed by changing the length of the cracks occurred downward at the region where the diaphragm plate and side of the rib are connected.

3. Details of the Longitudinal Ribs

Triangular longitudinal rib examined analytically in this study is shown in Fig. 3. The cross-sections of the rib studied here are the details of existence ribs used in Bosporus bridge in Istanbul [23, 24]. The distance between two ribs is 300 mm. The connection plate of the ribs is modelled the same for each rib detail. The length of the lap splice is modelled as 15 mm and the distance between the ribs is defined as 150 mm. The

connections are welded through ribs and the sides of the connection plate. The welding used to connect the ribs to the upper plate is not taken into account in the analysis. The depth of the ribs is defined as 1500 mm the height of the diaphragm is 750 mm selected so that no stress concentration could occur under the rib. Diaphragm is welded both on the sides of the rib at the centre of the rib and top plate and defined as fix bottom side of the diaphragm plate. The perpendicular edge of the diaphragm is not constraint which are free to move and the thickness is 8 mm (Fig. 4).

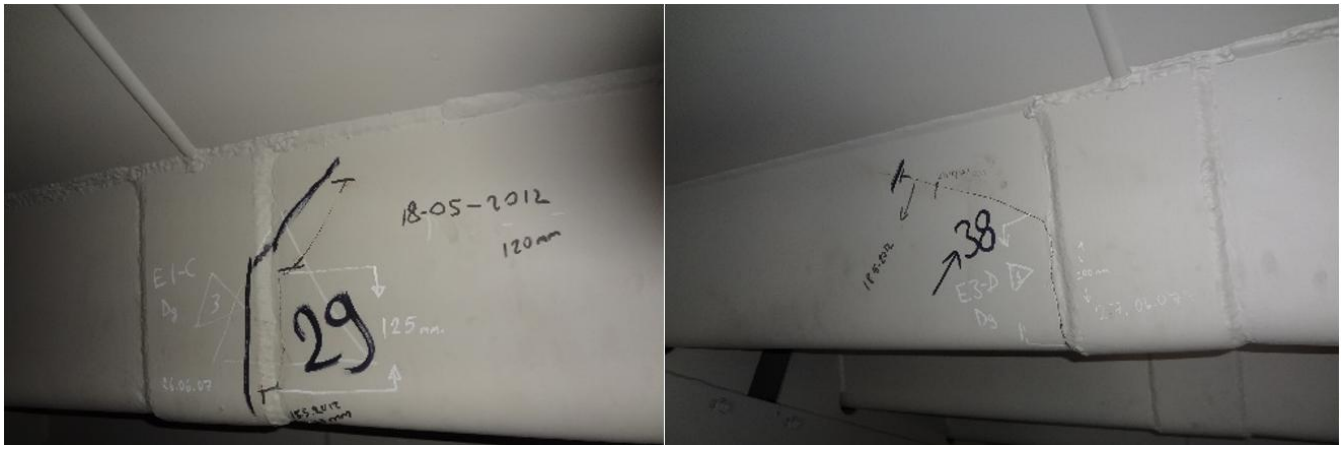

Figure(2): Triangular longitudinal rib to rib connection region fatigue cracks.

Figure(3): Triangular longitudinal ribs to diaphragm plate region fatigue cracks.

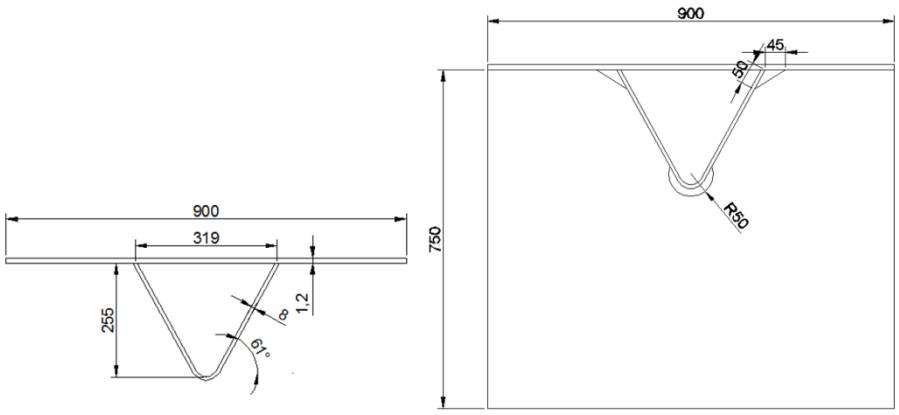

Figure(4): Triangular rib and diaphragm plate details (dimensions in mm).

4. General crack path of the ribs

Cracks are generally occurred at the connection areas of the ribs. These areas are the regions where the ribs are connected side by side and the point ribs are connected to the diaphragm plates. Cracks occurred at the connection region of the ribs are shown in Fig. 2. The second type of the cracks is shown Fig. 3. The third type of cracks develops downward at the welds between the diaphragm plate and the longitudinal rib (Fig.5b). These three types of cracks are investigated in this study.

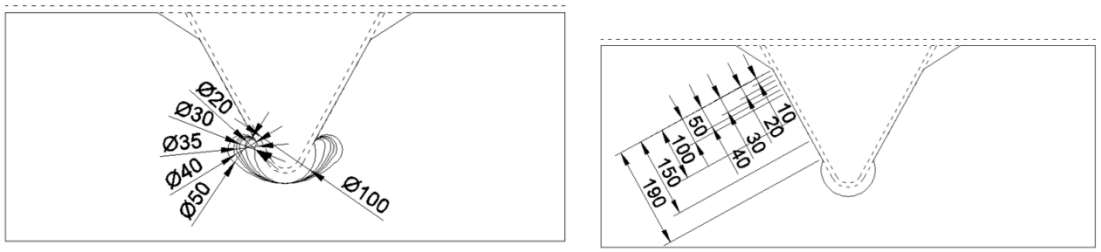

Figure(5): Diaphragm plate bottom fatigue crack repair with different hole diameter and crack between diaphragm plate and rib different crack length details (dimensions in mm).

5. Finite Element Modelling of the Ribs

In this study, the longitudinal rib and the components of the deck used in orthotropic bridge decks and a part of a tire (275/70 R22.5) used for transportation buses are modelled using a finite element program. The surface area of the tire gets larger when

the axial load from the transportation vehicle is applied, thus larger surfaces area is accounted in the FE analysis. The width of the model is defined as the depth of the longitudinal rib. The longitudinal rib in this study consists of triangular cross-section.

The longitudinal ribs, the upper plate and the tire are defined using steel material. The young modulus and poison ratio are given as 210 GPa and 0.1, respectively. The road is modelled using asphalt material and the young modulus and poison ratio are 2.5 GPa and 0.3 respectively. The reason of modelling the tire with steel material is that the most important part of the analysis is to evaluate the longitudinal rib and not to have any unexpected deformations in the tire. All the materials in the finite element model are defined using solid homogenous material type. The boundary conditions of the longitudinal rib and the upper plate at each end location are constrained in displacement and released in rotation. The connections between the asphalt and the upper plate, and the longitudinal rib and the plate are modelled using tie constraint in the analysis.

The thicknesses of the plates are 8 mm and 12 mm for the longitudinal rib and the upper plate respectively. The thickness of the asphalt is taken as 33 mm. The weld thickness in the connection region is defined as 5.5 mm. An 8 mm thick plate is used to connect the longitudinal ribs and the length of the lap splice is defined as 15 mm. The connection plate is taken as 180 mm long. The interaction between the connection plate, the weld and the longitudinal rib is chosen as tie constraint to provide full connection. The thickness of the diaphragm plate is 8 mm and height of the plate is 750 mm diaphragm plate and longitudinal rib connect with tie constraint and weld between diaphragm plate and rib is not defined.

The mesh size for the whole finite element model is around 10 mm and an 8-node linear brick element (C3D8R) is defined for the mesh element as shown in (Fig. 6). The axial load of 100 kN concentrated force of is applied at the centre of the tire. This load is taken from Turkish bridge code weight hos H30S24 truck having 240 kN axle load. There are 4 tires at each axle and thus a load of a tire is 60 kN. The normal load from a tire is accounted as 90 kN when the dynamic amplification factor is taken as 1.5.

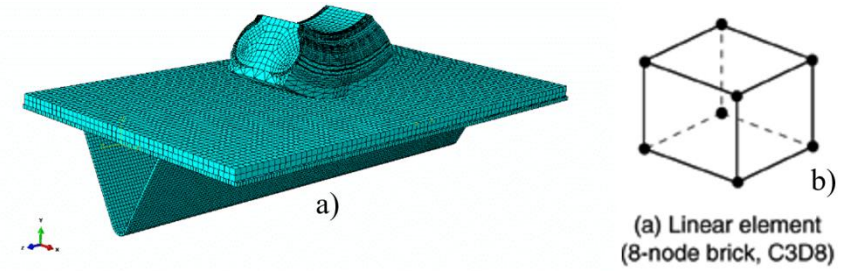

Figure(6): Finite element assembly mesh (a) and element type (b)

In this part of the analysis, longitudinal ribs are continuous under the bridge deck. The stresses on the longitudinal rib of a bridge deck due to tire loading are examined along the deck and away from the support regions of the bridge. The finite element model is built as if the tire passes in the middle of the longitudinal rib (Fig. 7). Hard contact interaction and friction are defined between the tire and the asphalt surface.

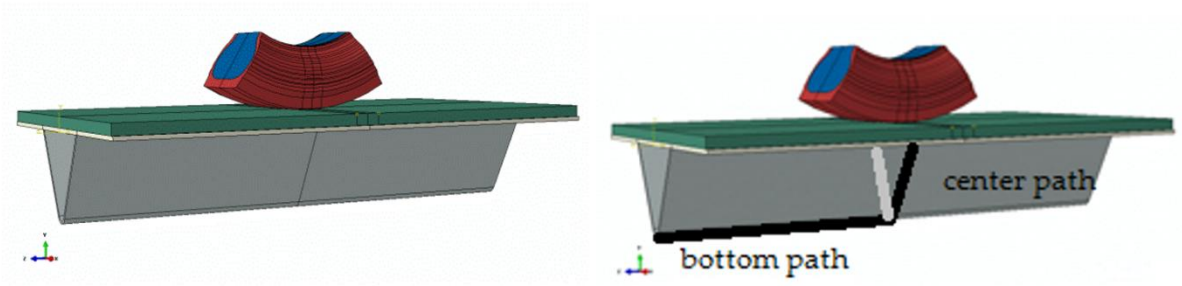

Figure(7): Finite element modelling continuous rib cross-sections and bottom and center paths

The connection region of the longitudinal ribs is also considered in this study. This region is generally constructed 1 m away from one end of the sector plate under the bridge deck for the real bridges. A finite element model of the connection plate and the weld to be used to combine the upper plate and the longitudinal rib is created. The thickness of the weld is chosen as 5.5 mm and applied around the thickness of the connection plate as a triangular welding. The lap splice of the connection plate on the ribs is 15 mm and the length of the plate is 180 mm (Fig. 8). Full interactions (tie constraint) between the plate and the weld and between the weld and the longitudinal rib are provided.

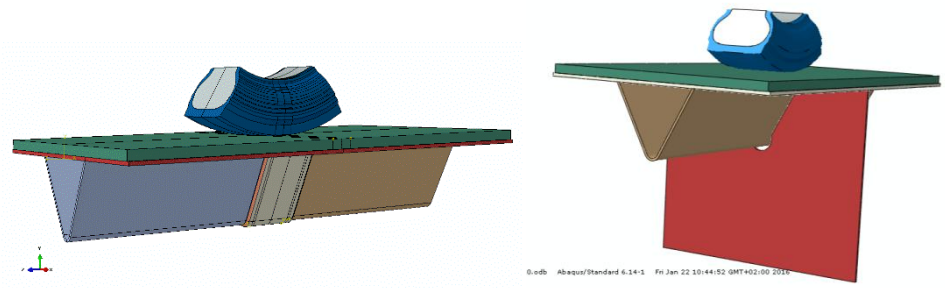

Figure(8): Finite element modelling rib connection area and diaphragm plate with continuous longitudinal rib

6. Parametric Analysis of the Ribs

The maximum principal stresses and the maximum deformations of the triangular longitudinal ribs are evaluated. The stress and the deformation contours along the vertical line perpendicular to the tire axis are shown in Fig. 9. In the model continuous rib, rib to rib connection region, and rib with diaphragm plate the maximum principal stress as seen in Fig. 9.

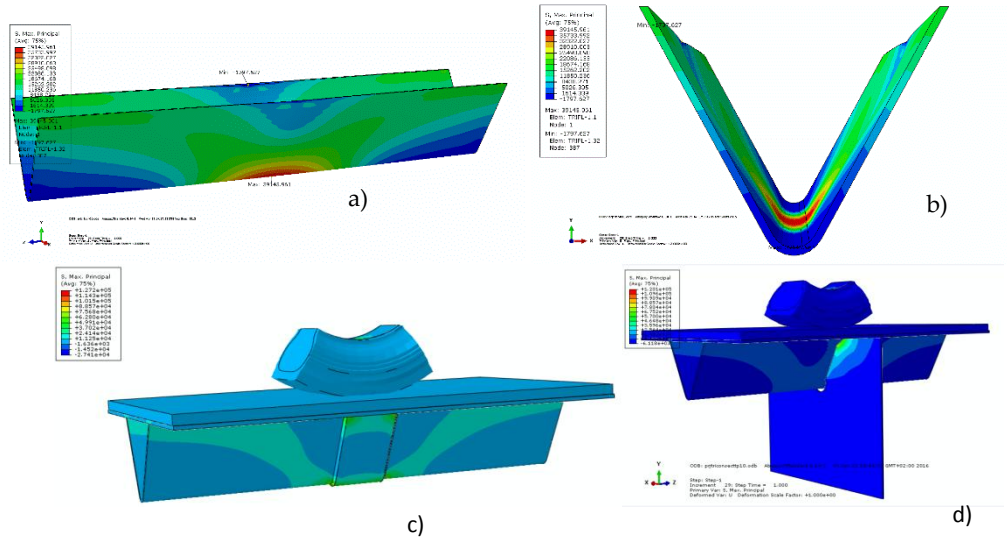

Figure(9): Max. Principal stress contours in the continuous rib (a) section view (b), and on the connection area (c) diaphragm plate with longitudinal rib (d)

6.1 Effect of Tire position on the ribs

The tire position is changed along the centre of the rib in this part of the analysis. The maximum principal stresses on the centre axis of the rib and on the longitudinal axis of the continuous rib are obtained according to the position of the tire and shown in the Fig. 10-11. The aim of the analysis is to examine the location of the tire since the tire does not always affect an orthotropic deck on the centre of the rib. The position of the tire was defined as 0, 50, 100, 150, 200, 250 mm where zero shows the centre of the rib and 250 mm shows the furthest location from the centre. The stresses on the centre line (centre path) of the longitudinal rib are illustrated in Fig. 10-11. In the FE models, only one rib with a specified length (1500 mm) was considered and there was no interaction defined from on the rib.

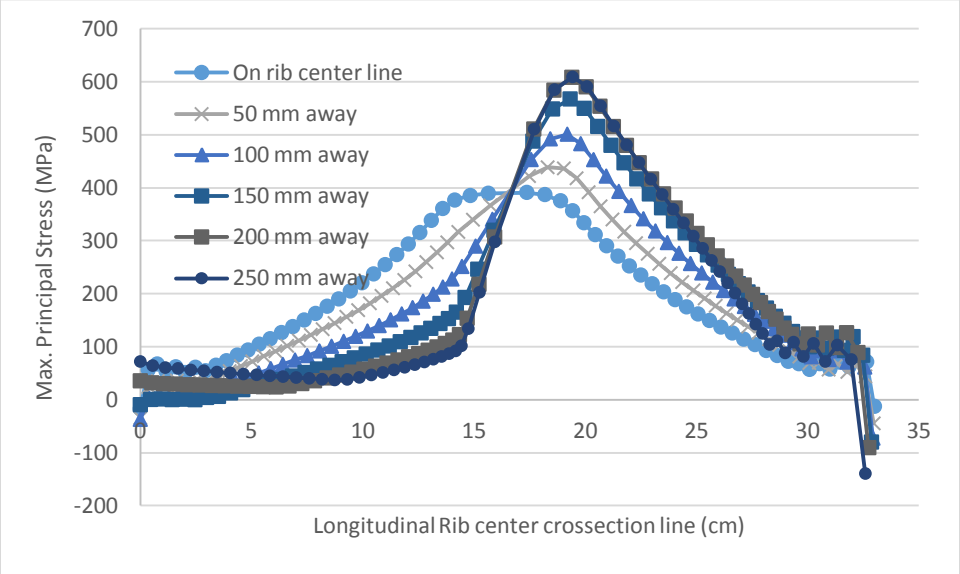

Figure(10): Longitudinal rib cross-section on the centre of the model

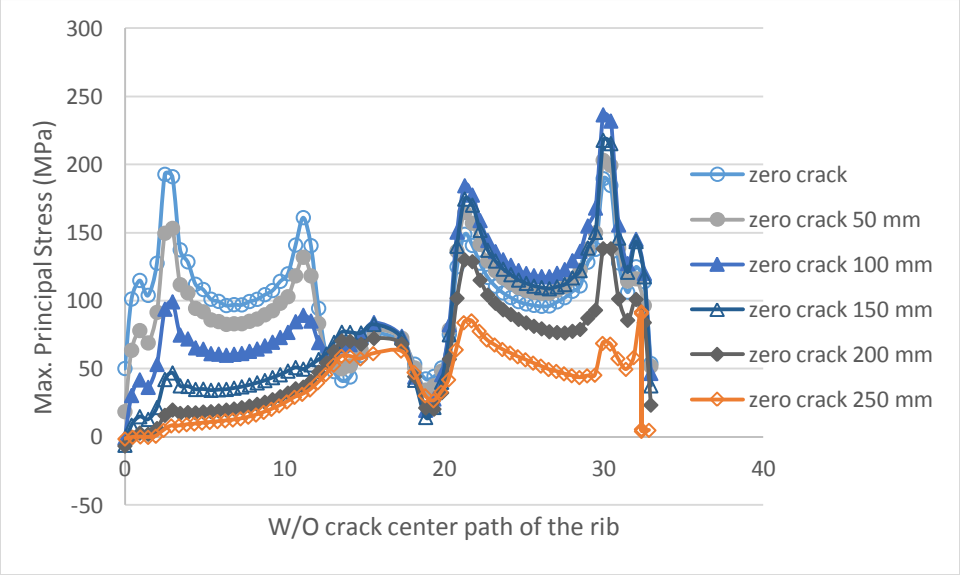

Figure(11): Longitudinal rib cross-section on the center of the model with diaphragm plate

6.2 Effect of crack repair with hole on the diaphragm plate

In this part of the analysis, the fatigue cracks at the region where the longitudinal ribs reach to the diaphragm plates are evaluated. The diameter of the drilled hole at the bottom of the ribs is changed to reduce the stress on the crack paths on the diaphragm plate. The diameter of the drilled hole is chosen between 20 mm - 50 mm (Fig.5a). The

stress distribution along the centre path is shown in Fig. 12 and the stress distribution along the circumference length of the drilled hole is shown Fig. 13

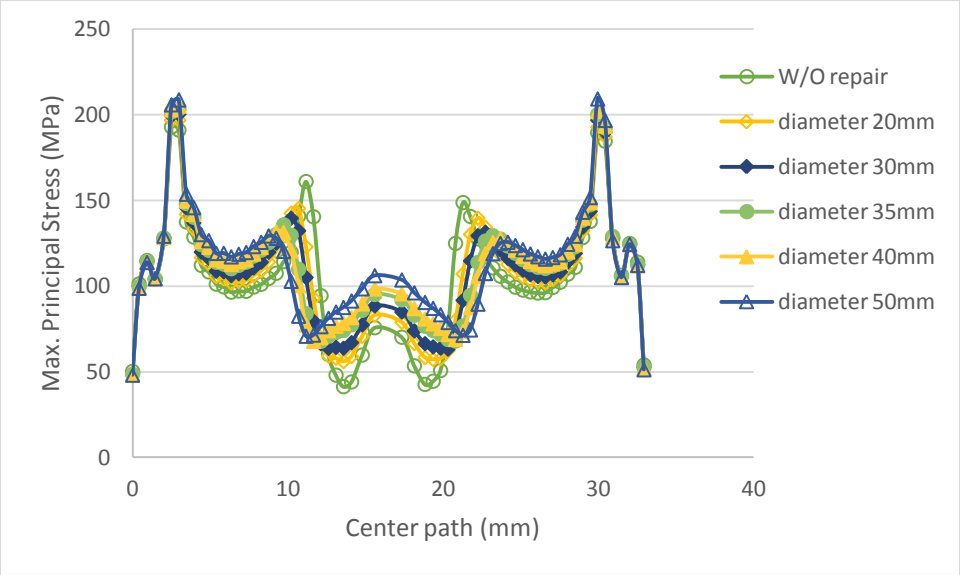

Figure(12): Longitudinal rib cross-section on the center of the model with diaphragm plate

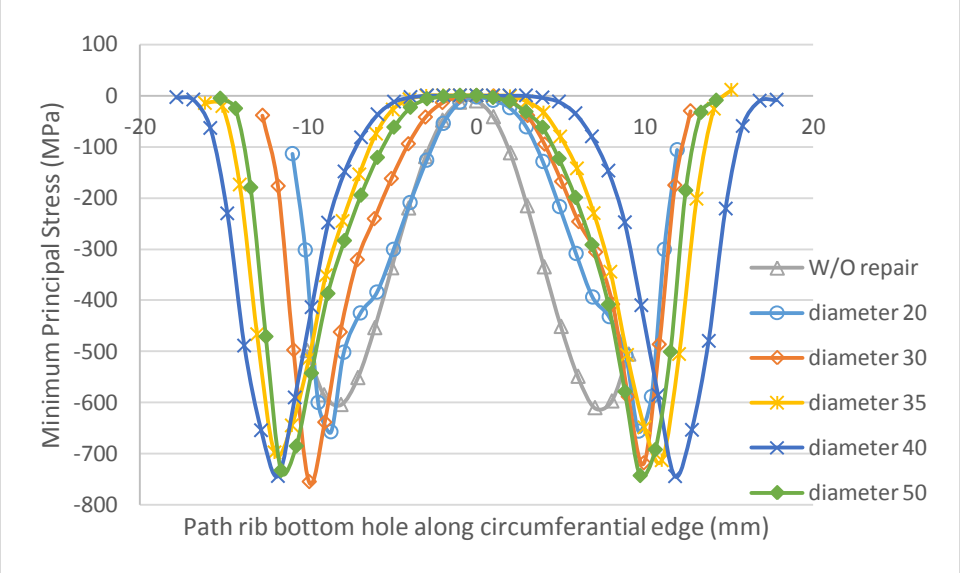

Figure(13): Longitudinal rib cross-section on the center of the model with diaphragm plate

6.3 Effect of crack length between diaphragm plate and longitudinal rib

The crack length along the welds between the diaphragm plate and the longitudinal rib altered from 10 mm to 190 mm in order to evaluate the effect of the crack length on

one side of the rib. The cracks defined as leaving 1 mm space between the diaphragm plate and the rib on the diaphragm plate (Fig.5b). The stress distribution for different crack length is shown in Figure 14.

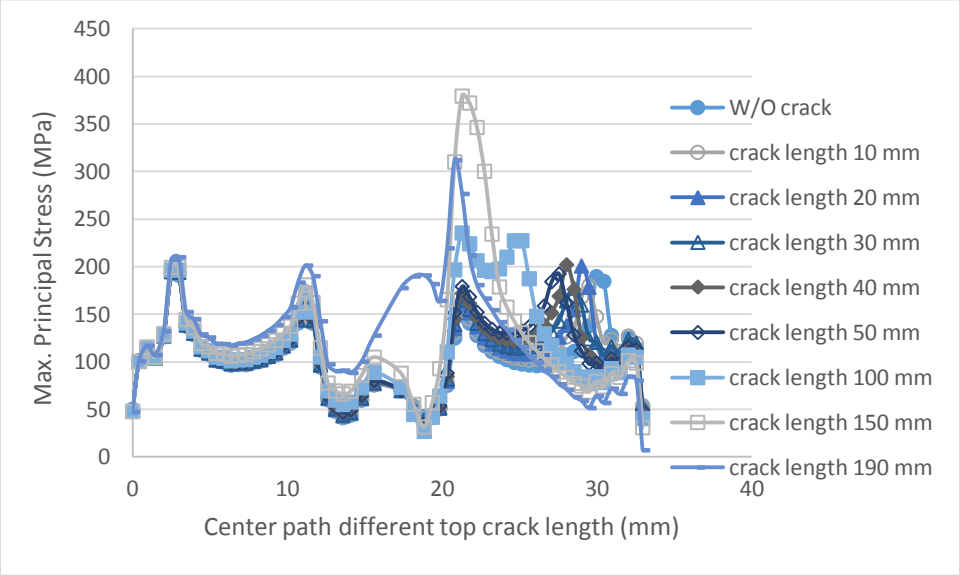

Figure(14): Longitudinal rib cross-section on the center of the model with diaphragm plate

7. Conclusions

The conclusion below are obtained from the FE analysis results.

- The stresses on the ribs are calculated under the maximum tire loading (100 kN) which is considered as the maximum load of one tire when the truck is fully loaded. The stress are higher away from the connection region along the bottom path of the rib for the model with connection plate when the tire is the centre position. However, the stresses on the welds around the connection plate are concentrated as shown in Fig 10. This results explains where the cracks start to grow as also shown in the Fig. 2. These findings are in line with the real situation.

- There is no difference obtained in the stress along the longitudinal axis of the rib when the position of the tire is changed. However, the maximum principal stresses occurred at the bottom point path and as well as on the bottom path of the rib when cross-sectional stresses are evaluated. The maximum stresses occur away from the centre of the rib as shown Fig. 10.
- The maximum stress values obtained in the cross-section of the rib coincides when the tire is 200 and 250 mm from centre. It can be concluded that the stress distribution may be obtained as the tire is 100 or 150 mm away from the centre since the effect of the length of the rib and the interaction between other ribs are excluded in the analysis. The maximum stress obtained when the tire is 150 mm away from the centre line is 1.16 times higher than the stress found in the analysis with the tire on the centre (Fig. 11). It may be observed that the fatigue cracks start to occur to the closed side of bottom of the rib. Tire position may effect to the maximum principal stress on the rib %22 higher depend on the centre loading.
- The maximum stress on the ribs when the crack on the diaphragm plate is repaired with different drilled hole diameter did not change (Fig. 12). Moreover, the maximum stresses along circumferential path increased comparing to without drilled hole. It is concluded that this repair method does not alleviate the stress concentration around the crack location. Especially, the ratio of the diameter of the drilled hole to the diameter of the arc at the bottom of the ribs is greater than 80% the stress concentration is growing around the drilled hole (Fig.13).
- The highest max principal stress occurred on diaphragm plate and ribs connection region when crack reached 150 mm long (Fig. 14). It is shown that

the crack length increases rapidly at this point. The maximum stress is doubled up when the crack length is 150 mm comparing to the maximum stress with no crack in the connection.

List of abbreviations:

FEM : Finite Element Method

FE : Finite Element

kN : Kilo Newton

FE model : Finite Element Model

GPa : Giga Pascal (kN/mm^2)

References

1. Z.X. Li, T.H.T. Chan, and T.Q. Zhou, *Accumulative damage near crack tip for welded bridge members: fatigue life determination.* Theoretical and Applied Fracture Mechanics, 2005. **43**(2): p. 245-260.
2. M. Aygül, M. Bokesjö, M. Heshmati, and M. Al-Emrani, *A comparative study of different fatigue failure assessments of welded bridge details.* International Journal of Fatigue, 2013. **49**(0): p. 62-72.
3. H.-T. Nguyen, Q.-T. Chu, and S.-E. Kim, *Fatigue analysis of a pre-fabricated orthotropic steel deck for light-weight vehicles.* Journal of Constructional Steel Research, 2011. **67**(4): p. 647-655.
4. S. Teixeira de Freitas, H. Kolstein, and F. Bijlaard, *Fatigue behavior of bonded and sandwich systems for strengthening orthotropic bridge decks.* Composite Structures, 2013. **97**(0): p. 117-128.
5. Z.G. Xiao, K. Yamada, J. Inoue, and K. Yamaguchi, *Fatigue cracks in longitudinal ribs of steel orthotropic deck.* International Journal of Fatigue, 2006. **28**(4): p. 409-416.
6. C. Miki, *Fatigue damage in orthotropic steel bridge decks and retrofit works.* International Journal of Steel Structures, 2006. **6**(4): p. 255-267.
7. Z.X. Li, T.H.T. Chan, and J.M. Ko, *Fatigue damage model for bridge under traffic loading: application made to Tsing Ma Bridge.* Theoretical and Applied Fracture Mechanics, 2001. **35**(1): p. 81-91.
8. B.N. Kaan, F. Alemdar, C.R. Bennett, A. Matamoros, R. Barrett-Gonzalez, and S. Rolfe, *Fatigue enhancement of welded details in steel bridges using CFRP overlay elements.* Journal of Composites for Construction, 2011. **16**(2): p. 138-149.
9. R.C. Battista, M.S. Pfeil, and E.M.L. Carvalho, *Fatigue life estimates for a slender orthotropic steel deck.* Journal of Constructional Steel Research, 2008. **64**(1): p. 134-143.
10. L. Frýba and L. Gajdoš, *Fatigue properties of orthotropic decks on railway bridges.* Engineering Structures, 1999. **21**(7): p. 639-652.
11. Z.-G. Xiao, T. Chen, and X.-L. Zhao, *Fatigue strength evaluation of transverse fillet welded joints subjected to bending loads.* International Journal of Fatigue, 2012. **38**(0): p. 57-64.
12. K. Kiss and L. Dunai, *Fracture mechanics based fatigue analysis of steel bridge decks by two-level cracked models.* Computers & Structures, 2002. **80**(27–30): p. 2321-2331.
13. F. Alemdar, A.B. Matamoros, C.R. Bennett, R. Barrett-Gonzalez, and S.T. Rolfe. *Improved method for bonding CFRP overlays to steel for fatigue repair*. in *Proc., ASCE/SEI Structures Congress*. 2011.
14. L. Frýba and S. Urushadze, *Improvement of fatigue properties of orthotropic decks.* Engineering Structures, 2011. **33**(4): p. 1166-1169.
15. M. Aygül, M. Al-Emrani, and S. Urushadze, *Modelling and fatigue life assessment of orthotropic bridge deck details using FEM.* International Journal of Fatigue, 2012. **40**(0): p. 129-142.
16. F. Alemdar, *Repair of bridge steel girders damaged by distortion-induced fatigue*. 2011, The University of Kansas.
17. F. Alemdar, D. Nagati, A. Matamoros, C. Bennett, and S. Rolfe, *Repairing Distortion-Induced Fatigue Cracks in Steel Bridge Girders Using Angles-with-*

Plate Retrofit Technique. I: Physical Simulations. Journal of Structural Engineering, 2013.

18. F. Alemdar, T. Overman, A. Matamoros, C. Bennett, and S. Rolfe, *Repairing Distortion-Induced Fatigue Cracks in Steel Bridge Girders Using Angles-with-Plate Retrofit Technique. II: Computer Simulations.* Journal of Structural Engineering, 2013.
19. M.A. Wahab and M.S. Alam, *The significance of weld imperfections and surface peening on fatigue crack propagation life of butt-welded joints.* Journal of Materials Processing Technology, 2004. **153–154**(0): p. 931-937.
20. Z.-G. Xiao, K. Yamada, S. Ya, and X.-L. Zhao, *Stress analyses and fatigue evaluation of rib-to-deck joints in steel orthotropic decks.* International Journal of Fatigue, 2008. **30**(8): p. 1387-1397.
21. J. Sim and H. Oh, *Structural behavior of strengthened bridge deck specimens under fatigue loading.* Engineering Structures, 2004. **26**(14): p. 2219-2230.
22. F. Alemdar, A. Matamoros, C. Bennett, R. Barrett-Gonzalez, and S.T. Rolfe, *Use of CFRP overlays to strengthen welded connections under fatigue loading.* Journal of Bridge Engineering, 2011. **17**(3): p. 420-431.
23. F. Alemdar, *Evaluation of the Performance of Stress Measures for Longitudinal Ribs on Orthotropic deck Using Finite Element Analysis.* 2015.
24. H.S. Celasun, *Asma Köprüler*. Vol. 160. 1981: İDMM Academy. 326.

ARID Journals

ARID International Journal for Science and Technology (AIJST)
ISSN: 2662-009X

Journal home page: http://arid.my/j/aijst

مَجلةُ أُريد الدَّوليةُ للعُلومِ والتِّكنولوجيا

العدد 7 ، المجلد 4 ، حزيران 2021 م

Traditional Radiation Therapy for Treatment Breast Cancer and Radiation Effects on Normal Tissues

Abbood Abbas Abbood

International Sakharov Environmental Institute of Belarusian State University (ISEI BSU)
23/1 Dolgobrodskaya Street, Minsk, 220070, Belarus
Belarusian/Minsk

العلاج الإشعاعي التقليدي لعلاج مريضات سرطان الثدي وتأثير جرعات الإشعاعية على الأنسجة الطبيعة

عبود عباس عبود

جامعة بيلاروسيا الحكومية -بيلاروسيا/مينسك

abbood.abbas.abbood@gmail.com
arid.my/0004-6707
https://doi.org/10.36772/arid.aijst.2021.475

ARTICLE INFO
Article history:
Received 18/02/2021
Received in revised form 22/03/2021
Accepted 19/05/2021
Available online 15/06/2021
https://doi.org/10.36772/arid.aijst.2020.475

ABSTRACT

The study aims to investigate the effect of traditional radiotherapy on cancer cells and normal cells near the tumor. This study aims to investigate recent advances in radiation therapy using high-energy targeted radiation doses for tumors with low radiation effects on normal cells near tumors or without radiological effects on normal cells. A study of five breast cancer patient's was taken. Three breast cancer patients had treatment by traditional radiation therapy. The other two patients were treated with modern radiation therapy. Traditional radiation therapy can affect patients with breast cancer in areas such as the spinal cord, heart, liver, and lungs. Treating the right side of the breast will impact the patient's liver and right lung. Treating the left side of the breast will have an impact on the heart and left side of the lung.

Keywords: Radiation therapy, cancer breast, lung, heart, spinal cord.

This paper is a revised and expanded version of a paper entitled 'Traditional radiation therapy for treatment breast cancer and radiation effects on normal tissues' presented at Fourth (1 international) student conference veterinary medicine and sustainable development goals, Egypt, 9 March 2021.

الملخص

تهدف هذه الدراسة إلى معرفة تأثير العلاج الإشعاعي التقليدي على الخلايا السرطانية والخلايا الطبيعية القريبة من الورم. تهدف الدراسة أيضا على فهم التطورات الحديثة في العلاج الإشعاعي باستخدام الجرعات الإشعاعية عالية الطاقة للاستهداف الأورام ذات التأثيرات الإشعاعية المنخفضة على الخلايا الطبيعية القريبة من الأورام أو بدون التأثيرات الإشعاعية على الخلايا الطبيعية. تم في هذا البحث دراسة العلاج الإشعاعي الحديثة وتأثير العلاج الإشعاعي التقليدي للنساء المصابات بسرطان الثدي على المناطق (القلب، العمود الفقري، الكبد، الرئة). حيث تم أخذ (5) عينة (مريضة) كما في النتائج والمناقشة. إن التركيز على دراسة التأثير العلاج الإشعاعي من المواضيع المهمة في وقتنا الحالي وذلك لان العلاج الإشعاعي التقليدي يترك إثر سلبي على المريض بصورة عامة حيث إن تأثير الإشعاع يكون على الخلايا السليمة وغير السليمة وهذا مأتم ملاحظته في جمع حالات سرطان الثدي قيد الدراسة: إن علاج سرطان الثدي الأيسر يؤدي إلى أن نسبة الإشعاع التي يستلمها القلب والعمود الفقري والرئة اليسرى كبيرة مما هي عليه عند علاج سرطان الثدي الأيمن وذلك لقربه من المنطقة العلاجية. إن علاج سرطان الثدي الأيمن يؤدي إلى أن نسبة الإشعاع التي يستلمها الكبد والعمود الفقري والرئة اليمنى كبيرة مما هي عليه عند علاج سرطان الثدي الأيسر وذلك لقربهم من المنطقة العلاجية.

كلمات مفتاحية: العلاج الإشعاعي التقليدي، سرطان الثدي، القلب، الرئة.

1- Introduction:

Traditional radiation therapy is the use of high-energy x-rays to destroying cancer cells but depending on the radiation doses it can have an effect on healthy cells. Traditional radiation therapy is often the most common radiation treatment but there are additional treatments that are also used to treat cancer cells such as surgery and/or chemotherapy. With traditional radiation therapy the division of the number of sessions, allows healthy cells to recover and repair themselves which contributes to cut the side effects of this type of treatment. Traditional radiation therapy sends x-rays or photon beams to the cancerous tumor but it can also send these beams beyond the tumor which will then affect healthy tissues nearby and can cause substantial side effects [1,2].

Nowadays, with the advances of radiation therapy have today using (proton therapy, brachytherapy, or treatment planning. etc.) able to send radiation doses of high-energy on cancer cells that stops at the tumor, making it less likely to affect healthy tissues that are near the tumor. Recent advancements have improved efficacy, reduced risks, and decrease the implications of radiation therapy. These advances involve Volumetric Modulated Arc Therapy (VMAT), Three-Dimensional Conformal Radiation Therapy (3DCRT), Stereotactic Radiotherapy (SRT), Brachytherapy, Intensity-Modulated Radiation Therapy (IMRT), Nano Therapy, Radio-Immunotherapy (RIT), and others. Each of these modalities is the improved radiation targeting to a tumor, thereby limiting radiation exposure to healthy tissues. The modalities also deliver a lethal dose of radiation to the tumor cells. The use of recent advances in the treatment planning process distinguishes it from other forms of traditional radiotherapy of the high-resolution tumor-focused radiation dose delivery plan. As a result, the higher and more effective dose for the radiation is delivered

directly to cancerous cells. At the same time, this greatly decreases the high dosage of radiation on the healthy tissues surrounding them [1,3,4].

The current problem, to date, is the use of traditional radiation therapy in the treatment of cancerous cells and using the high dosage of radiation that kills the cancerous cells but has an effect on normal cells. With recent advancements in methods of radiation therapy for cancerous cell, these new methods reduce the effects of radiation doses on normal cells that are near the tumor. The objective of this study is to use methods of radiation therapy for the treatment of cancer cells using the most recent advancements of devices for radiation therapy.

The study aims to identify the most improved and efficient procedure, reduced risk, reduction of radiation therapy side-effect, and the best radiation methods that target only the tumor. The study also aims to provide the best methods of high beam doses on tumors with low side effects on normal cells.

Among the study problems presented by the current research on the questions main.

Some define certain sub-questions:

What is traditional therapy?

What is radiation therapy?

What are the methods of radiation therapy for cancerous cells?

The importance of the current study stems from the fact that it's recent studies on the effects of radiation doses on healthy cells and the importance in:

Rational

Theoretical aspect

The current research is considered one of the studies that accompany continuous studies. It is important to keep pace with developments in cancer cell therapies, in general. We must always consider the continuation of previous research and studies in

cancer cell treatments, keeping in mind the importance of radiation therapy for the treatment of cancerous cells is a modern and advanced process.

Practical aspect

Adding and presenting scientific results that are of interest to researchers in the fields of treatments for cancer cells.

2- Material and Methods

The methods of patient's treatment of breast cancer by traditional radiation therapy and radiation therapy.

2-1 Radiation Therapy

The last studies on radiation therapy for treating breast cancer and research were discovered a century ago. One of the most common and effective uses in cancer treatments is radiotherapy. Generally, radiation doses of high energy are used to destroy cancer cells and shrink tumors. Types of radiotherapy include Brachytherapy and external beam radiation. Brachytherapy (internal radiation therapy) is a type of radiation therapy that involves inserting seeds, ribbons, or capsules containing a source of radiation into or near the tumor. To destroy cancer cells and shrink tumors. The most prevalent type of radiotherapy is external beam radiation. This includes an external beam therapy that guides radiation doses of high energy on cancer cells from outside the body and radiation from a variety of different angles that reaches the tumor. Radiation therapy is more effective in radiation with different intensities, the aim is for radiation doses to focus on tumor locations without causing damage to the normal tissue. Using radiation therapy for the treatment of almost all types of cancer [2,3,4].

2-2 Breast Cancer

Breast cancer is a condition in which out-of-control cells develop in the breast. Different kinds of breast cancer are present. The type of breast cancer depends on which cells transform into cancer in the breast. Breast cancer may start in various parts of the breast. Many tumors are benign in the breast, but certain types of abnormal cells may begin to split out of control and become malignant. When a tumor is breast cancerous, it can spread from its first place to nearby tissues, and when the infection develops further. Cancer can reach the lymphatic vessels or into the bloodstream and this will allow cancer to spread to other places further in the body. Types of breast cancer include invasive ductal carcinoma and invasive lobules carcinoma. The cancer cells spreads into other areas of the breast tissue beyond the ducts. Invasive cancer cells may also spread to other areas of the body. There are also other less common types of breast cancer, such as medullary external symbol, Paget disease, breast cancer that is inflammatory, and mucinous [5,6].

Ductal carcinoma in situ (DCIS) is a breast illness that may lead to breast cancer. Cancer cells are only found in the lining of the ducts and have not spread on other breast tissue [5].

Staging breast cancer is a way of identifying the extent to which breast cancer has spread and the size of the tumor, whether it has spread to lymph nodes, or whether the tumor has spread to remote parts of the body. The TNM method is the most common instrument that uses in staging breast cancer [7]. These divisions generally depend on three factors which are the following:

- (T), describes the tumor size and any cancer spread to surrounding tissue
- (N), describes cancer spread to nearby lymph nodes

- (M), describes metastasis (spread for cancer on other parts of the body). Staging helps diagnose where cancer is found, whether and/or where it has spread, and whether other areas of the body cancer treatment were performed. It depends on the type of breast cancer that has spread and how far. There are methods such as Surgery, Hormonal therapy, Chemotherapy, Radiation therapy, Biological therapy, and other treatment [7].

High beam radiation therapy is used to treat breast cancer in different situations, some of which can be mentioned as follows [5]:

- Radiation therapy has only been used to treat breast cancer.
- The use of radiation therapy can merge with surgery, chemotherapy, and other treatments to treat breast cancer.
- After breast surgery, the use of radiation therapy in this case aims to reduce the chance of the tumor appearing again in the breast or the lymph nodes.
- After mastectomy, especially if cancer has spread to the lymph nodes.
- The condition in which breast cancer spreads to other parts of the breast such as the brain or bones.

3- Results and Discussion

The treatment of breast cancer in this study was conducted by traditional radiation therapy and radiation therapy. A study was done to illustrate the effects of radiation on sensitive areas for breast cancer patients (liver, heart, lung, spinal cord). The study will explain cases to effect of traditional radiotherapy on healthy tissues and cancer cells. Using a radiation dosimeter in the treatment of the cancerous tumor and is device measures the dose uptake for ionization radiation and using the unit of measurement for the calculation amount for radiation a patient is subjected to is gray (GY). This is also known as centigray (CGY) and as shown below.

Case 1: The patient with left breast cancer was treated with traditional radiotherapy and was diagnosed with CT scan and had stage breast cancer ($T_2N_0M_0$). Using radiation doses done the total volume (2358.05cc), the minimum dose is (0.0 CGY), the maximum dose is (4374.0CGY), the mean dose is (3012.0 CGY), cursor volume (76.79%), and as shown in the graph. the number of sessions is 15 fraction (Fx), and the beam dose rate effect is larger on the left lung (476 CGY), heart (1056 CGY), beam dose rate effect is less on the right lung (19 CGY), and right side breast (27 CGY). Using a much higher beam dosage (GTV), (CTV), (PTV) as shown in the red color for killing the cancerous cells in the right breast causing a radiation effect on the healthy cells (from 100 volumes to 4000 doses). Note, a beam dose rate effect larger on the left lung as shown in the green color (from 100 volumes to 3600 doses), heart as shown in the blue color (from 100 volumes to 3600 doses), and spinal cord but less effect on the right lung as shown in the yellow color (from 100 volumes to 500 doses), and right breast as shown in the green color (from 100 volumes to 700 doses), and liver than beam dose as shown in figure 1.

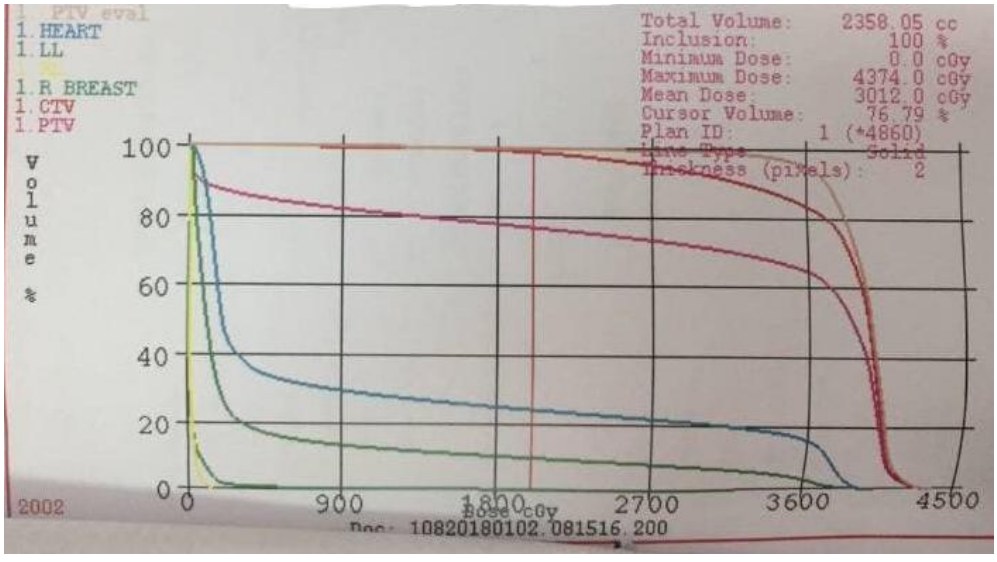

Figure(1): Graph volume-dose for treatment of left breast cancer

Case 2: The patient with left breast cancer was treated with traditional radiotherapy and was diagnosed with CT scan and had stage breast cancer ($T_2N_2M_0$). Using radiation doses done the total volume (1527.33cc), the minimum dose is (173.0 CGY), the maximum dose is (4538.0 CGY), the mean dose is (3725.0 CGY), cursor volume (97.95%), and as shown in the graph. The beam dose rate effects are larger on the left lung (1642 CGY), heart (671CGY). The beam dose rate has a less effect on the right lung (41CGY), and right side breast (10 CGY). Using high beam dosage for the killing of cancerous cells in the left breast causes a radiation effect on normal tissue at the same time (from 100 volumes to 4500 doses) as shown in the red. Note, a larger beam dose affects the left lung, heart, and spinal cord as shown in the red and yellow color but has a less effect on the right lung, liver, and right breast as shown in the blue color as shown in figure 2.

Figure(2): Graph volume-dose for treatment of left breast cancer by traditional radiation therapy

Case 3: The patient with right breast cancer was treated with traditional radiotherapy and was diagnosed with CT scan and had stage breast cancer ($T_2N_1M_0$). Using radiation doses done the total volume (1233.20 cc), the minimum dose is (296.0 CGY), the maximum dose is (4322.0CGY), the mean dose is (3798.0 CGY), cursor volume (99.64%), and as shown in the graph. Beam dose rate effect larger on right lung (1322 CGY), beam dose rate effect less on the heart (75 CGY), and left side breast (15 CGY) and left lung (23 CGY). Using a high beam dose for the killing cancerous cells in the right breast with radiation effect on healthy cells (from 100 volumes to 4050 doses). Note, a high beam dose rate effect is larger on the right lung as shown in the yellow color, liver as shown in the green color, and spinal cord as shown in the red color (from 100 volumes to 4500 doses) but less effect on the left lung as shown in the yellow color (from 100 volumes to 900 doses), the heart as shown in the red color (from 100 volumes to 1800 doses), and the left breast as shown in figure 3.

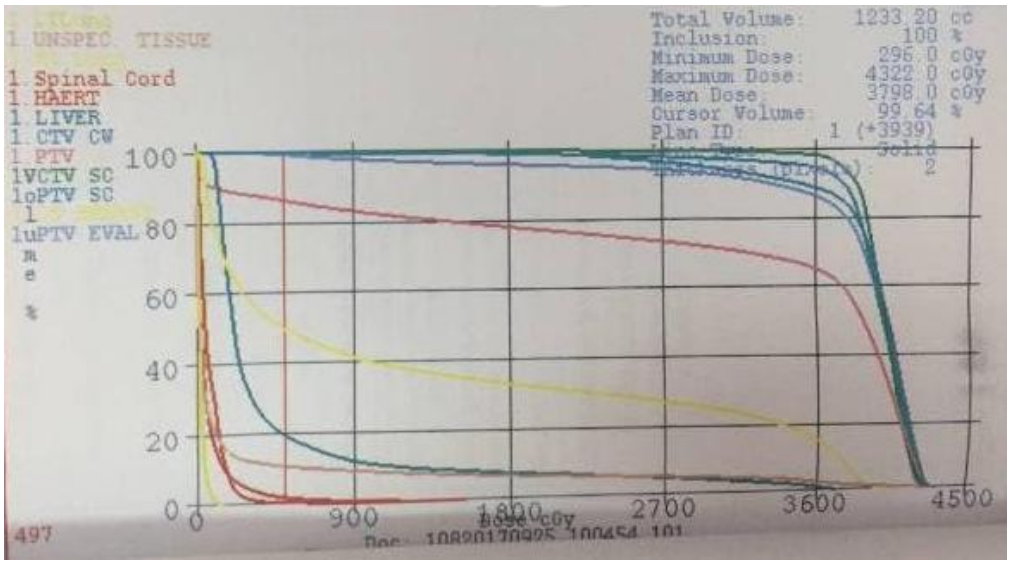

Figure(3): Graph volume-dose for treatment of right breast cancer

Case 4: Post-mastectomy patient with radiotherapy of the right breast using a 6-domain sliding window for IMRT treatment for the treatment of supra / infraclavian and internal lymph nodes but with preservation of normal tissue from a high dose beam [3] as shown in figure 4.

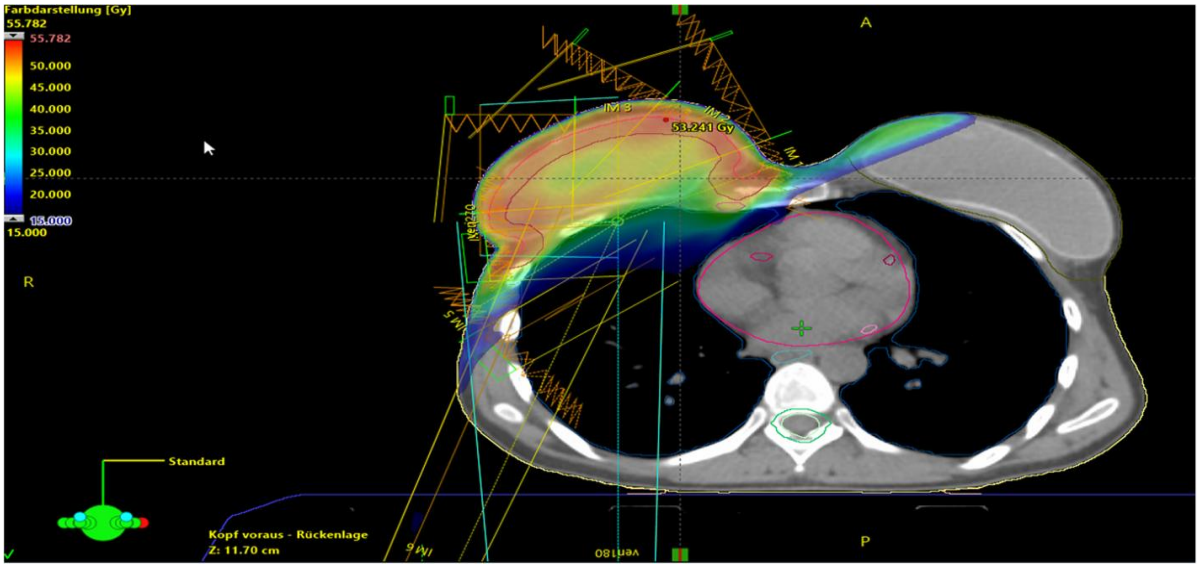

Figure(4): Right breast cancer patient [3]

Case 5: The patient was undergoing left breast radiation therapy using a 3-field sliding window IMRT technique. It is more effective, targets the tumor more directly and has

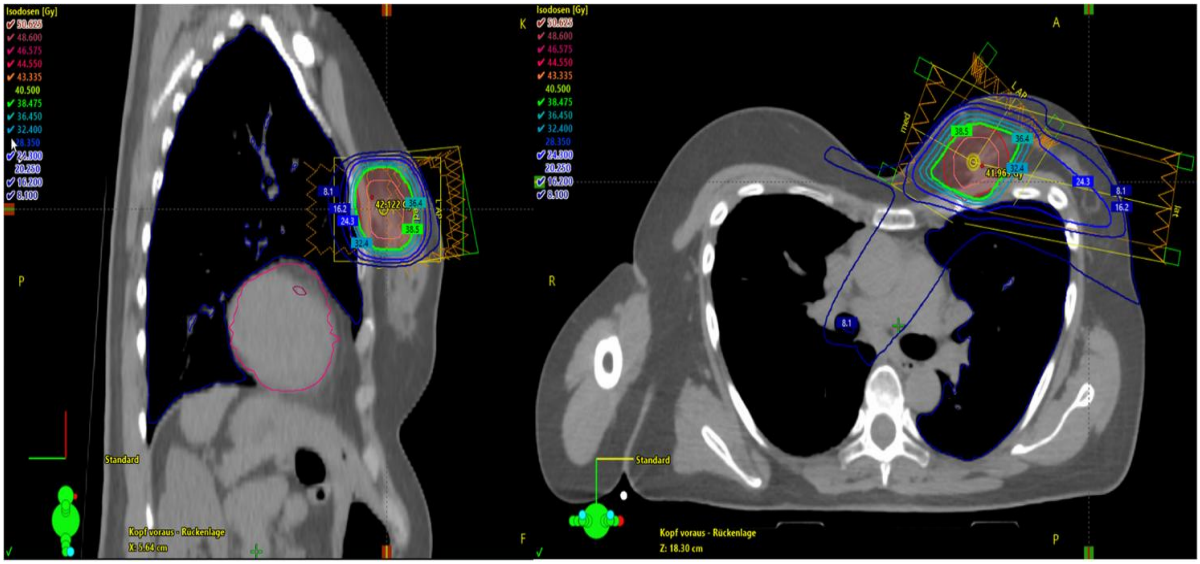

fewer side effects than traditional radiation therapy [3] as shown in figure 5.

Figure(5): Left breast cancer patient [3]

4- Conclusions:

This study was done on the effect of traditional radiation therapy for breast cancer patients and on recent developments in radiation therapy that allows us to switch from two-dimensional to three-dimensional and four-dimensional imaging which provides more focused therapy. The study is intended to provide more reliable tumor radiation doses and biological targeting. This would cause the radiation dose to increase, thereby being more efficient at treating cancer and reducing the amount of time it takes to re-treat. Radiation therapy has three cases:

The effect on the left breast on normal cells of traditional radiation therapy has a greater impact on the heart, spinal cord, and left lung when compared to the right side which has a less of an effect. The right side is less affected by traditional radiation therapy as in case 1 and in case 2.

The effect of traditional radiation therapy on the right side breast on normal cells on the spinal cord, liver, and right lung is more than the left side, which is less affected by traditional radiation therapy as in case 3.

Treating breast cancer using recent advances radiation therapy, proton therapy, brachytherapy, or using in treatment planning (3D, IMRT, VMAT, SIB, to other). These are perfect treatments for the patient's cancer. These methods kill cancerous cells with a more active radiation dose on the tumor with side-effects that are low on normal cells than with high dose beam as in the cases: case 5, case 6.

Recommendations

I believe recent advances in radiation therapy are the alternative to traditional radiation therapy because it focuses more on removing the cancerous tumor with a less effect on healthy tissues.

Abbreviations

RT	Radiation therapy	RIT	Radio-immunotherapy
RTP	Radiation treatment planning	GTV	Gross tumor volume
IMRT	Intensity-modulated radiation therapy	CTV	Clinical target volume
VMAT	Volumetric modulated arc therapy	PTV	Planning target volume
3DCRT	Three-dimensional conformal radiation therapy	CGY	Centigray
		FX	Fraction
SRT	Stereotactic radiotherapy	CC	Cubic centimeter
SIB	Simultaneous integrated boost		

References

1. Issam El Naqa. A guide to outcome modeling in radiotherapy and oncology listening to the data. CRC Press. 1st edition. 2018.
2. Markus MacGill. what to know about radiation therapy? Medical news today. 2019 (accessed 10 February 2021). https://www.medicalnewstoday.com/articles/158513.
3. J. Haussmann, S. Corradini, C. Nestle-Kraemling, E. Bölke, F. J. D. Njanang, B. Tamaskovics, k. Orth, E. Ruckhaeberle, T. Fehm, S. Mohrmann, I. Simiantonakis, W. Budach, C. Matuschek. Recent advances in radiotherapy of breast cancer. Radiation Oncology, 15(2020) 1-10.
4. C. Garibaldi, B. A. Jereczek-Fossa, G. Marvaso, S. Dicuonzo, D. P. Rojas, F. Cattani, A. Starzyńska, D. Ciardo, A. Surgo, M. C. Leonardi, R. Ricotti. Recent advances in radiation oncology. Ecancermedicalscience. 11(2017)1-19.
5. J. Strauss, W. Small, G. E. Woloschak. Breast cancer biology for the radiation oncologist. Springer. 2015.
6. Jaime Herndon. A Comprehensive Guide to Breast Cancer. Health line; 2019 (accessed 2 January 2021) https://www.healthline.com/health/breast-cancer.
7. A. E. Giuliano, J. L. Connolly, S. B. Edge, E. A. Mittendorf, H. S. Rugo, L. J. Solin, D. L. Weaver, D. J. Winchester, G. N. Hortobagyi. Breast Cancer—Major changes in the American Joint Committee on Cancer eighth edition cancer staging manual. A cancer journal for clinicians. Volume 67, Issue4(2017) 1-14.

ARID Journals

ARID International Journal for Science and Technology (AIJST)

ISSN: 2662-009X

Journal home page: http://arid.my/j/aijst

مَجلةُ أُريد الدَّوليةُ للعُلومِ والتِّكنولوجيا

العدد 7 ، المجلد 4 ، حزيران 2021 م

Requirements for controlling the accident's cost problems for construction projects

Zuhair Nafea Alani

Architectural and Interior Design Engineering Department -College of Engineering

Gulf University – Bahrain

متطلبات السيطرة على المشاكل الكلفوية لحوادث العمل للمشاريع الإنشائية

زهير نافع العاني

قسم الهندسة المعمارية والتصميم الداخلي-الجامعة الخليجية – مملكة البحرين

coo@gulfuniversity.edu.bh

https://doi.org/10.36772/arid.aijst.2021.476

ARTICLE INFO
Article history:
Received 09/01/2021
Received in revised form 15/03/2021
Accepted 17/05/2021
Available online 15/06/2021
https://doi.org/10.36772/arid.aijst.2021.476

ABSTRACT

The construction sector is one of the most accident-prone sectors during onsite work. Therefore, it increases the costs of the projects and add more amount to the budget i.e., the workers' hospitalization charges on injuries, and casualties led to it. The current study reviews the site cost issues due to the accidents caused during the construction projects with their suggested solutions. This research has reviewed thirty Sudanese Construction sector projects and analyses their results in detail to obtain the possible solutions as a part of an integrated site management system for accident cost problem (diagnosing and solving). It also used to reduce accidents, and to prevent any extra costs which might occur due to it.

Keywords: Construction projects, Site accidents, Site costs, Site management

الخلاصة

قطاع التشييد من أكثر القطاعات عرضة إلى وقوع الكثير من الحوادث أثناء تنفيذ الأعمال الإنشائية وبالتالي زيادة تكاليف المشاريع المنفذة إضافة الى إصابات العاملين والتي يؤدي بعضها إلى الوفاة. ومن هذا المنطلق فإن البحث في العوامل المؤدية إلى وقوع الحوادث والسبل الكفيلة للحد منها هي من أولويات الإدارات العليا في هذا القطاع الحيوي.
يتناول البحث شرح للمشاكل الموقعية التي تسبب في وقوع حوادث العمل والتي بالتالي تؤدي إلى زيادة في تكاليف العمال خلال

مراحل التنفيذ، مع الحلول المقترحة لها. تم تقسيم البحث إلى ثلاثة أجزاء، تناول الجزء الأول مراجعة نظرية للدراسة، والجزء الثاني تناول المسح الميداني تم القيام به أثناء الدراسة، لثلاثين مشروعا إنشائيا في عدد من مواقع التشييد في السودان – كحالة دراسية، وذلك من أجل التعرف على المشاكل الموقعية مقارنة مع الدراسة النظرية.

أما الجزء الثالث من البحث فقد تناول وضع الإستنتاجات التي توصل اليها الباحث وهي عباره عن مجموعة حلول والتي يمكن اعتمادها من قبل الإدارة الموقعية لغرض التقليل وحل المشاكل الموقعية والتي قد تحدث مسببة وقوع حوادث عمل التي تؤدي إلى زيادة في تكاليف الأعمال.

الكلمات المفتاحية: المشاريع الإنشائية، حوادث العمل، التكاليف الموقعية، إدارة الموقع.

1. Introduction

The construction industry has experienced a lot of occupational injuries, and construction work is considered one of the most dangerous occupations due to the dynamic and temporary nature of the workplace. Specifically, most construction work takes place outdoors and work conditions (e.g., temperature, humidity, and light conditions) and the number of required workers frequently changes, which increases the difficulty of safety management [1].

The current study has reviewed relevant literature to seek solutions of upsurge in the budget due to the onsite accidents during construction projects.

This research has been divided into three parts, the first part deal with reviewing the literature of the research, and through the second part, thirty projects, are selected from Sudanese construction sector – as a case study. These cases have been investigated to identify the site accident challenges and then compared with the literature. The third part of the research concludes a set of possible solutions as a part of an integrated site management system for accident cost problem (diagnosing and solving), to be followed by the site management, to reduce accidents, and therefore preventing any extra costs which might occur due to it.

2- THE LITERATURE REVIEW

2-1:*Classification of construction accidents*

Accident is defined as "any sudden, unexpected or planned emergency occurring during the work or causing what is related to it, and this includes any exposure to natural, mechanical or chemical hazards or acute stress and other risks that may lead to death, physical injury or acute illness to the injured worker. And the accident may lead to damages and damage to the facility or

production means without injuring any of the workers. Or it may lead to injury to one or more workers in addition to damage to the facility and the means of production" [2].

Some common types of construction accidents include:

- Crane or hoist accidents. Cranes and hoists are important construction tools. However, lack of training, operator errors, and other factors can lead to serious accidents on construction sites. [3]
- Falls from heights. Scaffolding accidents, ladder accidents, roofing accidents, and other falls from heights can be lethal. [3]
- Slip and falls. A slip and fall on the ground can cause broken bones, sprains, and other injuries. [3]
- Repetitive stress injuries. Repetitive nature of some construction work can result in repetitive stress injuries in the back, wrists, ankles, and joints. [3]
- Gas leaks, fires, and explosions. Gas leaks, fires, and explosions can be sudden and deadly. Carbon monoxide, for example, can be dangerous in a confined construction space. [3]
- Forklift accidents. Without proper training and alert operators, forklifts can be dangerous and may result in serious construction accidents. [3]
- Trench accidents. A trench collapse or an accident within a trench can be devastating. A construction worker may be trapped and unable to get out on their own. [3]
- Elevator shaft accidents. Construction workers may be at risk of falling down elevator shafts if safety precautions are not observed. [3]
- Electrocutions. Electrical equipment, overhead electrical wires, wiring, and lightning all create risks of electrocution for construction workers. [3]

- Machinery accidents. Heavy machines perform great deal of construction operations, but these also create risk situations for construction workers either because of malfunction of machinery or operator's fault. [3].

- Struck-by accidents. Motor vehicles are common on construction sites. Construction worker is at risk of being hit by a motor vehicle or part of machinery while working on a construction site. [3]

- Caught-between accidents. A limb of a person or entire body may get caught by a piece of equipment or crushed by the debris of a construction incident. [3]

- Exposure to hazardous or toxic chemicals. Inhalation of chemicals or toxic vapors by construction workers can cause severe respiratory problems. [3]

2-2:*Classification of Site Accident costs*

The cost of workday loss caused by minor occupational accidents are almost 35 % of major workday losses. These costs present the importance of preventive measures for workers' health and safety in construction. [4]

Costs caused by occupational accidents are well investigated in many different studies and they are subdivided into two categories as:

Direct costs include Medical costs, ambulance fee, Doctor's fees, hospital fee, rehabilitative services, cost of medication, therapy, insurance compensation payment to the injured worker [5].

Indirect costs include workday loss, working time loss in workplace, time loss for investigating the accident and legal processes, pausing the production after the accident, delay in workflow and program, damage in working machines or stopping to use these machines, low efficiency of

workers, loss of reputation for the company, fine payments for late delivery. Thus, it is indicated that indirect costs are much higher than the direct costs in total. [4]

2-3: The Factors Affecting Site Accidents Costs and their applicable solutions.

2-3-1: The Factors Affecting Site Accidents Costs:

***2-3-1-1: Excavations Works*:** the most affecting factors which can cause accidents during excavations are: [6]

- Unshoring the sides of excavation or sloping to the angle of repose may causes cave-in.
- Equipment operates near the top edge of the excavation.
- Keeping or storing the materials near the edge of the excavation.
- Electrical cables or and flammable gases pipes damaged during excavation causing possible hazards.
- No emergency exit is provided for employees working in a trench deeper than 4ft.

2-3-1-2: Individual falls: the unsecured railings will be the most affective factor for increasing the risk of accidents. [6]

***2-3-1-3: Steel erections*:** steel erection is very hazardous construction task, the factors which can cause accidents during steel erection on site are: [6]

- Workers are not provided with gloves, hard hats, and eye protection when they engaged in welding, cutting, and chipping operations.
- Shortage of scaffolds, or scaffolds without guard rails and safety belts can cause individual falls.
- No safety nets are provided when working on high places above the ground.
- weather is responsible for many of the hazards at the steel erection sites.

***2-3-1-4: Equipment operations*:**

The most factors which might increase accidents due to equipment operations are: [6]

-Using the equipment in improper purpose.

-Employing unexperienced operators.

- Exceeding the equipment design limits.

-loading the equipment in a way that affects the safety of driving or operating them.

- The position of the equipment near the edge of the excavation when unloading.

-Bad site illumination.

***2-3-1-5: Marine or over-water construction*:**

Marine or over-water construction presents all the usual construction hazards plus additional hazards posed by the marine environment, these additional hazards include slippery surfaces, increased tripping, and height hazards, as well as weather and wave actions. Factors which can add other risk of accidents are: [6]

-Bad illumination.

-Lack of ramps or walkways.

-unguarded decks or surfaces over water.

***2-3-1-6: Environmental Health in construction*:**

The major Environmental Health problems encountered in construction consist of noise, dust, toxic materials, heat and cold. [6]

2-3-2: applicable solutions to be considered to avoid accidents are:

2-3-2-1: For Excavations Works:

- Sides of excavations should be properly shored by one of the shoring systems, such as: sheeting, lagging, or sheet piling [7].

-When employees are required to work in a trench 4ft (1.2m.) or more in depth, provide an adequate means of emergency exit located with (7.6 m.) of the worker.

-Avoid the operation of equipment near the top edge of an excavation because this increases the chance of slope failure.

- Materials should not be stored near the edge of an excavation to decrease the chance of slop failure when workers are required to enter the excavation. No spoil or other material may be stored within (0.6 m.) of the edge of the excavation.

-Watch out for buried lines and containers when excavation. Possible hazards include toxic and flammable gasses, electricity and collapse of side slopes may occur due to sudden release of liquids.

2-3-2-2: For individual falls:

The procedures to be followed to prevent workers failure are: [8]

-Properly guard all opening above ground level.

-Provide guard rails, safety lines, safety belts, and/or safety nets for workers on scaffolds or steel work.

-Temporary structures should be properly designed, constructed, and braced.

2-3-2-3: For steel erections:

To prevent accidents during steel erections, the following steps should be followed: [9]

-workers engaged in welding, cutting, and chipping operations should be provided with hard hats, gloves, and eye protection.

-Prevent workers from falls from high places during erection by:

* Providing, whenever possible, temporary floors and scaffolds with rails.

* Providing lifelines and safety belts when guard rails are not feasible.

* Providing safety nets where the potential fall exceeds (7.6m.) or two stories.

2-3-2-4: For Equipment operations*:*

-Machines should be equipped with the required safety features and operators use seat belts when provided.

-The designed limits of equipment should not be exceeded, especially when operating cranes.

-Workers not to be allowed to ride on equipment unless proper seating is provided.

-Provide good site illumination to have clear roads to avoid accidents during transport.

-Ensuring that any guards or safety devices removed during equipment repair are promptly replaced. [7]

2-3-2-5: For Marine or over-water construction:

-Ramp or safe walkway must be provided.

- Access ways must be adequately illuminated free of obstructions.

-Working areas should have nonslip surfaces.

-Workers on unguarded decks or surfaces over water must wear approved life jackets or buoyant vests. Life rings and a rescue boat must also be available.

-Workers more than 25ft. (7.6m.) above a water surface must be protected by safety belts and safely nets. [7]

***2-3-2-6: For Environmental Health in construction*:**

-Workers who are concerned with cutting materials, especially asbestos, should be provided with noise cabs to avoid them from toxic dust effect.

-For people working in tunnels, dust problems can be avoided by ventilate a tunnel. Blasting, mucking, and using water instead of air to remove the cuttings to avoid dust caused by drilling.

-Methods of reducing heat effect on workers include the use of mechanical equipment, scheduling hot work for the cooler part of the day, use of sun shields, providing cool rest areas, providing water supply easily accessible to workers, and the use of proper hot-weather clothing.

-The provisions of workers with adequate clothing and warming areas will be successful requirements for cold weather construction.

- Giving the workers adequate rest allowances to avoid stresses and accidents due to working more than allowable hours under extreme temperature in hot weather construction. [6]

3- Controlling accident costs:

In the light of the above discussed facts, it seems crucial that onsite accident costs must also be included in the monthly report of the actual costs of the project along with the monthly costs of main elements such as (labor, machinery, materials, incentives, contractors, and subcontractors work etc.)

Safety is an important part of project management, and it is no less important than planning, scheduling of work, estimating work quantities, and controlling costs, and it must be considered. Achieve safety in the design stage and during the project implementation stages. Accidents do not .affect workers only, but also their families [10]

So, to control accidents costs during the implementation of the work, the "safety program" can be a reason for preventing these accidents [11].

4. THE FIELD WORK

Through this part of the research, a survey has been conducted on thirty selected Sudanese projects to identify the actual accidents site rising cost concerns. The field work was also added to get the in-depth information from site management experts in relation to the accidents during construction, and their suggested solutions for these problems (if any) to compare with the consulted literature.

4-1 The characteristics of the respondents

Table (1) illustrates the respondents (experts) selected for the survey. The table below shows their years of experience, which is ranged from 5-40 years:

- 40% of experience have (8-15) years.
- 13% of experience have (16-20) years.
- 30% of experience have (21-25) years.
- 17% of experience have (26-40) years.

Majority (60%) of the respondents have more than 16 years of experience. Most (63%) of the respondents are civil engineers, while 20% are architectural, and 17% respondents are mechanical and electrical engineers. A large number (73%) of them are working as site and project managers, which provided substantial information and in-depth knowledge of field experience which is quite useful for the research undertaken.

4-2 Preparing the Questionnaire List (Q.L.)

The review of literature related to the Accident site cost problems has been carried out from the thirty Sudanese survey projects. In depth field knowledge from the survey projects have been obtained from the respondents.

The Questionnaire List (Q.L.) has been prepared from the literature which includes all the site cost challenges (factors) that are affecting the accident site costs with their possible solutions that would reduce these costs.

As a result of eliciting most of the problems that might increase accident site costs, through the (Q.L.), the total number of these problems (factors) have finally reached in number to (24), distributed as follows:

1- Excavations, 6 problems

2- Individual fall, 6 problems

3- Work on water, 2 problem

4- Scaffolding , 3 problems

5-Work environment, 7 problems

4-3 The Analysis of the tabulated results

The results which have been concluded from the (Q.L.) answers were analyzed, and tabulated, as shown in Table (2) and Table (3), the following figures were calculated and presented for each of the thirty selected projects.

A- The number of existed site cost problems found in the selected research projects.

B- The percentage of existing site cost problems out of total known problems.

C- The number of problems that were addressed and solved during the implementation by the management of these projects.

D- The percentage of site cost addressed and resolved.

E- The number of problems that still exist that have not been addressed and resolved, and their types and percentage.

4-4 Analysis of percentages table.

Tables (2) shows the number of existing site cost problems, and their percentages.

While **Table (3)** shows Number of issues, solved by project management, and problems that still exist, and their percentages, where Only (60%) of the selected projects have solved more than 50% of their cost problems.

Also, table (3) indicates the affecting factors (problems) on site costs such as: scaffolding, individual fall, excavation. Table (4) shows the percentages of these problems in the selected projects according to their significant effectiveness on site costs.

A- 93% of the projects still have unsolved problems regarding scaffolding.

B- 90% of the projects still have unsolved problems regarding individual fall at work.

C- 83% of the projects still have unsolved problems regarding excavation work.

D- 70% of the projects still have unsolved problems regarding work environment.

Figure (1) shows the number of problems which cause site accidents and still exist in the selected Projects.

The analysis of Tables (2) and (3) helps the top management in diagnosing and evaluating the efficiency and performance of project site management in identifying and solving cost problems, through knowing who can solve most of their cost problems (specially the most effective on increasing site costs), and managers who have the largest percentage of problems that have unsolved.

If the percentage of unsolved problems exceeds 25% in any construction project, this gives a good indication to top management in identify the site cost problems that will have a significant impact in increasing the total costs of the project, and thus effective corrective measures are taken to solve these problems.

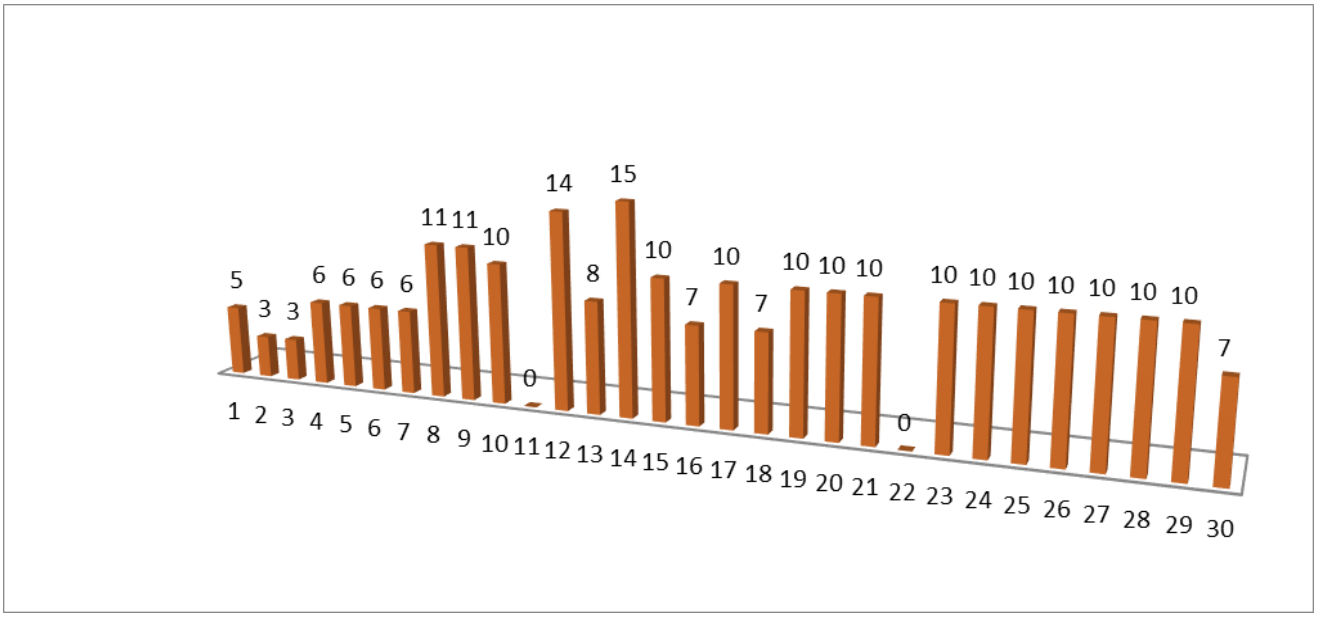

Figure(1): unsolved Accident cost problems in 30 construction projects

Table(1): Respondence characteristics

Projects Numbers	Years of experience	Projects Numbers	specialization	Projects Numbers	position
6,7,11,15,16,17,22,23,26,28,29,30	8-15	1,2,3,5,10,11,12,13,14,19,20,22,23,24,25,26,27,29,30	Civil engineer	1,7,8,17,18,27	Project manager
1,13,20,24	16-20	4,8,16,18,21,28	Architect	2,6,10,11,12,13,15,19,20,22,23,24,25,26,28,29	Site manager
2,3,4,5,8,10,12,18,27	21-25	6,9	Mechanical engineer	3,9,14,16,21,30	Designer
9,14,19,21,25	26-30	7,15,17	Electrical engineer	4,5	planner

Table(2): number of problems exist for each project and their percentages.

Projects Numbers	Total number of problems	Number of problems exist (in each project)	% of problems exist (in each project)
1,10,15,16,21,30	24	20	%83
2,8,14,18,28	24	19	%79
3,12,17,23,25	24	22	%92
4,5,9,24,27	24	21	%88
6,13,19,26,29	24	18	%75
7,20	24	17	%71
11	24	15	%63
22	24	14	%58

Table(3): Number of problems solved by project management, and problems that still exist and their types.

Project No.	Number of problems exist in each project	Number of problems solved in each project	% of problems solved in each project	Number of unsolved problems in each project	Number and Type of unsolved problems in each project
12	22	8	%36	14	(4) problems regarding individual Fall (2) problems regarding Scaffolding (5) problems regarding excavation (1) problems regarding work environment (2) problems regarding work on water
14	19	4	%21	15	(3) problems regarding individual Fall (3) problems regarding Scaffolding (4) problems regarding excavation (5) problems regarding work environment
8	19	8	%42	11	(3) problems regarding individual Fall (2) problems regarding Scaffolding (4) problems regarding excavation (2) problems regarding work environment
9	21	10	%48	11	
10,21	20	10	%50	10	(3) problems regarding individual Fall (2) problems regarding Scaffolding (3) problems regarding excavation (2) problems regarding work environment
26,29	18	8	%44	10	
15	20	10	%50	10	(3) problems regarding Scaffolding (3) problems regarding excavation (1) problems regarding work environment (3) problems regarding individual Fall
19	18	8	%44	10	
20	17	7	%41	10	
23,25	22	12	%55	10	(2) problems regarding individual Fall (3) problems regarding Scaffolding (4) problems regarding excavation (1) problems regarding work environment

17	22	12	%55	10	(2) problems regarding individual Fall (3) problems regarding Scaffolding (4) problems regarding excavation (1) problems regarding work environment
27	21	11	%52	10	(3) problems regarding individual Fall (4) problems regarding Scaffolding (3) problems regarding excavation
28	19	9	%47	10	
24	21	11	%52	10	(2) problems regarding individual Fall (2) problems regarding work on water (3) problems regarding excavation (2) problems regarding work environment (1) problems regarding Scaffolding
16,30	20	13	%65	7	(3) problems regarding individual Fall (2) problems regarding Scaffolding (4) problems regarding excavation (2) problems regarding work environment
18	19	12	%63	7	(2) problems regarding individual Fall (2) problems regarding Scaffolding (2) problems regarding excavation (1) problems regarding work environment
13	18	10	%56	8	(3) problems regarding individual Fall (1) problems regarding Scaffolding (2) problems regarding excavation (2) problems regarding work environment
4,5	21	15	%71	6	(2) problems regarding individual Fall (2) problems regarding Scaffolding (2) problems regarding excavation
6	18	12	%67	6	
7	17	11	%65	6	
1	20	15	%75	5	(2) problems regarding Fall (2) problems regarding Scaffolding (1) problem regarding Work environment
2	19	16	%84	3	(1) problems regarding Scaffolding (2) problems regarding Work environment

3	22	19	%86	3	(2) problems regarding individual Fall (1) problems regarding Scaffolding
11	15	15	%100	0	%0
22	14	14	%100	0	%0

Table(4): the types and percentages of problems according to their significant effectiveness on site costs

	Problems regarding **Scaffolding**	Problems regarding **Individual falls**	Problems regarding **excavation**	Problems regarding **Work environment**	Problems regarding **Work on water**
Projects No.	1,2,3,4,5,6,7,8,9,10, 12,13,14,15,16,17, 18,19,20,21,23,24, 25,26,27,28,29,30	1,3,4,5,6,7,8,9,10, 12,13,14,15,16,17, 18,19,20,21,23,24, 25,26,27,28,29,30	4,5,6,7,8,9,10,12, 13,14,15,16,17,18, 19,20,21,23,24,25, 26,27,28,29,30	1,2, 8,9,10,12,13, 14,15,16,17,18,19, 20,21,23,24,25,26, 29,30	12,24
No. of projects (out of 30)	28	27	25	21	2
% of projects (out of 30)	93%	90%	83%	70%	6%

5- THE CONCLUSION

Thus, in a nutshell, the most significant affecting factors that cause site accidents, which led to extra site costs, are those related to Excavations, Individual falls, Scaffolding, and Work environment.

Only (60%) of the selected projects have solved more than 50% of their cost problems. The top management should address the above-mentioned entities in mind to identify and solve some or all their cost problems related to work accidents.

This guide can be used as an efficient evaluation parameter. This evaluation would be a good incentive to encourage project managers to reduce site cost problems during the implementation of construction work.

-As a method for monitoring and controlling site costs by diagnosing the most significant accidents, cost problems for each project, so that the top management can take the proper action to rectify such problems quickly to save costs.

-Practicing safety program may be considered as the remedy to reduce the site accidents costs.

REFERENCES

1- K. Yang, K. Kim, S. Go, "Towards Effective Safety Cost Budgeting for Apartment Construction: A Case Study of Occupational Safety and Health Expenses in South Korea", an Article, https://www.mdpi.com/journal/sustainability/ 13/ 1335. (Accessed: Jan. 27, 2021).

2- Massoudi Kulthum, Mokrin Heba, "Work Accidents, Their Causes and Methods of Reducing them", research paper, "Altaamin lilearab", www. @insurance4arabs, (Accessed December 2013).

3- B. V. Ova," Best practices to improve construction site safety, in the specific conditions of processing plant building", University of Mining and Geology "St. Ivan Rilski", 1700 Sofia, Bulgaria, MATEC Web of Conferences (305) (00014) (2020) - 2.

4- F. Yilmaz and U. B. Çelebi," The Importance of Safety in Construction Sector", *Business and Economics Research Journal* Volume (6) Number (2) (2015)- 26.

5- K.K. Bentil." The impact of construction Related Accidents on the cost and productivity of building Construction Projects*", International council for Building Research Studies and Documentation (CIB),* Vol. (6) (1990) -15.

6- R. Alani and Z.N. Alani " Having an efficient management system for controlling accident site cost problems of Iraqi projects", The First Engineering Scientific Conference, Civil Engineering Research Program, College of Engineering, Anbar University, Ministry of Higher Education and Scientific Research, Iraq, Sep. (1998).

7- S.W. Nunnaly, " Construction Methods and Management" 2nd Ed. By prentice-Hall, Inc. New Jersey,1987.

8- C. Hendrickson, and T. Au, "Project Management for Construction" By prentice-Hall, Inc. USA,1989.

9- W. Hammer, "Occupational Safety Management and Engineering", By Prentice-Hall, Inc. New Jersey,1976.

10- Garold D. Oberlender," Project Management for Engineering and Construction", 2nd Edition, McGraw- Hill International Editions, Civil Engineering Series, Singapore,2000.

11- Robert L. Peorifoy, Clifford J. Schexnayder, Robert L. Schmitt, Avida Shapira, "Construction Planning, Equipment, and Methods", 9th Edition, McGraw- Hill Education, New York, 2018.